



**TÉCNICO**  
LISBOA



## The Kerr black hole hypothesis: a review of methods and results

João Miguel Arsénio Rico

Thesis to obtain the Master of Science Degree in  
**Engineering Physics**

### Examination Committee

Chairperson: Doctor José Pizarro de Sande e Lemos  
Supervisor: Doctor Vitor Manuel dos Santos Cardoso  
Members of the Committee: Doctor Jorge Miguel Cruz Pereira Varelas da Rocha  
Doctor Paolo Pani

September 2013



# Acknowledgements

Life and physics are hard. It is often easy to forget how much there is beyond the formulas we understand and that some of our basic assumptions are wrong. Experiment rules regardless of pet theories, and we are fortunate for the opportunity to at least refine our intuitions. It is essential to keep questioning, keep working, keep humble. Life and physics are a pleasure, and for the most part people are the reason why.

I want to start by thanking Vitor Cardoso, my thesis supervisor, for all the help, patience and encouragement throughout this project. An excellent researcher and an excellent supervisor are not the same thing, and I have been extremely fortunate because Vitor really is both. His sheer energy, constant good spirits and relentless enthusiasm for Physics are an inspiring example for me, and I have yet to measure all that I have learned from him. I also want to thank Paolo Pani for being such a great co-supervisor! Thank you for all the guidance and fun through this initiation to research and black hole physics. It has been a real pleasure and privilege to work with both of you.

I thank Jorge Rocha, my thesis examiner, for a very careful reading of the manuscript and valuable comments and suggestions. Thanks to everyone at CENTRA and the Gravity Group for making it an exceptionally good and fun environment to work in!

Yes, the physics students at IST are a remarkably interesting and diverse group of intelligent people. Here life is never boring, one finds many friends, and classes, labs, dinners, nights out, study sessions, football games and trips provided so many memorable moments. And so many of them with these two very smart, very fun and very kind friends, Francisco and Pedro.

Is there anything better than hanging out with your group of long time friends? For continuously putting up with me and for all the good times: Ana, Cláudia, Francisco, Joana, João, Liron, Luís, Rui, Sebastião and Tiago! Speaking of putting up with and good times, who would I be without my beautiful, smart, fun sisters, Sara and Inês?

Without my family's love, support and sacrifice none of this would have been possible. I owe them the most. And high above all, my Mother. I could not possibly thank her adequately in these notes, so let me at least thank her for the talks and, yes, for all the little snacks! For giving me every opportunity to pursue what I wanted and making me the most privileged person I know of. For all the little and big things the best Mother does.

And finally: Thank you, Zara. For the all the love and laughter, all the trust and passion. For being my best friend and bringing out the best in me. For the dreams we share and surprising me each day. For being the laughing, smart, beautiful explorer you are.



# Resumo

Apesar de um formalismo geral e poderoso para testar e impor limites experimentais a teorias da gravitação no regime de campo fraco e de baixas velocidades já existir há várias décadas (o formalismo parametrizado pós-Newtoniano), um formalismo experimental e teórico análogo para testar o regime de campos gravíticos fortes e curvaturas espaço-temporais elevadas ainda se encontra em desenvolvimento. Esta dissertação centra-se em investigações recentes com vista a testar a *hipótese de buraco negro de Kerr*, uma das mais notáveis previsões da Teoria da Relatividade Geral de Einstein. Esta hipótese afirma que todos os buracos negros astrofísicos isolados são descritos pela solução de Kerr, sendo deste modo inteiramente definidos por apenas dois parâmetros: a sua massa e o seu momento angular. Descrevem-se propriedades relevantes da solução de Kerr e dos espaços-tempos estacionários, axialmente simétricos e assintoticamente planos, assim como as duas principais linhas experimentais e observacionais: a detecção de ondas gravitacionais e observações no espectro electromagnético. São apresentadas algumas das abordagens específicas, com ênfase em EMRI's (*Extreme Mass-Ratio Inspiral*) e radiação quasinormal, e na modelação de discos de acreção através do método de *continuum fitting* e do método dos perfis das linhas de ferro relativisticamente alargadas. Discutimos e generalizamos espaços-tempos parametricamente deformados de Kerr, e estudamos a importância relativa dos parâmetros de diferentes ordens, assim como a possibilidade da sua correspondência a diversas soluções de buracos negros em teorias alternativas da gravitação.

**Palavras-Chave:** Buracos negros; Momentos multipolares em espaços-tempos curvos; Ondas gravitacionais; Discos de acreção.



# Abstract

While a general, powerful framework for testing and constraining gravity theories in the weak field, slow-moving regime exists for several decades (the parametrized post-Newtonian formalism), an analogous experimental and theoretical framework to test the strong-field and strong-curvature regime of gravity is still being developed. This thesis focuses on recent work to test the *Kerr black hole hypothesis*, one of the most remarkable strong-field predictions of Einstein's General Theory of Relativity. This hypothesis states that all astrophysical black holes in isolation are described by the Kerr solution, and therefore completely defined by just two parameters: their mass and angular momentum. Relevant properties of the Kerr solution and of general stationary axisymmetric asymptotically flat vacuum spacetimes are described, as well as the two main avenues to test strong-field gravity: gravitational-wave detection and electromagnetic observations. Specific approaches are presented, with focus on extreme mass-ratio inspirals, quasinormal ringdown and on accretion disc modelling by relativistically broadened iron line profiles and by the continuum fitting method. We discuss and extend parametrically deformed Kerr spacetimes, and study the relative importance of different order parameters, as well as the possibility of its matching to rotating black hole solutions in alternative theories of gravity.

**Keywords:** Black holes; Multipole moments in curved spacetimes; Gravitational waves; Accretion discs.



This work was supported by Fundação para a Ciência e Tecnologia, under the grant PTDC/FIS/098025/2008. The research included in this thesis was carried out at Centro Multidisciplinar de Astrofísica (CENTRA) in the Physics Department of Instituto Superior Técnico.



# Contents

Acknowledgements . . . . .	iii
Resumo . . . . .	v
Abstract . . . . .	vii
<b>Contents</b>	<b>xii</b>
<b>List of Tables</b>	<b>xiii</b>
<b>List of Figures</b>	<b>xv</b>
<b>1 Introduction</b>	<b>1</b>
1.1 Outline . . . . .	3
<b>2 The Kerr black hole hypothesis</b>	<b>4</b>
2.1 The Kerr spacetime and uniqueness theorems . . . . .	4
2.2 Stationary, axisymmetric, asymptotically flat, vacuum spacetimes . . . . .	7
2.2.1 The Ernst equation . . . . .	10
2.2.2 Geroch-Hansen multipole moments for axisymmetric spacetimes . . . . .	12
<b>3 Observational routes: the gravitational and the electromagnetic spectrum</b>	<b>15</b>
3.1 Extreme mass-ratio inspirals (EMRIs) . . . . .	15
3.2 Quasinormal ringdown . . . . .	21
3.3 Accretion disc emission . . . . .	22
3.4 Other electromagnetic spectrum tests . . . . .	27
<b>4 Non-Kerr spacetimes</b>	<b>28</b>
4.1 Bumpy black holes . . . . .	28
4.1.1 Bumpy black holes . . . . .	28
4.1.2 Quasi-Kerr spacetimes . . . . .	34
4.1.3 Bumpy black holes in alternative theories . . . . .	37
4.2 Manko-Novikov spacetimes . . . . .	39
4.3 Johannsen-Psaltis spacetimes . . . . .	45
4.3.1 Dependence on higher order parameters . . . . .	49
4.3.2 A generalization of the Johannsen-Psaltis metric . . . . .	51

4.3.3 Non-matching to alternative theories . . . . .	52
<b>5 Conclusions</b>	<b>55</b>
<b>A The Newman-Janis algorithm</b>	<b>57</b>
<b>Bibliography</b>	<b>67</b>

# List of Tables

3.1	EMRI event rates for different NGO and LISA configurations. . . . .	16
3.2	PPE parameters for some alternative theories of gravity. . . . .	20
4.1	Changes to the Geroch-Hansen multipole moments of bumpy black holes. . . . .	34
4.2	Inner accretion disc edges and Killing horizon topology for the Johannsen-Psaltis spacetime. . . . .	46



# List of Figures

2.1	Kerr values of $r_{ISCO}$ , $r_{photon}$ , $r_{bound}$ . . . . .	10
3.1	Surface of section of the outer region for the Manko-Novikov spacetime; rotation number as a function of the radius $\rho$ . . . . .	21
3.2	Ringdown efficiency for detection of the fundamental model as a function of the mass $M$ ; Comparative SNRs for EMRI inspiral and ringdown of an equal-mass, non-spinning massive-black-hole binary. . . . .	23
3.3	Ray-tracing geometry. . . . .	23
3.4	Iron line profiles dependence on different model parameters. . . . .	24
3.5	Continuum fitting method dependence on different model parameters. . . . .	26
4.1	Shifts to Schwarzschild black hole orbital frequencies due to an $l = 2$ bump. . . . .	35
4.2	Shifts to Kerr black hole orbital frequencies for an $l = 2$ bump. . . . .	35
4.3	Number of cycles $\mathcal{N}$ required to accumulate $\pi/2$ difference in periastron shifts for the quasi-Kerr spacetime. . . . .	36
4.4	Comparing quasi-Kerr and Kerr approximate hybrid waveforms. . . . .	37
4.5	Boundaries of the ergoregion and of the region with closed timelike curves for $a/M = 0.9$ . . . . .	43
4.6	The permissible regions of motion for the Manko-Novikov spacetime. . . . .	44
4.7	Poincaré maps of the outer and inner region in the Manko-Novikov spacetime. . . . .	44
4.8	ISCO type and location for the Johannsen-Psaltis spacetime. . . . .	47
4.9	Broad K iron line generated around a JP BH as a function of the parameters of the model; $\chi^2$ from the comparison of the broad K iron line generated around a Kerr BH and a JP BH. . . . .	48
4.10	Thermal spectrum of a thin disk around a JP BH as a function of the parameters of the model; $\chi^2$ from the comparison of thermal spectrum of a thin accretion disk around a Kerr BH and a JP BH. . . . .	49
4.11	ISCO radius, frequency and energy as a function of the parameters $\epsilon_3$ and $\epsilon_4$ for the JP metric . . . . .	50
4.12	Shifts to the ISCO frequencies in the JP and JP2 metrics, in the small parameter limit, as a function of the spin. . . . .	53



# Chapter 1

## Introduction

The concept of a black hole is centuries old. John Michell was the first to discuss, in 1783, the existence of objects so compact that not even light could escape its gravitational pull, having also discussed the possible detection of these dark stars by observations of binary systems [1]. In 1916, less than two months after Albert Einstein published the final equations of his General Theory of Relativity (GR), Karl Schwarzschild discovered their most simple non-trivial solution, which represents a static spherical black hole (although the modern, relativistic notion of a black hole would only be understood decades later). Rotating black holes remained elusive until Roy Kerr discovered one such exact solution, in 1963 [2]. At least as remarkable as the discovery of theoretical black hole solutions of Einstein's equations is the fact that our current understanding of stellar structure and evolution places as most likely their existence, by a formation process involving the gravitational collapse of large stars, from work that started already in 1930 by Subrahmanyan Chandrasekhar.

In the decade that followed the discovery of Kerr's solution, the work of many people revealed many of its special properties of integrability, separability and uniqueness. Specially important are the uniqueness (or no-hair) theorems that Israel, Hawking, Carter, Robinson and others [3–6] have proved (under different mathematical assumptions): *the unique end-state of gravitational collapse in a stationary, axisymmetric, rotating, asymptotically flat, vacuum spacetime, if we require that there be no closed timelike curves and that singularities are always hidden behind an event horizon, is the Kerr metric.* Except for very short transient periods such as mergers, black holes in the universe are expected to satisfy the conditions of the theorem above to a very high degree of precision, and all astrophysical black holes are thought to be described solely by the Kerr solution and its two parameters, in what has been called the *Kerr Black Hole Hypothesis*. In Chandrasekhar's often-quoted words:

"Kerr's solution has also surpassing theoretical interest: it has many properties that have the aura of the miraculous about them. These properties are revealed when one considers the problem of the reflection and transmission of waves of different sorts (electromagnetic, gravitational, neutrino, and electron waves) by the Kerr black hole. [...]"

What, may we inquire, are these properties? In many ways, the most striking feature is the separability of all the standard equations of mathematical physics in Kerr geometry." [7]

"In my entire scientific life, extending over forty-five years, the most shattering experience has been the realization that an exact solution of Einstein's equations of general relativity, discovered by the New Zealand mathematician, Roy Kerr, provides the absolutely exact representation of untold numbers of massive black holes that populate the universe." [8]

General relativity has passed all experimental tests so far: from the classical tests of Mercury's perihelion precession, light's deflection by the Sun and light's gravitational redshift to binary pulsar systems, among others. However even these latter do not probe the regime of strong gravity. Taking  $M$ ,  $R$  and  $v/c$  as a system's characteristic mass, length and velocity, respectively, one can characterize the strength of the gravitational field [9, 10] by its dimensionless compactness  $C = \frac{GM}{Rc^2}$  and spacetime curvature  $\xi = \frac{GM}{R^3c^2}$ , where  $G$  is Newton's constant and  $c$  the speed of light in vacuum. For a body orbiting the surface of the Sun or for a binary pulsar system  $C \sim 10^{-6}$ ,  $v/c \sim 10^{-3}$  and  $\xi \sim 10^{-28} \text{cm}^{-2}$ , while on the surface of a neutron star or event horizon of a stellar mass black hole one has  $C \sim 0.1 - 1$  and  $\xi \sim 10^{-13} \text{cm}^{-2}$ , and  $v/c \sim 0.4$  prior to merger.

While Einstein's Equivalence Principle, tested at least at the level of 1 part in  $10^{13}$  [11], makes life very hard for non-metric theories of gravity [12], dozens of alternative metric theories have since been proposed - even as late back as Gunnar Nordström's in 1913. Most of these are by now ruled out by Solar System experiments, binary pulsars systems and the Parametrized Post Newtonian (PPN) framework [13], but many alternative theories that include GR as a special case remain only constrained, and do predict qualitative and quantitative differences from GR in the strong field regime.

So far however no general consistent framework to test strong field gravity has been developed, and current approaches have been divided in two kinds [14]: a top-down and bottom-up approach. In the top-down case, one modifies and parametrizes the action, and studies how these deviations can be constrained by observations (something which can involve tremendous amount of work for one single alternative theory). In the bottom-up approach one adopts a phenomenological parametrization of the observations and spacetime geometry and infers how these should modify the underlying theory, while aiming for generic tests of gravity theories such as those of Lorentz and parity violation, variable  $G$  and massive graviton, and polarization modes of gravitational waves [10, 15].

On the experimental side, the next decades promise a second golden age of general relativity. The first detection of gravitational waves is around the corner, and will potentially be achieved in the next 5-10 years with the LIGO/VIRGO Earth-based detectors [16]; in parallel, the space-based detector LISA (to launch perhaps before 2030) will open the field of millihertz gravitational wave astronomy. In the last few years, X-ray observations of accretions discs already provided measurements of the spin of stellar mass and supermassive black holes (e.g., [17-19]), to name one example of strong field phenomena that increasingly accurate observations in the electromagnetic spectrum have the potential to deliver.

In this thesis I review recent work and standard tools in different approaches to test the Kerr black hole hypothesis, with emphasis on how to quantify and experimentally measure deviations from the Kerr geometry, focusing on several specific metrics that deviate parametrically from Kerr and, on the experimental side, on measurements of the spin of astrophysical black holes through continuum fitting and iron line profiles methods, and on extreme mass ratio inspirals. I follow closely some of the original

references on several instances. Geometrized units are used unless otherwise stated, that is, the speed of light  $c$  and the gravitational constant  $G$  are equal to one.

## 1.1 Outline

In chapter 2, the main properties of the Kerr spacetime are described, as well as those of a general stationary axisymmetric asymptotically flat vacuum spacetime, including a discussion of the Ernst equation and relativistic multipole moments, in what is mostly textbook material [20, 21]. Gravitational waves and electromagnetic spectrum tests of the Kerr black hole hypothesis are presented in chapter 3, with focus on extreme mass ratio inspirals, quasinormal ringdown and on the continuum fitting and relativistically broadened iron lines profiles methods for accretion disks. In chapter 4, some specific spacetimes that parametrically deviate from the Kerr solution and recent studies of their properties and proposals for tests of the Kerr black hole hypothesis are reviewed: the different proposals within the original bumpy black hole formalism [22–24], the quasi-Kerr metric [25], the Manko-Novikov spacetime [26] and the metric put forward by Johannsen and Psaltis [27]. In the last subsections the relative importance of higher order parameters of the Johannsen-Psaltis metric is studied and, by constructing a generalization of this metric, the possibility of its matching to solutions in alternative theories of gravity is argued against.

# Chapter 2

## The Kerr black hole hypothesis

### 2.1 The Kerr spacetime and uniqueness theorems

The Kerr line element in Boyer-Lindquist coordinates takes the form

$$ds^2 = - \left( 1 - \frac{2Mr}{\Sigma} \right) dt^2 - \frac{4aMr \sin^2 \theta}{\Sigma} dt d\phi + \frac{\Sigma}{\Delta} dr^2 + \Sigma d\theta^2 + \left( r^2 + a^2 + \frac{2a^2 Mr \sin^2 \theta}{\Sigma} \right) d\phi^2, \quad (2.1)$$

where  $M$  is the mass of the black hole and  $J = aM$  is its angular momentum, and where

$$\Sigma = r^2 + a^2 \cos^2 \theta, \quad \Delta = r^2 - 2Mr + a^2. \quad (2.2)$$

For  $a = 0$  this is the Schwarzschild metric, and for  $M = 0$  it is Minkowski spacetime in oblate spheroidal coordinates. It is clear that in Boyer-Lindquist coordinates the Kerr metric is singular for  $\Sigma = 0$  or  $\Delta = 0$ . The former case corresponds to a true singularity since the curvature invariant  $R_{abcd}R^{abcd}$  is infinite there. The latter case has two roots,

$$r_{\pm} = M \pm \sqrt{M^2 - a^2}, \quad (2.3)$$

both coordinate singularities, at which every curvature invariant is finite. The surfaces  $r = r_+$  and  $r = r_-$  define the outer and inner event horizon, respectively.

An important feature of the Kerr black hole, which is absent in the non-rotating case, is the existence of an ergosphere: the region between the outer event horizon and the stationary limit surface (which corresponds to the surface  $r = M + \sqrt{M^2 - a^2 \cos^2 \theta}$  in the Kerr case). By definition, inside this region the asymptotic time translation Killing vector becomes spacelike, that is,  $\xi_{(t)}^2 = g_{tt} > 0$ , requiring a stationary observer to move faster than light. In the Kerr spacetime, the stationary limit surface is also the infinite redshift surface since

$$1 + z \equiv \frac{\lambda_{\infty}}{\lambda_r} = \frac{dt}{d\tau} = \frac{1}{\sqrt{g_{tt}}}, \quad (2.4)$$

where  $z$  is the redshift factor,  $\lambda_r$  is the wavelength of the radiation emitted at  $r$ ,  $\lambda_{\infty}$  the wavelength received at infinity and  $\tau$  the local time of an observer at  $r$ . As first pointed out by Penrose in 1969

[28], the existence of an ergosphere provides a way to extract energy from a rotating black by sending a test particle to the ergosphere where it is then split in two particles: one with positive energy which escapes the black hole and one with negative energy absorbed by the black hole, therefore decreasing its energy. Superradiance is an analogous effect for waves [29]: when reaching a black hole part of the wave is absorbed and part is reflected, and in some cases the absorbed wave carries negative energy while the reflected wave is amplified. For a wave of the form  $\phi = \text{Re} \{ \phi_0(r, \theta) e^{-i\omega t} e^{-im\phi} \}$  this happens when  $0 < \omega < m\Omega_H$ , where  $\Omega_H = \frac{a}{r_+^2 + a^2}$  is the angular velocity of the outer horizon. In the presence of an effective “mirror”, such as the one provided by the timelike boundary in AdS spacetime or the potential of a massive bosonic field, this amplification could lead to a black hole bomb [30, 31].

The Kerr solution is a stationary and axisymmetric spacetime, possessing two Killing vectors  $\xi_{(t)}^a$  and  $\xi_{(\phi)}^a$  which respectively provide the conservation of energy,  $E$ , and axial angular momentum,  $L_z$ , for orbiting test particles, as described in the following section. A crucial property of the Kerr metric is the existence of an additional constant of motion, discovered by Carter [32] through the separability of the Hamilton-Jacobi equation. The existence of Carter’s constant makes the equations of motion completely integrable in Kerr spacetime and its solution can be written in action-angle variables, triperiodic in the frequencies  $\Omega_r$ ,  $\Omega_\theta$  and  $\Omega_\phi$  [33]. Walker and Penrose [34] showed that Carter’s constant,  $K$ , is quadratic in the particle momenta and related to a Killing tensor  $K^{ab}$  via  $K = K^{ab} p_a p_b$ . This Killing tensor can in turn be written [35] in terms of a Killing-Yano tensor  $f_{ab}$  through  $K_{ab} = f_{ac} f_b^c$ . A Killing-Yano is an  $n$ -rank anti-symmetric tensor that satisfies  $\nabla_{(a_1} f_{a_2) a_3 \dots a_{n+1}} = 0$ . Every Killing-Yano tensor  $f_{a_1 \dots a_n}$  defines a Killing tensor  $K_{ab}$  via  $K_{ab} = f_{aa_2 \dots a_n} f_b^{a_2 \dots a_n}$ , although the reverse is not true. The Kerr Killing-Yano tensor also generates its Killing vectors [36] via  $\xi_{(t)}^a = \frac{1}{3} \nabla_b (*f)^{ba}$  and  $\xi_{(\phi)}^a = -K^a_b \xi_{(t)}^b$ , where  $*$  is the Hodge dual. Carter [37] has also shown that the Killing-Yano tensor is derivable from a Killing-Yano potential basis form  $\mathbf{b}$ , as  $\mathbf{f} = *d\mathbf{b}$ . The Petrov type D of the spacetime, which accounts for Kerr’s separability properties, was shown by Collinson [38] to be implied from the existence of the Killing-Yano 2-tensor.

A series of papers between 1967 and 1975 led to the following uniqueness theorem [39]: *Let  $(M, g)$  be a good vacuum spacetime with a non-empty black hole region and with a Killing vector field which is timelike in the asymptotic regions. Then  $(M, g)$  is diffeomorphically isometric to a Kerr spacetime.* Also known as ‘no-hair theorem’ or ‘no-hair conjecture’ (a term coined by John Wheeler, “the hair being anything that might stick out of the hole to reveal the details of the star from which it was formed” [40]), this result has been proved under different mathematical assumptions and definitions of “good spacetime”. Currently the three main gaps in its proof are [41] the assumption of analyticity of the spacetime and of the non-degeneracy of the horizon, and the possibility of multi-component solutions (for 5 dimensions, for example, the black Saturn solutions [42] provide a two-component counter-example to the conjecture). These three assumptions (analyticity, non-degeneracy and connectedness) are thought to be spurious but such a proof for the general case has not yet been achieved. We describe the main original results for the vacuum case, with no description of the specific mathematical assumptions. Hawking [5] proved that the event horizon of any stationary black hole has spherical topology, and that the event horizon is a Killing horizon which is static or axially symmetric. Here the proof splits in two, and the static case was

actually the first part of the uniqueness theorems to be proved: in 1967 Israel [3] showed that any static black hole with a spherical topology event horizon necessarily is the Schwarzschild solution. (This then is a converse to Birkhoff's theorem: that the exterior vacuum solution of any spherically symmetric spacetime is necessarily static and described by the Schwarzschild solution.) Carter [6] used Ernst's formulation of Einstein's equations [43] to show that all stationary axisymmetric black holes with a spherical topology event horizon are described by disjoint families of solutions not deformable into each other and uniquely determined by only two parameters: the mass and angular momentum. That the Kerr family is the unique such solution was shown by Robinson [4] in 1975.

The Kerr-Newman solution [?] is a generalization to the case of a charged black hole and has also been found to be the unique stationary asymptotically flat electro-vacuum black hole [44, 45] but although uniqueness theorems for the Einstein-Maxwell system stand on similar ground to the vacuum case, generalized uniqueness theorems for other systems such as the Yang-Mills equations or dilatonic fields, or for higher dimensional black holes, were already found to be violated and several specific counter-examples have been constructed [41].

The uniqueness theorem stated above is specially important since the dark compact objects we observe in the Universe probably satisfy its conditions, that is, they are stationary asymptotically-flat vacuum black holes to a high degree of precision. The theoretical work behind why such hypothesis is accepted today goes back to Chandrasekhar [46], and Oppenheimer and Volkoff [47] in the 1930s. However it wasn't until decades later that significant breakthrough occurred, with Penrose's introduction of the concept of a *trapped surface* [48]. Hawking and Penrose proved the well-known *singularity theorems* [49], which state that when a trapped surface forms the appearance of spacetimes singularities inside it is inevitable. That given sufficient matter compactification a trapped surface must form was proved by Schoen and Yau [50]. The unphysical nature of spacetime singularities lead Roger Penrose to conjecture that naked singularities do not exist, that is, that all singularities should be hidden behind an event horizon. This is known as the Cosmic Censorship Hypothesis and is one of the most important unsolved problems in General Relativity [28, 51, 52]. Finally, several studies have indicated that charged black holes very likely become uncharged by neutralizing with the surrounding plasma [53, 54] and that non-stationary black holes very quickly radiate away any bumps and enter an equilibrium state [55].

Assuming General Relativity to be valid, one can therefore expect that all isolated astrophysical black holes are described by the Kerr solution, in what has been called the *Kerr black hole hypothesis*. Of course, extreme phenomena such as collisions and mergers of black holes and other compact objects are excluded in such considerations, but after the merger the black hole is believed to very quickly radiate perturbations away and enter a stationary state. The hypothesis applies to black holes in accretion discs as well since the mass of the disc is estimated to be smaller than that of the black hole by several orders of magnitude.

## 2.2 Stationary, axisymmetric, asymptotically flat, vacuum spacetimes

In the absence of a general model-independent framework to test strong-field gravity, a recurring approach has been to take the simplifying assumption that the astrophysical system under study is, to a high degree of precision, a stationary, axisymmetric, asymptotically flat and vacuum spacetime.

Within general relativity, the most general stationary axisymmetric vacuum solution is the Lewis-Papapetrou metric [56], which can be written in the form

$$ds^2 = -e^{2\psi}(dt - \omega d\phi)^2 + e^{-2\psi}[\rho^2 d\phi^2 + e^{2\gamma}(d\rho^2 + dz^2)] \quad (2.5)$$

where  $\psi$ ,  $\gamma$  and  $\omega$  are functions of only  $\rho$  and  $z$ .

In the Hamiltonian approach, the second order geodesic equations are written as first order differential equations as

$$\dot{q}^\mu = \frac{\partial H}{\partial p_\mu}, \quad \dot{p}_\mu = -\frac{\partial H}{\partial x^\mu} \quad (2.6)$$

where the  $H = \frac{1}{2}g^{\mu\nu}p_\mu p_\nu$  is the Hamiltonian,  $q^\mu = (t, r, \theta, \phi)$  and  $p_\mu = (p_t, p_r, p_\theta, p_\phi)$  are the generalized coordinates and momenta respectively, and the dot represents differentiation with respect to the proper time  $\tau$ . Liouville's theorem on integrable systems states that in a Hamiltonian system with a  $2n$ -dimensional phase space, if  $n$  independent first integrals in involution are known, then the system is integrable by quadratures. Two functions  $F(q, p)$  and  $G(q, p)$  of the canonical variables are said to be in involution if  $\{F, G\} = 0$ , that is, if their the Poisson bracket  $\{F, G\} \equiv \sum_{k=1}^n \left( \frac{\partial F}{\partial q^k} \frac{\partial G}{\partial p_k} - \frac{\partial F}{\partial p_k} \frac{\partial G}{\partial q^k} \right)$  is zero. A first integral is a function  $F(q, p)$  which is in involution with the Hamiltonian, that is,  $\{F, H\} = 0$ . The Hamiltonian itself is a first integral, and because the metric (2.5) does not depend on  $t$  and  $\phi$  it is clear that  $p_t$  and  $p_\phi$  are also first integrals of the motion. On a stationary, axisymmetric vacuum spacetime one therefore always has at least three constants of motion: the mass of the test particle  $m^2 = -2H$ , its energy  $E = -p_t$  and axial angular momentum  $L_z = p_\phi$ . In the search for a fourth integral of motion, if one chooses to look for a constant of the form  $K = K^{\mu_1 \dots \mu_n} p_{\mu_1} \dots p_{\mu_n}$ , then  $K^{\mu_1 \dots \mu_n}$  is necessarily a Killing tensor. Carter's constant is of this kind and, in Boyer-Lindquist coordinates, it is written as

$$K = K^{\mu\nu} p_\mu p_\nu = m^2 a^2 \cos^2 \theta + p_\theta^2 + \left( \frac{p_\theta}{\sin \theta} \right)^2. \quad (2.7)$$

Whether there exist other stationary axisymmetric vacuum spacetimes which also possess a (generalized) Carter's constant is a relevant unsolved problem for gravitational wave astronomy, in particular, for gravitational wave templates for EMRI's [24, 57, 58]. The more general problem of integrability and its relation to separability and Killing tensors in Riemannian manifolds and general relativity has also been studied by several authors, e.g. [59, 60].

In part for the simplicity it affords, circular and equatorial (or nearly circular and nearly equatorial) geodesic motion in stationary axisymmetric vacuum spacetimes has been recurrently studied, from accretion discs to extreme mass ratio inspirals. Given an axisymmetric stationary asymptotically flat

spacetime with metric of the form

$$ds^2 = g_{tt}dt^2 + 2g_{t\phi}dtd\phi + g_{rr}dr^2 + g_{\theta\theta}d\theta^2 + g_{\phi\phi}d\phi^2, \quad (2.8)$$

where the metric functions are independent of  $t$  and  $\phi$ , one can write the conserved specific energy  $E$  and axial angular momentum  $L_z$  of the test particle as

$$E = -g_{tt}\dot{t} - g_{t\phi}\dot{\phi}, \quad L_z = g_{t\phi}\dot{t} + g_{\phi\phi}\dot{\phi}, \quad (2.9)$$

which can be inverted to

$$\dot{t} = \frac{g_{\phi\phi}E + g_{t\phi}L}{g_{t\phi}^2 - g_{tt}g_{\phi\phi}}, \quad \dot{\phi} = -\frac{g_{t\phi}E + g_{tt}L}{g_{t\phi}^2 - g_{tt}g_{\phi\phi}}. \quad (2.10)$$

Substituting the two equations in  $g_{\mu\nu}\dot{x}^\mu\dot{x}^\nu = -1$ , one obtains

$$g_{rr}\dot{r}^2 + g_{\theta\theta}\dot{\theta}^2 = V_{\text{eff}}(E, L, r, \theta), \quad (2.11)$$

where the effective potential is given by

$$V_{\text{eff}}(E, L, r, \theta) = \frac{g_{\phi\phi}E^2 + 2g_{t\phi}EL + g_{tt}L^2}{g_{t\phi}^2 - g_{tt}g_{\phi\phi}} - 1. \quad (2.12)$$

If one uses the Papapetrou metric of equation (2.5), then (2.11) can be reduced to

$$e^{-2(\phi+\gamma)}(\dot{\rho}^2 + \dot{z}^2) = V_{\text{eff}}(E, L_z, \rho, z). \quad (2.13)$$

Since the left side of the equation is non-negative, motion is only allowed in regions where  $V_{\text{eff}} \geq 0$ .

The geodesic equation can be written in the form

$$\frac{d}{d\tau} \left( g_{\mu\alpha} \frac{dx^\alpha}{d\tau} \right) = \frac{1}{2} \partial_\mu g_{\alpha\beta} \frac{dx^\alpha}{d\tau} \frac{dx^\beta}{d\tau}, \quad (2.14)$$

and, for a circular equatorial orbit, its  $r$ -component yields

$$\dot{\phi}^2 \partial_r g_{\phi\phi} + 2\dot{\phi}\dot{t} \partial_r g_{t\phi} + \dot{t}^2 \partial_r g_{tt} = 0. \quad (2.15)$$

Solving this equation for the azimuthal frequency  $\Omega_\phi \equiv d\phi/d\tau = \dot{\phi}/\dot{t}$ , one obtains

$$\Omega_\phi = \frac{-\partial_r g_{t\phi} \pm \sqrt{(\partial_r g_{t\phi})^2 - \partial_r g_{tt} \partial_r g_{\phi\phi}}}{\partial_r g_{\phi\phi}}, \quad (2.16)$$

where the upper (lower) sign is for prograde (retrograde) orbits. From  $g_{\mu\nu}\dot{x}^\mu\dot{x}^\nu = -1$ , one obtains  $\dot{t} = (-g_{tt} - 2\Omega_\phi g_{t\phi} - \Omega_\phi^2 g_{\phi\phi})^{-1/2}$  from which one finds the expressions for the energy and angular

momentum of a test particle in a circular equatorial orbit:

$$E = -\frac{g_{tt} + g_{t\phi}\Omega_\phi}{\sqrt{-g_{tt} - 2g_{t\phi}\Omega_\phi - g_{\phi\phi}\Omega_\phi^2}}, \quad L = \frac{g_{t\phi} + g_{\phi\phi}\Omega_\phi}{\sqrt{-g_{tt} - 2g_{t\phi}\Omega_\phi - g_{\phi\phi}\Omega_\phi^2}}. \quad (2.17)$$

The radial and vertical oscillation frequencies for nearly circular and nearly equatorial orbits can be obtained if one considers equation (2.11) for constant angle  $\theta$  and constant radius  $r$  [61], respectively:

$$\left(\frac{dr}{dt}\right)^2 = \frac{2V_{\text{eff}}}{g_{rr}t^2}, \quad \left(\frac{d\theta}{dt}\right)^2 = \frac{2V_{\text{eff}}}{g_{\theta\theta}t^2}. \quad (2.18)$$

and by writing  $r = r_0 + \delta r$  and  $\theta = \pi/2 + \delta\theta$ . Taking the coordinate time derivative leads to the equations:

$$\frac{d^2(\delta r)}{dt^2} + \Omega_r^2 \delta r = 0, \quad \frac{d^2(\delta\theta)}{dt^2} + \Omega_\theta^2 \delta\theta = 0, \quad (2.19)$$

where

$$\Omega_r^2 = -\frac{1}{2g_{rr}t^2} \frac{\partial^2 V_{\text{eff}}}{\partial r^2}, \quad \Omega_\theta^2 = -\frac{1}{2g_{\theta\theta}t^2} \frac{\partial^2 V_{\text{eff}}}{\partial \theta^2}. \quad (2.20)$$

If one is using cylindrical coordinates,  $\theta$  can be replaced by  $z$  in the equations above.

Stable circular equatorial orbits satisfy the conditions  $\partial_r^2 V_{\text{eff}} \leq 0$  and  $\partial_\theta^2 V_{\text{eff}} \leq 0$ , so that  $\Omega_r^2 \geq 0$  and  $\Omega_\theta^2 \geq 0$ . If one of these is not satisfied, say the radial condition, then a small perturbation in the radial direction to a circular orbit would lead the particle to follow an entirely different orbit, and one therefore says the orbit is radially unstable (or vertically unstable, in the other case). Although for the Kerr spacetime the vertical condition is satisfied at any radius, it is not necessarily so in other spacetimes where vertical instabilities can exist besides radial ones. In the Kerr case, for each value of the spin, there is a value  $r \equiv r_{\text{ISCO}}$  (the Innermost Stable Circular Orbit) for which all inner orbits are radially unstable and all outer are radially stable. In non-Kerr spacetimes, the situation may be different and there may be disconnected intervals of  $r$  which verify both stability conditions.

For the Kerr metric, in Boyer-Lindquist coordinates, the expressions for the energy and angular momentum for circular equatorial orbits take the form [62]

$$E = \frac{r^2 - 2Mr \pm a\sqrt{Mr}}{r(r^2 - 3Mr \pm 2a\sqrt{Mr})^{1/2}}, \quad L = \frac{\sqrt{Mr}(r^2 \mp 2a\sqrt{Mr} + a^2)}{r(r^2 - 3Mr \pm 2a\sqrt{Mr})^{1/2}} \quad (2.21)$$

and the Keplerian frequency is given by

$$\Omega_\phi = \pm \frac{M^{1/2}}{r^{3/2} \pm aM^{1/2}}, \quad (2.22)$$

where the upper (lower) sign is for prograde (retrograde) orbits. The oscillation frequencies are given by

$$\Omega_r^2 = \frac{M(r^2 - 6Mr \pm 8a\sqrt{Mr} - 3a^2)}{r^2(r^{3/2} \pm a\sqrt{M})^2}, \quad \Omega_\theta^2 = \frac{M(r^2 \mp 4a\sqrt{Mr} + 3a^2)}{r^2(r^{3/2} \pm a\sqrt{M})^2}. \quad (2.23)$$

As shown in figure 2.1, the radius of the innermost stable circular orbit for Kerr is a monotonic

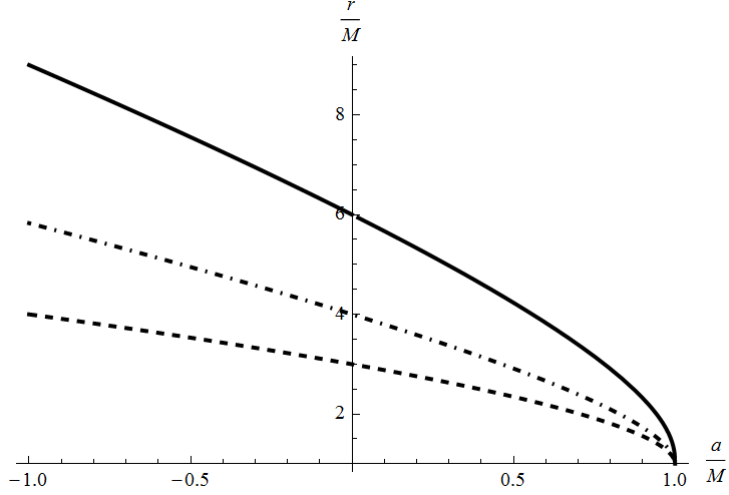


Figure 2.1: Kerr values of  $r_{ISCO}$  (solid), of the innermost circular photon orbit  $r_{\text{photon}} = 2M \left[1 + \cos\left(\frac{2}{3} \cos^{-1}(\mp a/M)\right)\right]$  (dashed), and the marginally bound orbit  $r_{\text{bound}} = 2M \pm a + 2\sqrt{M^2 \pm aM}$  (dot-dashed) [62].

function of the spin (a crucial fact in black hole spin measurements, see section 3.3) and is given by

$$r_{ISCO} = M \left\{ 3 + Z_2 \mp [(3 - Z_1)(3 + Z_1 + 2Z_2)]^{1/2} \right\}, \quad (2.24)$$

where

$$Z_1 = 1 + \left(1 - \frac{a^2}{M^2}\right)^{1/3} \left[ \left(1 + \frac{a}{M}\right)^{1/3} + \left(1 - \frac{a}{M}\right)^{1/3} \right], \quad Z_2 = \left(3 \frac{a^2}{M^2} + Z_1^2\right)^{1/2}. \quad (2.25)$$

### 2.2.1 The Ernst equation

The problem of finding and studying stationary axisymmetric vacuum solutions in General Relativity was greatly simplified by Ernst's discovery [43, 63, 64] that the Einstein equations reduce to a single complex equation in this case.

From Einstein's equations and the Lewis-Papapetrou metric (equation (2.5)) one can obtain the field equations:

$$\nabla^2 \psi + \frac{1}{2} \rho^{-2} e^{4\psi} (\vec{\nabla} \omega)^2 = 0 \quad (2.26)$$

$$\vec{\nabla} \cdot (\rho^{-2} e^{4\psi} \vec{\nabla} \omega) = 0 \quad (2.27)$$

Because equation (2.27) can be regarded as the integrability condition of the following two equations:

$$\rho^{-1} e^{4\psi} \frac{\partial \omega}{\partial z} = \frac{\partial \chi}{\partial \rho} \quad (2.28)$$

$$\rho^{-1} e^{4\psi} \frac{\partial \omega}{\partial \rho} = -\frac{\partial \chi}{\partial z}, \quad (2.29)$$

substituting  $\nabla\omega$  for  $\nabla\chi$ , equation (2.26) can be rewritten, as

$$e^{4\psi}\nabla^2\psi + \frac{1}{2}(\vec{\nabla}\chi)^2 = 0. \quad (2.30)$$

Defining  $F \equiv e^{2\psi}$ , the previous equation can be written as

$$F\nabla^2F = (\vec{\nabla}F)^2 - (\vec{\nabla}\chi)^2. \quad (2.31)$$

The integrability condition for  $\vec{\nabla}\chi$  is

$$\vec{\nabla} \cdot (F^{-2}\vec{\nabla}\chi) = 0. \quad (2.32)$$

Defining the Ernst potential  $\mathcal{E}$  as

$$\mathcal{E} \equiv F + i\chi, \quad (2.33)$$

equations (2.31) and (2.32) can be written as a single complex equation known as the Ernst equation

$$(\text{Re}\mathcal{E})\nabla^2\mathcal{E} = \vec{\nabla}\mathcal{E} \cdot \vec{\nabla}\mathcal{E}. \quad (2.34)$$

A usual alternative form of the Ernst equation is

$$(\xi\xi^* - 1)\vec{\nabla}^2\xi = 2\xi^*(\vec{\nabla}\xi) \cdot (\vec{\nabla}\xi), \quad (2.35)$$

with the new potential defined as

$$\mathcal{E} = \frac{\xi - 1}{\xi + 1}. \quad (2.36)$$

Ernst also found a generalization of this equation for the case of the Einstein-Maxwell equations [63] and both formulations brought an important development to finding new exact solutions [65], an example of which is the Manko-Novikov family of solutions, a generalization of the Kerr-Newman spacetime with an infinite number of parameters, described in section 4.2. The usefulness of these formulations includes its use in the proofs of the black hole uniqueness theorems [6] and in deriving easier methods to compute relativistic multipole moments for electrovacuum spacetimes, such as the one devised by Fodor, Hoenselaers and Perjés [66–68] and used by Ryan in mapping the spacetime geometry during an extreme mass-ratio inspiral [69, 70] (see section 3.1).

Given the Ernst potential  $\mathcal{E}$ , one can obtain the metric functions  $\psi$ ,  $\omega$  and  $\gamma$ , via

$$g_{tt} = -e^{2\psi} = -F = -i\chi - \mathcal{E}, \quad g_{t\phi} = F\omega = F \int_{\rho}^{\infty} d\rho' \frac{\rho'}{F^2} \left( \frac{\partial\chi}{\partial z} \right) \Big|_{z=\text{constant}} \quad (2.37)$$

and

$$\gamma = \frac{1}{4} \int_{\rho}^{\infty} d\rho' \left[ \frac{\rho'}{g_{tt}^2} \left( \frac{dg_{tt}}{d\rho'} \right)^2 - \frac{g_{tt}^2}{\rho'} \left( \frac{d(g_{t\phi}/g_{tt})}{d\rho'} \right)^2 \right]. \quad (2.38)$$

### 2.2.2 Geroch-Hansen multipole moments for axisymmetric spacetimes

Although multipole moment expansions are widely used in many areas of physics, in general relativity the tensorial nature of the fields and the non-linearity of the field equations makes it more difficult to work with and to generalize multipole moments. Despite these difficulties, multipole moment expansions can be very useful as, for example, they can provide a guide to the physical interpretation of the solutions of the field equations, and are a powerful tool in gravitational radiation studies.

The first invariant definition of spacetime multipole moments was given by Geroch [71] for the static asymptotically flat case and Hansen [72] later generalized it for the stationary case. The assumption of stationarity implies that there is a timelike Killing vector field  $\xi^a$  and one finds an analogue of the Euclidean space in Newtonian gravitation as the 3-manifold  $V$  of trajectories of this timelike Killing vector field, where one defines a field in terms of which the multipole moments are computed. The metric  $g_{ab}$  of the 4-manifold with signature  $(-, +, +, +)$  induces on  $V$  the positive definite metric

$$h_{ab} = \lambda g_{ab} + \xi_a \xi_b, \quad (2.39)$$

where  $\lambda = -\xi^a \xi_a$  is the norm of the Killing vector field. One defines its twist  $\omega_a$  by

$$\omega_a = \epsilon_{abcd} \xi^b \nabla^c \xi^d, \quad (2.40)$$

and from the Einstein vacuum equations one can define a scalar twist  $\omega$  by

$$\omega_a = \nabla_a \omega. \quad (2.41)$$

The fields  $\phi_M$  and  $\phi_J$ , analogues of the Newtonian mass and angular momentum potentials, are defined as

$$\phi_M = \frac{1}{4} \frac{\lambda^2 + \omega^2 - 1}{\lambda}, \quad \phi_J = \frac{1}{2} \frac{\omega}{\lambda}. \quad (2.42)$$

When  $\omega = 0$ , we have the static case.

The 3-manifold is asymptotically flat if there is a 3-manifold  $\tilde{V}$  with metric  $\tilde{h}_{ab}$  such that

1.  $\tilde{V} = V \cup \Lambda$ , where  $\Lambda$  is a single point,
2.  $\tilde{h}_{ab} = \Omega^2 h_{ab}$  is a smooth metric on  $\tilde{V}$ ,
3.  $\Omega|_\Lambda = 0$ ,  $\tilde{D}_a \Omega|_\Lambda = 0$ ,  $\tilde{D}_a \tilde{D}_b \Omega|_\Lambda = 2\tilde{h}_{ab}|_\Lambda$ ,

where  $\tilde{D}_a$  is the derivative operator associated with  $\tilde{h}_{ab}$ .

Having introduced  $V$  and its conformal compactification  $\tilde{V}$ , one defines the multipole moments of the fields  $\phi_M$  and  $\phi_J$ , and lets  $\phi$  denote either of them. Let  $\tilde{\phi} = \Omega^{-1/2} \phi = P$  and define recursively the sequence  $P, P_{a_1}, P_{a_1 a_2}, \dots$  of tensors:

$$P_{a_1 \dots a_n} = C \left[ \tilde{D}_{a_1} P_{a_2 \dots a_n} - \frac{(n-1)(2n-3)}{2} \tilde{R}_{a_1 a_2} P_{a_3 \dots a_n} \right], \quad (2.43)$$

where  $C[T_{a\dots b}]$  is the totally symmetric, trace-free part of  $T_{a\dots b}$ , and  $\tilde{R}_{ab}$  is the Ricci tensor of  $\tilde{V}$ . The multipole moments are defined as the tensors  $\{P_{a_1\dots a_n}(\Lambda)\}_{n=0}^\infty$ .

To define the multipole moments in a fully geometric way the freedom of choice associated with the coordinate origin still has to be eliminated. This can be achieved by choosing a conformal factor such that the dipole moment vanishes, which amounts to centering the system about a generalized center of mass. On the other hand, the potentials given by Hansen are not unique and there are different potentials that define the same multipole moments.

The computation of the multipole moments from its definition is quite involved, but Bäckdahl and Herberthson [73] have devised a method of calculation for stationary axisymmetric asymptotically flat spacetimes in which the multipole moments are given by the derivatives of a single scalar function evaluated at its origin (used by Vigeland [74] to calculate the Geroch-Hansen multipole moments of bumpy black spacetimes, see section 4.1.1).

Given an axisymmetric stationary asymptotically flat spacetime, this method requires finding the potential  $\phi = \phi_M + i\phi_J$  as defined in equation (2.42) (although other potentials will yield the exact same results as, for example, the Ernst potential  $\phi_E = (1 + \lambda - i\omega)/(1 + \lambda + i\omega)$ ) and the conformal factor  $\Omega$  of the conformal compactification of the metric of the 3-manifold of trajectories of the timelike Killing vector.

Starting from the Lewis-Papapetrou metric,

$$ds^2 = -e^{2\psi}(dt - \omega d\varphi)^2 + e^{-2\psi}[r^2 d\varphi^2 + e^{2\beta}(dr^2 + dz^2)] \quad (2.44)$$

this implies that the metric on  $V$  is

$$h_{ab} = \lambda g_{ab} + \xi_a \xi_b \sim r^2 d\varphi^2 + e^{2\beta}(dr^2 + dz^2). \quad (2.45)$$

Conformal compactification can be carried out by writing  $\Omega = R^2 e^{-\beta}$  and

$$\tilde{h}_{ab} = \Omega^2 h_{ab} \sim \tilde{\rho}^2 e^{-2\beta} d\varphi^2 + d\tilde{\rho}^2 + d\tilde{z}^2 = R^2 \sin^2 \theta e^{-2\beta} d\varphi^2 + dR^2 + R^2 d\theta^2 \quad (2.46)$$

where new variables  $\tilde{z}, \tilde{\rho}, R$  and  $\theta$  have been defined by  $\tilde{z} = R \cos \theta = \frac{z}{r^2 + z^2}$  and  $\tilde{\rho} = R \sin \theta = \frac{r}{r^2 + z^2}$ , and where  $R = 0$  corresponds to the point at infinity,  $\Lambda$ .

Then now one has the functions  $\phi = \phi(R, \theta)$ ,  $\beta = \beta(R, \theta)$  and  $\Omega = \Omega(R, \theta)$ , and defines a new function  $\tilde{\phi} = \Omega^{-1/2} \phi$ . The next step is to write these in the cylindrical coordinates  $\tilde{z}$  and  $\tilde{\rho}$  defined above as  $\tilde{\phi}(\tilde{z}, \tilde{\rho})$  and  $\tilde{\beta}(\tilde{z}, \tilde{\rho})$  and to define the functions

$$\tilde{\phi}_L(R) = \tilde{\phi}(R, iR), \quad (2.47)$$

$$\beta_L(R) = \beta(R, iR), \quad (2.48)$$

$$\kappa_L(R) = -\ln \left[ 1 - R \int_0^R \frac{e^{2\beta_L(R')} - 1}{R'^2} dR' - RC \right] + \beta_L(R), \quad (2.49)$$

where  $C$  is an integration constant which can be set to zero.

The multipole moments are given by the following formula

$$\mathcal{M}_l = \frac{2^l l!}{(2l)!} \frac{d^l y}{d\rho^l}, \quad (2.50)$$

where the  $y(R) = e^{-\kappa_L(R)/2} \tilde{\phi}_L(R)$  and  $\rho(R) = R e^{\kappa_L(R) - \beta_L(R)}$ .

Applying the method above to the Kerr metric gives the following relations

$$\mathcal{M}_l = M_l + iS_l = M(ia)^l, \quad (2.51)$$

where  $M_l$  and  $S_l$  are the mass and mass current multipole moments, respectively. This relation has been a key part in proposals to test the Kerr black hole hypothesis. Because setting the values of  $M$  and  $a$  locks those of all other multipole moments, having independent measurements of three different moments is enough to perform a null-hypothesis test. While the first multipole moment, the mass  $M$ , can be measured from Newtonian far-field observations, sufficiently accurate measurements of the other moments require either probing the central region extremely closely (as with accretion discs tests, see section 3.3) or very clean and long observations (such as EMRIs, see section 3.1).

## Chapter 3

# Observational routes: the gravitational and the electromagnetic spectrum

Lisa says, On a night like this  
It'd be so nice if you gave me one great big kiss  
And Lisa says, Honey, for just one little smile  
I'll sing and play with you for the longest while.

---

*Lisa Says*, Lou Reed

### 3.1 Extreme mass-ratio inspirals (EMRIs)

Extreme mass-ratio inspirals (EMRIs) are binary systems consisting of a compact stellar mass object, such as a black hole or neutron star, orbiting within astronomical units of the Schwarzschild radius of a supermassive object of  $\sim 10^4 - 10^7$  solar masses. By emission of gravitational waves, the stellar mass object slowly loses energy and inspirals to the central object taking several years and as much as several millions of orbits. The long duration of the inspiral serves as a microscope to the background geometry, and the extreme mass-ratio allows to treat the inspiral, as a first approximation, as a test particle adiabatically transiting from one geodesic to another in a time scale much larger than a single orbit.

Along with supermassive black hole coalescences and galactic binaries, EMRIs are the primary sources for future space-based gravitational wave observatories with LISA's mission design [75–77], consisting of 3 satellites separated by  $\sim 10^9$  meters and connected by 4 to 6 laser links, sensible to gravitational waves in the milli-Hertz range. Since NASA withdrew from LISA's joint program with ESA, a new European re-scaled project called eLISA/NGO (evolved LISA/New Gravitational wave Observatory) has been developed, with its first phase starting as early as 2015 with the launch of LISA Pathfinder. With less sensitivity than the original LISA design, NGO is believed to be able to answer most of the scientific

Detector	Black Hole Spin								
	$a = 0$			$a = 0.5$			$a = 0.9$		
	No. Events in $\mathcal{M}_1$	No. Events in $\mathcal{M}_2$	No. Events in $\mathcal{M}_3$	No. Events in $\mathcal{M}_1$	No. Events in $\mathcal{M}_2$	No. Events in $\mathcal{M}_3$	No. Events in $\mathcal{M}_1$	No. Events in $\mathcal{M}_2$	No. Events in $\mathcal{M}_3$
NGO	< 1	15	< 1	< 1	19	1	< 1	45	15
6-link NGO	2	35	< 1	2	57	3	2	70	35
2Gm NGO	5	45	2	2	55	5	3	95	45
4-link LISA	10	190	10	10	210	30	10	220	130
6-link LISA	40	280	20	30	290	50	30	300	160

Table 3.1: Estimates of the number of EMRI events for the mission duration of NGO and LISA (2 and 5 years, respectively) for different configurations.  $\mathcal{M}_1 \equiv 10^4 M_\odot < M < 10^5 M_\odot$ ,  $\mathcal{M}_2 \equiv 10^5 M_\odot < M < 10^6 M_\odot$ ,  $\mathcal{M}_3 \equiv 10^6 M_\odot < M$ . From Gair and Porter [78]. The estimated event rates for neutron stars and white dwarfs EMRIs are always less than 1% that of black hole EMRIs.

issues intended for LISA, including constraints on the Hubble constant and local slope of the black hole mass function [78], the main difference being the estimated event rates, as shown in Table 3.1 for different mission designs. These values of the event rates suffer from uncertainties of at least two orders of magnitude.

Based on a conjecture by Thorne, the first framework to test the Kerr black hole hypothesis using gravitational waves was introduced by Ryan in 1995 [69]. Thorne’s conjecture (which has evolved over time [79]) states that gravitational waves emitted during an EMRI or IMRI (Intermediate Mass-Ratio Inspiral) essentially encode all the information on the spacetime geometry of the central body, on the tidal coupling between the central and orbiting bodies, and on the evolving orbital elements (the semi-latus rectum  $p(t)$ , eccentricity  $e(t)$  and inclination angle  $\iota(t)$ ).

In essence, Ryan showed that for quasi-circular and quasi-equatorial orbits some observables can be written as a series expansion in the orbit’s evolving dimensionless parameter  $v \equiv (M\Omega_\phi)^{1/3} = (\pi Mf)^{1/3}$  (which is the inspiraling body’s linear velocity in the Newtonian limit), with coefficients given by different combinations of the Geroch-Hansen mass and current multipole moments  $M_l$  and  $S_l$ , in such a way that they could be extracted given enough precision in the measurements.

Ryan made several simplifying assumptions, namely that: (a) the spacetime is general-relativistic, vacuum, stationary, axisymmetric, reflection symmetric and asymptotically flat (so that one can define Geroch-Hansen multipole moments and the Ernst potential), (b) the inspiraling body can be described as a test particle whose orbit evolves adiabatically from one geodesic to another due to the emission of gravitational radiation, (c) the inspiraling object follows a quasi-circular and quasi-equatorial geodesic orbit, and (d) there is no tidal coupling, so that all energy lost by the orbit is emitted as gravitational waves.

Ryan considered the following observables: the precession frequencies  $\Omega_\phi - \Omega_z$  and  $\Omega_\phi - \Omega_\rho$ , the gravitational wave energy per logarithmic interval of frequency  $f = \Omega_\phi/\pi$  denoted by  $\Delta E(f)$ , and the number of gravitational wave cycles spent in a logarithmic interval of frequency,  $\Delta N(f)$ . The radial and vertical oscillations frequencies can be calculated from equations (2.20). The radial and vertical precession frequencies which modulate the gravitational wave are given by  $\Omega_\phi - \Omega_\rho$  and  $\Omega_\phi - \Omega_z$ , respectively, but for the rest of this section we follow instead Ryan’s notation and call the precession frequencies  $\Omega_\alpha$ , which

are then given by

$$\Omega_\alpha = \Omega_\phi - \left( -\frac{g^{\alpha\alpha}}{2} \left[ (g_{tt} + g_{t\phi}\Omega_\phi)^2 \left( \frac{g_{\phi\phi}}{\rho^2} \right)_{,\alpha\alpha} - 2(g_{tt} + g_{t\phi}\Omega_\phi)(g_{t\phi} + g_{\phi\phi}\Omega_\phi) \left( \frac{g_{t\phi}}{\rho^2} \right)_{,\alpha\alpha} + (g_{t\phi} + g_{\phi\phi}\Omega_\phi)^2 \left( \frac{g_{tt}}{\rho^2} \right)_{,\alpha\alpha} \right] \right)^{1/2}, \quad (3.1)$$

where  $\alpha$  stands for  $\rho$  and  $z$ .

Since there is no tidal coupling, the energy carried by the wave,  $dE_{\text{gw}}$ , is equal to the energy lost by the orbit,  $-dE$ , and the wave energy per logarithmic interval of frequency is given by

$$\Delta E \equiv \frac{dE_{\text{gw}}}{d(\ln f)} = -\Omega_\phi \frac{dE}{d\Omega_\phi}. \quad (3.2)$$

The number of gravitational wave cycles per logarithmic interval of frequency is given by

$$\Delta N(f) \equiv \frac{f^2}{df/dt} = \frac{\Delta E(f)}{dE_{\text{gw}}/dt}. \quad (3.3)$$

As described in section 2.2.1, given the Ernst potential  $\mathcal{E} = F + i\chi$  or  $\xi$ , given by

$$\mathcal{E} = \frac{\sqrt{\rho^2 + z^2} - \xi}{\sqrt{\rho^2 + z^2} + \xi}, \quad (3.4)$$

one can find all the metric functions  $F$ ,  $\omega$  and  $\gamma$  (equations (2.37) and (2.38)).

Essential in Ryan's scheme is a method devised by Fodor, Hoenselaers and Perjés [66] to compute the Geroch-Hansen multipole moments from the Ernst potential. They showed that the latter could be written as

$$\xi = \sum_{j,k=0}^{\infty} a_{jk} \frac{\rho^j z^k}{(\rho^2 + z^2)^{j+k}}, \quad (3.5)$$

where, through a recursive scheme which will not be described here,  $a_{jk}$  can be written as a function of the multipole moments  $M_l$  and  $S_l$ . One can therefore compute the metric and its derivatives as a series in  $1/\rho$  since only quantities at the equatorial plane are needed, so that  $z = 0$  in the final expressions. Finally, expanding the orbital frequency, equation (2.16), in powers of  $1/\rho$  and inverting this series, one obtains  $1/\rho$  as a series in  $\Omega_\phi$ , or  $v = (M\Omega_\phi)^{1/3}$ , which can then be substituted in the expansion series of the observables to obtain,

$$\frac{\Delta E}{\mu} = \frac{1}{3}v^2 - \frac{1}{2}v^4 + \frac{20}{9} \frac{S_1}{M^2} v^5 + \left( -\frac{27}{8} v^6 + \frac{M_2}{M^3} \right) + \frac{28}{3} \frac{S_1}{M^2} v^7 + \left( -\frac{225}{16} + \frac{80}{27} \frac{S_1^2}{M^4} + \frac{70}{9} \frac{M_2}{M^3} \right) v^8 + \dots \quad (3.6)$$

$$\frac{\Omega_\rho}{\Omega_\phi} = 3v^2 - 4 \frac{S_1}{M^2} v^3 + \left( \frac{9}{2} - \frac{3}{2} \frac{M_2}{M^3} \right) v^4 - 10 \frac{S_1}{M^2} v^5 + \left( \frac{27}{2} - 2 \frac{S_1^2}{M^4} - \frac{21}{2} \frac{M_2}{M^3} \right) v^6 + \dots, \quad (3.7)$$

$$\frac{\Omega_z}{\Omega_\phi} = 2 \frac{S_1}{M^2} v^3 + \frac{3}{2} \frac{M_2}{M^3} v^4 + \left( 7 \frac{S_1^2}{M^4} + 3 \frac{M_2}{M^3} \right) v^6 + \left( 11 \frac{S_1 M_2}{M^5} - 6 \frac{S_3}{M^4} \right) v^7 \dots, \quad (3.8)$$

$$\Delta N = \frac{5}{96\pi} \left( \frac{M}{\mu} \right) v^{-5} \left[ 1 + \frac{743}{336} v^2 - 4\pi |v|^3 + \frac{113}{12} \frac{S_1}{M^2} v^3 + \left( \frac{3058673}{1016064} - \frac{1}{16} \frac{S_1^2}{M^4} + 5 \frac{M_2}{M^3} \right) v^4 \right. \quad (3.9)$$

$$\left. - \sum_{l=4,6,\dots} \frac{(-1)^{l/2} (4l+2)(l+1)!! M_l v^{2l}}{3l!! M^{l+1}} + \sum_{l=3,5,\dots} \frac{(-1)^{(l-1)/2} (8l+20)l!! S_l v^{2l+1}}{3(l-1)!! M^{l+1}} \right]. \quad (3.10)$$

One can see how the different multipole moments are redundantly encoded in the different observables. The formula for  $\Delta N$  is valid to the second post-Newtonian order and included the quadrupole formula for the gravitational wave luminosity:

$$\left. \frac{dE_{\text{gw}}}{dt} \right|_{I_{ij}} = \frac{32}{5} \mu^2 \rho^4 \Omega_\phi^6, \quad (3.11)$$

and a contribution due to motion of the inspiraling object,

$$\left. \frac{dE_{\text{gw}}}{dt} \right|_{J_{ij}} = \frac{32}{5} \left( \frac{\mu}{M} \right)^2 v^{10} \left[ \frac{1}{36} v^2 - \frac{1}{12} \frac{S_1}{M^2} v^3 + \frac{1}{16} \frac{S_1^2}{M^4} v^4 \right], \quad (3.12)$$

as explained in Ryan's paper.

In a following paper [80], Ryan computed the accuracy in obtaining the multipole moments from these types of inspirals from LISA's observations using a Fisher matrix analysis. Ryan calculated for example that for a body with mass  $10M_\odot$  inspiraling a central body with mass  $10^6 M_\odot$ , LISA could measure  $M_2/M^3$  to within  $\sim 5 \times 10^{-1}$ , assuming a signal-to-noise ratio (SNR) of 100 and two years of data. More recently, Barack and Cutler [81] by focusing on deviations at the quadrupolar moment and using their analytic kludge waveforms [82] extended the analysis to a more realistic model including generic orbits and taking into account modulations caused by the motion of LISA's satellites. They calculated that for an inspiraling black hole of  $10M_\odot$  and one year of data,  $M_2/M^3$  could be measured to within  $\sim 10^{-4}$ ,  $10^{-3}$  and  $\sim 10^{-2}$  when the central black hole had  $10^{5.5}$ ,  $10^6$  and  $10^{6.5}$  solar masses, respectively. Although their analysis was still approximate they argued that the accuracy results should hold within one order of magnitude. Rodriguez, Mandel and Gair [83] carried out a similar analysis for the case of IMRIs, which might be detectable by Earth-based observatories such as LIGO and VIRGO, and concluded that using 3.5PN waveforms one could measure the central object's quadrupole moment to about a 15 % error, which would get degraded to a  $\sim 100$  % fractional error if only 2PN waveforms were used.

In the years following, Ryan's results were generalized in different directions. By using the extension of the recursive method of calculating the multipole moments from the Ernst potential to the electrovacuum case [67, 68], Sotiriou and Apostolatos [70] have shown that the assumption of a vacuum spacetime can be dropped and that one can still read all the multipole moments from the same observables, which are now a power series with coefficients as functions of the mass and mass currents moments  $M_l$  and  $S_l$  as well as of the electric and magnetic moments  $E_l$  and  $H_l$ . Li and Lovelace [79] pointed out how to extract the evolving orbit parameters and have generalized Ryan's results by dropping the assumption of no tidal coupling.

While measuring with enough precision the mass  $M_0$ , spin  $S_1$  and a Kerr-deviating quadrupole moment  $M_2$  is enough to falsify the null-test hypothesis of a clean vacuum general-relativistic supermassive Kerr black hole, EMRIs have the potential to shows us beyond this. Although mostly as preliminary studies, alternative tests have been considered, whether by considering alternative theories of gravity or different types of central objects and surroundings. When considering EMRIs testing of alternative theories of gravity one should properly consider the three different levels at which the theory might differ from GR

and alter the signature of GW: on the geometry, that is, the metric tensor; on the radiation reaction force and on the gravitational wave emission, dependent on the field equations. The Kerr spacetime is also a solution in different theories of gravity [84], but this does not imply that, for example, the gravitational radiation emitted during an EMRI is indistinguishable from the GR case [85].

One example of an alternative theory that can be constrained by gravitational waves observations of EMRIs and IMRIs is the dynamical Chern-Simons (CS) gravity [86–89]. It has been found that for this theory the contributions to the signature in the gravitational waves comes from the difference in the orbits arising from a different spacetime geometry as well as from the different field equations and gravitational wave emission, and that one could constrain the theory parameter to about  $\xi^{1/4} \leq 10^2 \text{km}$ . However the spacetime curvature in EMRIs suppresses the CS corrections and stellar mass BH binaries, to which earth based observatories are sensible, were found to better constrain the theory parameter, to within  $\xi^{1/4} \leq O(10 - 100) \text{km}$  [90] which is six to seven orders of magnitude better than the Gravity Probe B [91] and LAGEOS [92] solar system constrains.

Yunes and Pretorius [93] have recently proposed what has been called the “parametrized post-Einsteinian” (PPE) framework, involving a generic deformation of  $l = 2$  harmonic of the response function in Fourier space as:

$$\tilde{h}_{\text{ppE}}^{l=2} = \tilde{h}^{\text{GR}}(1 + \alpha_{\text{ppE}} u^{a_{\text{ppE}}} e^{i\beta_{\text{ppE}} u^{b_{\text{ppE}}}}), \quad (3.13)$$

where the response function is given by  $h = F_+ h_+ + F_\times h_\times$ , where  $h_+$  and  $h_\times$  are the two polarization amplitudes of the gravitational waveform and  $F_+$  and  $F_\times$  are beam-pattern functions that characterize the intrinsic response of the detector and that depend on the orientation of the detector, direction to the source and on a polarization angle [94]. Similarly to the PPN framework, it aims at reducing GR bias in experiments: different theories of gravity correspond to different values of the 4 parameters  $(\alpha_{\text{ppE}}, a_{\text{ppE}}, \beta_{\text{ppE}}, b_{\text{ppE}})$  which are now to be fitted independently. Table 3.2 shows the different values these parameters take for some alternative theories. This deformation does not cover all possible alternative theories but it can be easily generalized at the cost of introducing more parameters and different functionals.

The effects surrounding matter can have on an EMRI will in general be twofold: if its mass is comparable to that of the supermassive black hole its gravitational field will distort the spacetime geometry and alter its multipole structure and orbits; secondly, the effect of hydrodynamic drag on the inspiraling body inside this material can be at least comparable to that of radiation reaction. Barausse, Rezzolla, Petroff and Ansorg [95, 96] have studied the influence of two different surrounding compact accretion torus close to the event horizon, one of mass comparable with the supermassive black hole and one with comparable angular momentum, and Yunes, Kocsis, Loeb and Haiman [97, 98] studied the effect of an accretion disc on an EMRI when the stellar mass object inspirals within the disc. Although dependent on the magnitude of the perturbations both effects were found to leave an observable signature on the waveforms, giving rise to a serious confusion problem which nonetheless has the potential to be solved from the evolution of the frequencies during the inspiral.

There have been several proposals of alternative types of compact objects, more exotic than neutron

Table 3.2: PPE parameters for some alternative theories. Because its amplitudes are zero the values of some parameters are irrelevant, in which case the symbol  $\cdot$  is used. General Relativity corresponds to  $(\alpha_{\text{ppE}}, \beta_{\text{ppE}}) = (0, 0)$ . From [10].

Theory	$\alpha_{\text{ppE}}$	$a_{\text{ppE}}$	$\beta_{\text{ppE}}$	$b_{\text{ppE}}$
Jordan-Brans-Dicke-Fierz	$-\frac{5}{96} \frac{S^2}{\omega_{\text{BD}}} \eta^{2/5}$	-2	$-\frac{5}{3584} \frac{S^2}{\omega_{\text{BD}}} \eta^{2/5}$	-7
Dissipative Einstein-Dilaton-Gauss-Bonnet gravity	0	$\cdot$	$-\frac{5}{7168} \zeta_3 \eta^{-18/5} \delta_m^2$	-7
Massive Graviton	0	$\cdot$	$-\frac{\pi^2 D \mathcal{M}_c}{\lambda_g^2 (1+z)}$	-3
Lorentz Violation	0	$\cdot$	$-\frac{\pi^{2-\gamma_{\text{LV}}}}{(1-\gamma_{\text{LV}})} \frac{D_{\gamma_{\text{LV}}}}{\lambda_{\text{LV}}^{2-\gamma_{\text{LV}}}} \frac{\mathcal{M}_c^{1-\gamma_{\text{LV}}}}{(1+z)^{1-\gamma_{\text{LV}}}}$	$-3\gamma_{\text{LV}} - 3$
$G(t)$ Theory	$-\frac{5}{512} \dot{G} \mathcal{M}_c$	-8	$-\frac{25}{65536} \dot{G}_c \mathcal{M}_c$	-13
Extra Dimensions	$\cdot$	$\cdot$	$-\frac{75}{2554344} \frac{dM}{dt} \eta^{-4} (3 - 26\eta + 24\eta^2)$	-13
Non-Dynamical Chern-Simons Gravity	$\alpha_{\text{PV}}$	3	$\beta_{\text{PV}}$	6
Dynamical Chern-Simons Gravity	0	$\cdot$	$\beta_{\text{dCS}}$	-1

stars and black holes, including boson stars, gravastars and quark stars. Kesden, Gair and Kamionkowski [99] have found that in the case the supermassive central object is a boson star stable orbits exist inside the Schwarzschild radius so that instead of disappearing behind the event horizon an inspiraling body would continue to emit gravitational radiation making it readily distinguishable from a black hole. Macedo, Pani, Cardoso and Crispino [100] have confirmed this conclusion by extending the analysis with a study of the gravitational radiation emitted. The case of an EMRI with a supermassive non-rotating gravastar was recently studied by Pani, Berti, Cardoso, Chen and Norte [101] and it was found that for quasi-circular orbits the gravitational wave power emitted would show characteristic peaks due to the excitation of the polar oscillation modes of the gravastar, a feature absent in the case of a black hole.

Recently, Apostolatos, Lukes-Gerakopoulos and Contopoulos have put forward [102–104] a test that could be a ‘smoking gun’ for ergodic motion and non-Kerrness: the observation of a plateau in the evolution of the ratio of frequencies  $f_\rho/f_z$ , which would not occur in an integrable system like Kerr.

The Kolmogorov-Arnold-Moser (KAM) theorem states that for an integrable Hamiltonian system (such as Kerr) a generic perturbation will not destroy most of the phase space tori, but that it will deform them instead (these are called non-resonant tori). On the other hand, the Poincaré-Birkhoff theorem states that the resonant tori are destroyed and that a chain of (Birkhoff) islands is formed on the Poincaré map. After the perturbation, from each resonant torus only a finite even number of periodic points survive. Half of these are unstable, while the other half are stable and form a chain of islands of stability. Each of these chains is characterized by a ratio of frequencies (constant along its non-vanishing width) which is equal to the ratio of the unperturbed resonant torus. Figure 3.1 shows some of these islands in the Manko-Novikov spacetime (see section 4.2). They were found with the aid of the rotation

number, which is defined as

$$\nu = \lim_{N \rightarrow \infty} \sum_{i=1}^N \frac{\Delta\theta_i}{2\pi} \quad (3.14)$$

where  $\Delta\theta_i$  is the angle formed by the  $i$ -th and  $(i+1)$ -th successive cross-sections on the surface of section, with respect to the center of the main island.

The essential idea is that during an inspiral the orbit evolves adiabatically from one geodesic to another and that it may at some point enter one of the Birkhoff chains. Then if one could continuously measure the ratio of the orbital frequencies a plateau could be observed, as represented in figure 3.1. Such

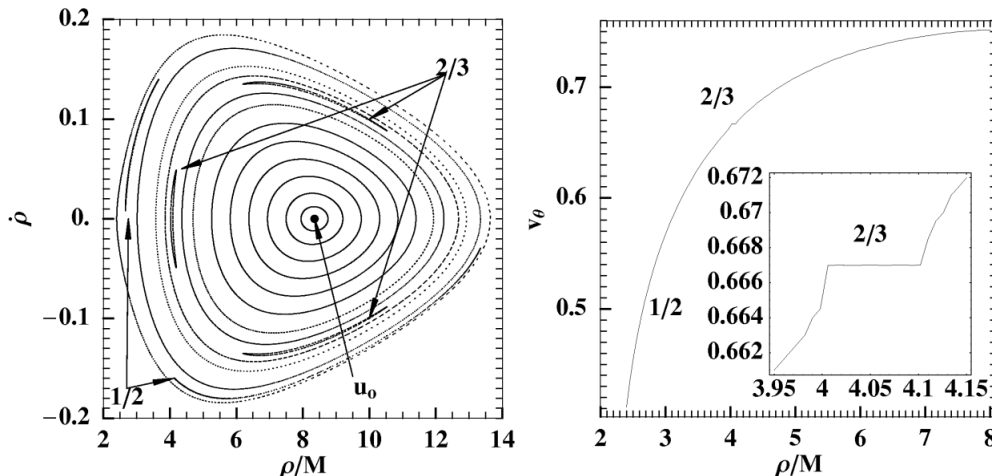


Figure 3.1: Left: The surface of section of the outer region on the  $(\rho, \dot{\rho})$  plane for the parameter set  $E = 0.95$ ,  $L_z = 3M$ ,  $a/M = 0.9$ ,  $q = 0.95$ . The fixed point at the center of the main island is indicated by  $u_0$ . Right: The rotation number vs.  $\rho$  along the line  $\dot{\rho} = 0$  of the surface of section presented in the left panel. A detail of the rotation curve around the  $2/3$ -resonance showing a plateau is embedded in the right panel. (Figure 3 of [103]).

an observation would be a clear indication that the spacetime is not a pure Kerr spacetime. Furthermore, although the analysis was done for the Manko-Novikov metric, it should be applicable to other ‘quasi-Kerr’ systems. Although promising, the usefulness of such a test depends crucially on how much time,  $\Delta t$ , an orbit would spend in a chain, i.e. on the plateau. The authors show that this time is in general larger for: larger deviations to the Kerr metric; larger inspiral mass ratios; and stronger resonances (lower integer ratios). It was found that  $\Delta t \approx 0.15(M/M_\odot)$  for a ratio of masses  $\mu/M = 8 \times 10^{-5}$ , a deviation  $q = 0.95$  and  $a = 0.9M$ .

## 3.2 Quasinormal ringdown

When a black hole is perturbed, as for example after a binary merger, it quickly radiates gravitational waves, in the so-called ringdown phase, until it reaches a stationary state. This radiation is a superposition of exponentially damped sinusoids, called quasinormal modes QNM [105–107]. The possibility to test strong field gravity and the Kerr black hole hypothesis using QNMs has been studied by several authors [101, 108–113]. The two gauge-invariant polarization amplitudes of the gravitational waveform,  $h_+$  and

$h_{\times}$ , measured by a detector at a distance  $r$  of the source can be expressed as [106]:

$$h_{+} = \frac{M}{r} \sum_{lmn} \operatorname{Re} \left\{ \mathcal{A}_{lmn}^{+} e^{i(\omega_{lmn}t + \phi_{lmn}^{+})} e^{-t/\tau_{lmn}} S_{lmn} \right\} \quad (3.15)$$

$$h_{\times} = \frac{M}{r} \sum_{lmn} \operatorname{Im} \left\{ \mathcal{A}_{lmn}^{\times} e^{i(\omega_{lmn}t + \phi_{lmn}^{\times})} e^{-t/\tau_{lmn}} S_{lmn} \right\}, \quad (3.16)$$

where  $\mathcal{A}_{lmn}^{+,\times}$ ,  $\phi_{lmn}^{+,\times}$ ,  $\omega_{lmn}$  and  $\tau_{lmn}$  are the real amplitude, real phase, complex frequency and real damping time of the wave, respectively, and where  $S_{lmn}$  are spin-weighted spheroidal harmonics. The real physical frequency  $f_{lmn}$  is given from  $\omega_{lmn} = 2\pi f_{lmn} + i/\tau_{lmn}$ . A certain frequency  $\omega_{lmn}$  can in general be given by different  $(M, a, l, m, n)$  multiplets, where  $M$  and  $a$  are the black hole's mass and rotation parameter, respectively. A necessary condition to extract  $(M, a)$  is measuring two modes  $\omega_{lmn}$  and  $\omega_{l'm'n'}$  - each measurement will yield a discrete set of  $(M, a)$  doublets, and the correct one should belong to both sets. However the  $n = 0, l = m = 2$  mode is expected to be the dominant one in most cases [114], and assuming this is the mode being detected one is able to extract  $M$  and  $a$  from the measurement of this single mode. The additional measurement of either the real frequency or the damping time of a second mode would in principle be enough for a null test of the Kerr black hole hypothesis. The astrophysical scenarios which could emit detectable ringdown radiation include the gravitational collapse and formation of black holes, accreting matter onto black holes, and binary mergers of neutron stars and black holes. The main factors affecting the detectability of QNMs are the mass and the spin of the black hole, the distance to the source, the ringdown efficiency  $\epsilon_{rd}$  which is defined as the fraction of the total mass-energy of the system radiated as QNMs, and the mass ratio of the progenitors. The left panel of figure 3.2 indicates how equal-mass mergers with a final black hole mass larger than  $\sim 10^5 M_{\odot}$  are expected to be detected by LISA, and the right panel shows how, depending on the redshifted black hole mass, the SNR from ringdown radiation can be larger than the inspiral radiation. Berti, Cardoso et al. [109, 111] concluded that given a SNR  $\sim 100$  tests of the Kerr black hole hypothesis with LISA and Earth-based detectors should be possible by measuring the fundamental QNM and either the frequency or damping time of a second mode.

### 3.3 Accretion disc emission

Binary systems consisting of a black hole surrounded by an accretion disc of matter from its companion star are one of the most promising avenues to probe strong field gravity. In this section we describe the method of ray-tracing which is one of the preferred techniques when computing and modelling accretion discs emission, and it is specially useful when considering light bending, returning radiation and non-Kerr spacetimes [116–118].

Ray-tracing consists of dividing the observer's sky into small elements and from each of these integrate the photon's path back in time to its emission location on the disc. Having a local emission profile, one then integrates over the observer's sky to obtain the emission profile as seen by the distant observer. Besides the parameters arising from the local emission profile, this modelling should still include the parameters from the spacetime and disc geometry, such as the mass and angular momentum of the

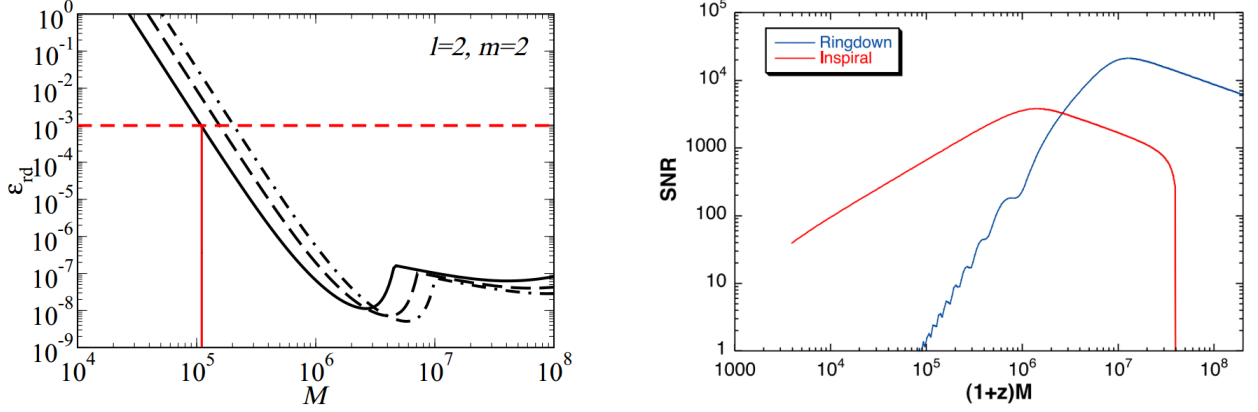


Figure 3.2: Left (figure 1 of [109]): Value of  $\epsilon_{rd}$  required to detect the fundamental mode with  $l = m = 2$  at a distance  $r = 3\text{Gpc}$ , with detection being defined by  $\text{SNR} = 10$ . The different curves correspond to 3 values of the dimensionless spin parameter:  $a/M = 0$  (solid),  $a/M = 0.8$  (dashed) and  $a/M = .98$  (dot-dashed). The red, dashed horizontal line marks the "pessimistic" prediction of  $\epsilon_{rd}$  from numerical head-on collision simulations. Right (figure 7 of [115]): LISA's comparative SNRs for the last year of inspiral and ringdown of an equal-mass, non-spinning massive-black-hole binary, as a function of the redshifted black-hole mass  $(1+z)M$ .

central object and the inner and outer edges of the disc, as well as the distance and inclination angle between the observer and the disc.

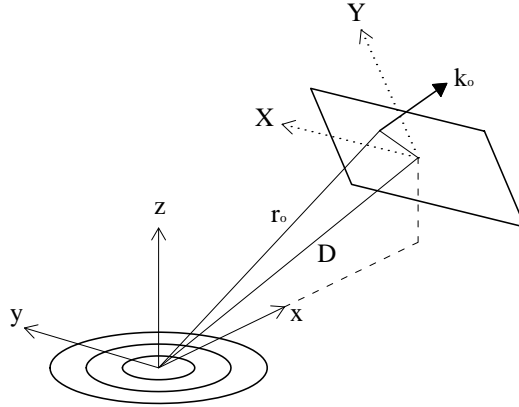


Figure 3.3: Ray-tracing geometry.

The flux seen by the observer can be written as

$$F_{E_{obs}} = N_{E_{obs}} E_{obs} = \int I_{obs}(E_{obs}) d\Omega_{obs}, \quad (3.17)$$

where  $N_{E_{obs}}$ ,  $E_{obs}$  and  $I_{obs}$  are, respectively, the photon flux number density, photon energy and specific intensity of the radiation as measured by a distant observer.

From Liouville's theorem (see page 588 of [119]), it follows that the flux can be written as

$$F_{E_{obs}} = \int g^3 I_e(E_e) d\Omega_{obs} \quad (3.18)$$

where the index  $e$  denotes the emitter, and  $g$  is the redshift factor given by

$$g = \frac{E_{obs}}{E_e} = \frac{(k_\mu u^\mu)_{obs}}{(k_\nu u^\nu)_e}. \quad (3.19)$$

The velocity of the distant observer is  $u_{obs}^\mu = (-1, 0, 0, 0)$  and, assuming stationarity and axisymmetry, the velocity of the emitter is  $u_e^\mu = (u_e^t, 0, 0, \Omega_\phi u_e^t)$ . From  $g_{\mu\nu} u_e^\mu u_e^\nu = -1$  one obtains

$$u_e^t = -\frac{1}{\sqrt{-g_{tt} - 2g_{t\phi}\Omega - g_{\phi\phi}\Omega^2}}, \quad (3.20)$$

so that the redshift factor can be written as

$$g = \frac{\sqrt{-g_{tt} - 2g_{t\phi}\Omega - g_{\phi\phi}\Omega^2}}{1 + \lambda\Omega}, \quad (3.21)$$

with

$$\lambda = \frac{k_\phi}{k_t} = r_0 |\sin \theta_0| \frac{k_0^\phi}{k_0^t}, \quad (3.22)$$

which is constant along the photon's path, and where the last equality comes from the equations (3.28) to (3.31) below.

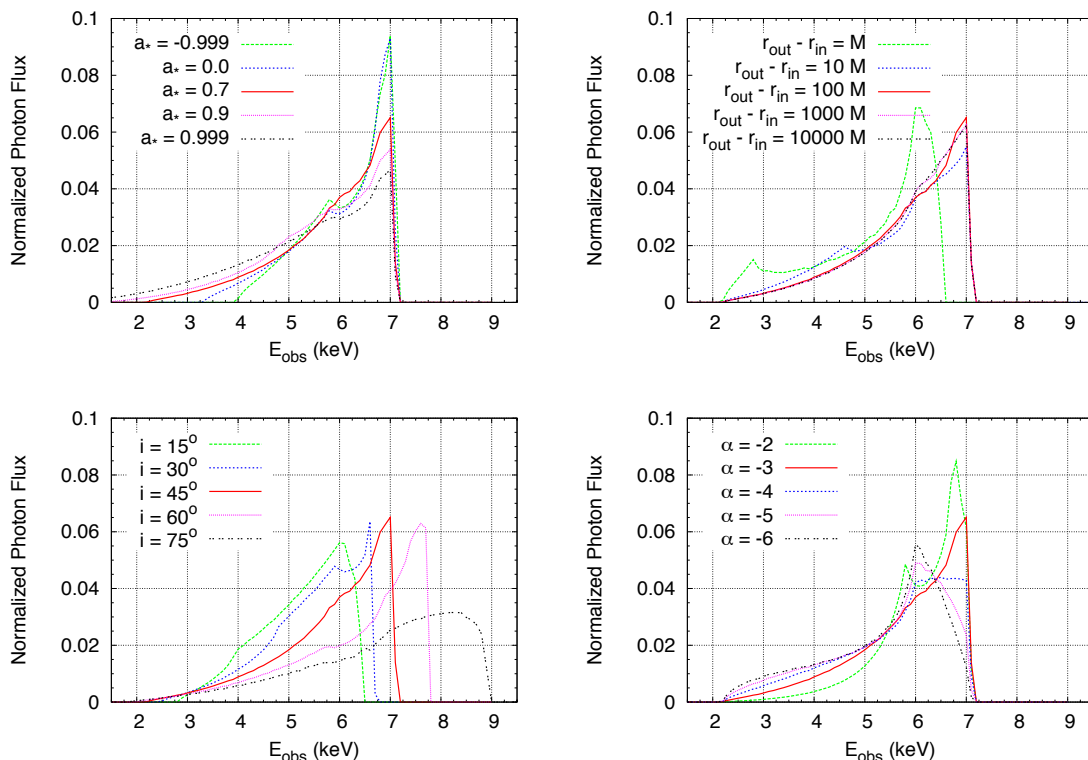


Figure 3.4: Iron line profiles dependence on different model parameters. From [120].

In terms of the coordinates  $X$  and  $Y$  (of the observer's sky) and the distance  $D$  and inclination angle

$i$  (see figure 3.3), the photon's initial conditions can be written as

$$t_0 = 0, \quad (3.23)$$

$$r_0 = (X^2 + Y^2 + D^2)^{1/2}, \quad (3.24)$$

$$\theta_0 = \arccos \frac{Y \sin i + D \cos i}{(X^2 + Y^2 + D^2)^{1/2}}, \quad (3.25)$$

$$\phi_0 = \arctan \frac{X}{D \sin i - Y \cos i}, \quad (3.26)$$

$$(3.27)$$

$$k_0^r = -\frac{D}{(X^2 + Y^2 + D^2)^{1/2}} |\mathbf{k}_0|, \quad (3.28)$$

$$k_0^\theta = \frac{\cos i - D \frac{Y \sin i + D \cos i}{X^2 + Y^2 + D^2}}{(X^2 + (D \sin i - Y \cos i)^2)^{1/2}} |\mathbf{k}_0|, \quad (3.29)$$

$$k_0^\phi = \frac{X \sin i}{X^2 + (D \sin i - Y \cos i)^2} |\mathbf{k}_0|, \quad (3.30)$$

$$k_0^t = ((k_0^r)^2 + r_0^2 (k_0^\theta)^2 + r_0^2 \sin^2 \theta_0 (k_0^\phi)^2)^{1/2}. \quad (3.31)$$

One is then ready to integrate the observer's sky given the specific radiation intensity of the emitter  $I_e$ . For the fluorescent iron line emission, this is usually considered to be given as [121, 122]

$$I_e(E_e) = \epsilon(r_e, \mu_e) \delta(E_e - E_{K_\alpha}) \propto r_e^{-\alpha} \delta(E_e - E_{K_\alpha}), \quad (3.32)$$

where  $\epsilon(r_e, \mu_e)$  is the emissivity and  $\alpha$  the power-law index. For the thermal spectrum, the emission is assumed to be that of a black body with an effective temperature  $T_{\text{eff}}$ , given by  $\mathcal{F}(r) = \sigma T_{\text{eff}}^4$ , where  $\sigma$  is the Stefan-Boltzmann constant and where  $\mathcal{F}(r)$  is the time-averaged energy flux emitted from the surface of the disc, which depends on spacetime metric and can be computed from the Novikov-Thorne model as described below (see equation (3.38)). Non-thermal effects are usually taken into account, on a first approximation, with a spectral hardening factor  $f_{\text{col}}$ , so that the temperature measured from the observed spectrum is  $T_{\text{col}}(r) = f_{\text{col}} T_{\text{eff}}(r)$ . Thus the intensity is given by

$$I_e(E_e) = f_{\text{col}}^{-4} B_\nu(T_{\text{col}}(r)) = \frac{2E_e^3}{f_{\text{col}}^4} \frac{\Upsilon}{\exp\left(\frac{E_e \sigma^{1/4}}{k_B f_{\text{col}} \mathcal{F}(r)^{1/4}}\right) - 1}, \quad (3.33)$$

where  $B_\nu$  is Planck's function,  $k_B$  is the Boltzmann constant,  $\mathcal{F}(r)$  is given by equation (3.38), and  $\Upsilon = 1$  for the case of isotropic emission and  $\Upsilon = \frac{1}{2} + \frac{3}{4} \cos \xi$  for limb-darkened emission (where  $\xi$  is the angle between the normal of the disc surface and the wavevector of the photon). Figures 3.4 and 3.5 show the dependence of the emission profiles on some of the model parameters.

In the following we briefly review the relativistic standard thin accretion disc theory, the so called Novikov-Thorne model [123–125], which provides a formula for the time-averaged energy flux emitted from the surface of the disc,  $\mathcal{F}(r)$ , for stationary and axisymmetric spacetimes. In this model the disc is assumed to have negligible self-gravity, and to be moving on the equatorial plane of a stationary, axisymmetric, asymptotically flat and reflection symmetric spacetime. The disc is assumed to be thin,

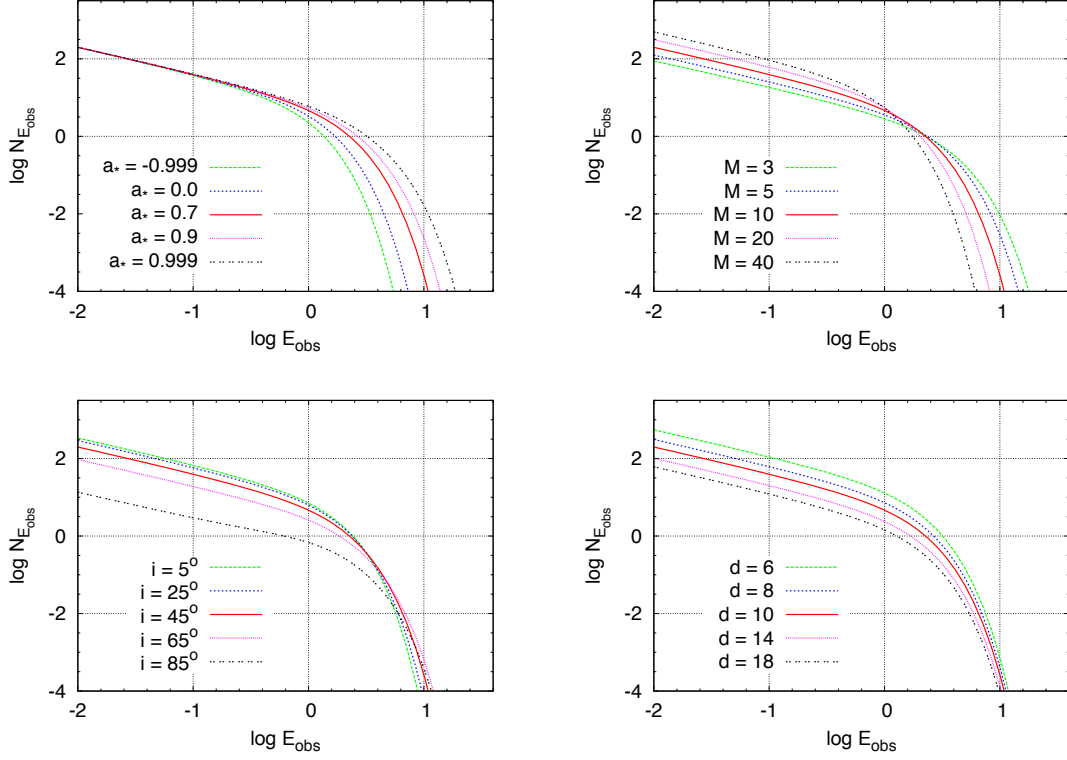


Figure 3.5: Iron line profiles dependence on different model parameters. From [120].

so that at any radius  $r$ , the thickness of the disc is much smaller than  $r$ , that is  $2H \ll r$ , where  $H$  is the height of the disc.

The stress energy tensor is decomposed in the following form

$$T^{\mu\nu} = \rho_0 u^\mu u^\nu + 2u^{(\mu} q^{\nu)} + t^{\mu\nu}, \quad (3.34)$$

where  $\rho_0$  is the density,  $u^\mu$  is the particle's four-velocity,  $q^\mu$  the energy flow vector and  $t^{\mu\nu}$  the stress tensor, with  $u_\mu q^\mu = 0$  and  $u_\mu t^{\mu\nu} = 0$ .

The three basic equations describing the time-averaged radial structure of the disc can be deduced from the conservation of rest mass, energy and angular momentum, respectively:

$$\nabla_\mu(\rho_0 u^\mu) = 0, \quad \nabla_\mu E^\mu = 0, \quad \nabla_\mu J^\mu = 0, \quad (3.35)$$

where  $-E^\mu \equiv T_\nu^\mu(\partial/\partial t)^\nu$  and  $J^\mu \equiv T_\nu^\mu(\partial/\partial\phi)^\nu$ .

From the conservation of the rest mass, one obtains the constancy of the accretion mass rate

$$\dot{M}_0 = -2\pi r \sqrt{-g} \Sigma u^r = \text{constant}, \quad (3.36)$$

where  $\Sigma$  is the surface density of the disc. The conservation of energy and angular momentum lead to

$$[\dot{M}_0 E - 2\pi r \Omega W_\phi^r]_{,r} = 4\pi r \mathcal{F} E, \quad [\dot{M}_0 L - 2\pi r W_\phi^r]_{,r} = 4\pi r \mathcal{F} L, \quad (3.37)$$

where  $\mathcal{F}(r)$  is the time-averaged energy flux emitted from the surface of the disc, and  $W_\phi^r$  the averaged torque, which one can eliminate in the above equations to obtain

$$\mathcal{F}(r) = \frac{\dot{M}_0}{4\pi\sqrt{-g}} f(r), \quad (3.38)$$

with

$$f(r) \equiv \frac{\Omega_{,r}}{(E - \Omega L)^2} \int_{r_{ms}}^r (E - \Omega L) L_{,r} dr = -\frac{p^t_{,r}}{p_\phi} \int_{r_{ms}}^r \frac{p_{\phi,r}}{p^t} dr. \quad (3.39)$$

### 3.4 Other electromagnetic spectrum tests

Several other tests to measure the quadrupole moment of black holes have been suggested [126]. Essentially any experiment that probes the strong field of compact objects and measures its angular momentum could also, in principle, constrain its quadrupole moment given enough precision. These proposals include: the tracking of the orbits of cluster stars [127–129] and radio pulsars [130–132] around Sgr\*A; modelling of the Quasi-Periodic Oscillations (QPO) frequencies observed from accretion discs [133, 134]; mean radiative efficiency tests [135]; X-ray polarimetry [136]; and black hole direct imaging [137–139].

# Chapter 4

## Non-Kerr spacetimes

In this chapter we review recent work on different approaches to measuring deviations from the Kerr metric by working with spacetime metrics which possess additional parameters besides the mass and spin of the Kerr solution. In section 4.1 we describe the bumpy black hole formalism, and in section 4.2 the Manko-Novikov metric (an example of an exact vacuum solution to the Einstein equations generalizing the Kerr spacetime) and its possible application to tests of strong field gravity. We describe a non-GR generalization of the Kerr metric put forward by Johannsen and Psaltis in section 4.3, and ensuing studies of the properties of this spacetime and its possible use in revealing deviations from Kerr's quadrupole moment. In the last subsections we study the relative importance of the higher order parameters in the Johannsen-Psaltis metric, and by constructing a further generalization of the spacetime argue against the possibility of its mapping to rotating black hole solutions in alternative theories of gravity.

### 4.1 Bumpy black holes

The term ‘bumpy black holes’ was coined by Collins and Hughes [22] in 2004, where they define them as ‘objects that have a multipolar structure that is very nearly, but not quite, that of a black hole’. They emphasize that as a trial spacetime the bumpy black hole should behave well deep into the strong field and exhibit a controllable deviation from the Kerr solution. The term has been used more generally as what we call in this review non-Kerr spacetimes, but here the term will be applied to the original approach and direct developments.

This section is divided in three parts. In the first we describe Collins and Hughes first attempt and the ensuing development by Vigeland and Hughes. In the second part we describe Glampedakis and Babak's construction of a quasi-Kerr spacetime, and the last section describes Vigeland, Yunes and Stein's two formalisms of bumpy black holes in alternative theories of gravity.

#### 4.1.1 Bumpy black holes

Collins and Hughes [22] have constructed a spacetime which is an axisymmetric perturbation of the Schwarzschild metric deviating at the quadrupole moment. Essentially the construction is the superpo-

sition of the Schwarzschild metric with two small perturbation functions representing a equatorial ring mass and two point masses on the axis of symmetry of opposite sign, one at the north pole and another at the south pole. This work was later generalized by Vigeland and Hughes [23, 74] for the case of a rotating black hole. In the following we describe these two constructions and the impact on observables.

The approach taken by Collins and Hughes was to start from the Weyl metric, which describes all static axisymmetric vacuum spacetimes,

$$ds^2 = -e^{2\psi} dt^2 + e^{2\gamma-2\psi} (d\rho^2 + dz^2) + e^{-2\psi} \rho^2 d\phi^2 \quad (4.1)$$

(which is equation (2.5) with  $\omega = 0$ ) and perturb the Schwarzschild solution, i.e. take  $\psi = \psi_0 + \psi_1$  and  $\gamma = \gamma_0 + \gamma_1$ , where  $\psi_0$  and  $\gamma_0$  are the functions of the Schwarzschild solution, and where the perturbations are taken to be small compared to these.

The non-trivial vacuum Einstein equations for the Weyl metric (4.1) reduce to

$$\frac{\partial^2 \psi}{\partial \rho^2} + \frac{1}{\rho} \frac{\partial \psi}{\partial \rho} + \frac{\partial^2 \psi}{\partial z^2} = 0, \quad (4.2)$$

$$\frac{\partial \gamma}{\partial \rho} = \rho \left[ \left( \frac{\partial \psi}{\partial \rho} \right)^2 - \left( \frac{\partial \psi}{\partial z} \right)^2 \right]. \quad (4.3)$$

$$\frac{\partial \gamma}{\partial z} = 2\rho \frac{\partial \psi}{\partial \rho} \frac{\partial \psi}{\partial z}. \quad (4.4)$$

It is noted that equation (4.2) is simply Laplace's equation in cylindrical coordinates. This is a key point in the construction due the the linearity of the solutions and is later exploited by Vigeland and Hughes [23], as explained below.

Changing to prolate spheroidal coordinates  $u \in [0, \pi]$  and  $v \in [0, \infty)$  which cover the entire exterior Schwarzschild spacetime (for  $u = 0$ , we are at the event horizon  $r = 2M$ ),

$$\rho = M \sinh u \sin v, \quad (4.5)$$

$$z = M \cosh u \cos v, \quad (4.6)$$

the line element becomes

$$ds^2 = -e^{2\psi} dt^2 + M^2 e^{2\gamma-2\psi} (\sinh^2 u + \sin^2 v) (du^2 + dv^2) + M^2 e^{-2\psi} \sinh^2 u \sin^2 v d\phi^2. \quad (4.7)$$

Now taking Schwarzschild as the background spacetime,

$$\psi_0 = \ln \tanh(u/2), \quad \gamma_0 = -\frac{1}{2} \ln \left( 1 + \frac{\sin^2 v}{\sinh^2 u} \right), \quad (4.8)$$

the Einstein equations reduce, to leading order in  $\psi_1$  and  $\gamma_1$ , to

$$\nabla^2 \psi_1 = 0, \quad (4.9)$$

$$\frac{\partial \gamma_1}{\partial u} = \frac{2[\tan v(\partial \psi_1 / \partial u) + \tanh u(\partial \psi_1 / \partial v)]}{\sinh u(\coth u \tan v + \tanh u \cot v)}, \quad (4.10)$$

$$\frac{\partial \gamma_1}{\partial v} = \frac{2[\tan v(\partial \psi_1 / \partial v) - \tanh u(\partial \psi_1 / \partial u)]}{\sinh u(\coth u \tan v + \tanh u \cot v)}. \quad (4.11)$$

In fact, equations (4.10) and (4.11) overdetermine the solution and there is a unique solution up to a constant of integration ([20], page 167), so that only equation (4.11) is used to calculate  $\gamma_1$ , after imposing a particular  $\psi_1$ .

A final change of coordinates

$$r = 2M \cosh^2(u/2), \quad \theta = v, \quad (4.12)$$

implying that

$$\rho = r \sin \theta \sqrt{1 - \frac{2M}{r}}, \quad z = (r - M) \cos \theta, \quad (4.13)$$

brings the perturbed metric into a more familiar Schwarzschild-like form

$$\begin{aligned} ds^2 &= -e^{2\psi_1} \left(1 - \frac{2M}{r}\right) dt^2 + e^{2\gamma_1 - 2\psi_1} \left(1 - \frac{2M}{r}\right)^{-1} dr^2 + r^2 e^{2\gamma_1 - 2\psi_1} d\theta^2 + r^2 \sin^2 \theta e^{-2\psi_1} d\phi^2 \\ &\equiv (\hat{g}_{\alpha\beta} + b_{\alpha\beta}) dx^\alpha dx^\beta \end{aligned} \quad (4.14)$$

where the potentials  $\psi_1$  and  $\gamma_1$  are left in exponential form only for notational convenience, as in fact they should expand to first order as  $e^{2\psi_1} \simeq 1 + 2\psi_1$  (and the same for  $\gamma_1$ ). The non zero components of  $b_{\alpha\beta}$  are given by

$$b_{tt} = -2\psi_1 \left(1 - \frac{2M}{r}\right), \quad (4.15)$$

$$b_{rr} = (2\gamma_1 - 2\psi_1) \left(1 - \frac{2M}{r}\right)^{-1}, \quad (4.16)$$

$$b_{\theta\theta} = (2\gamma_1 - 2\psi_1)r^2, \quad (4.17)$$

$$b_{\phi\phi} = -2\psi_1 r^2 \sin^2 \theta, \quad (4.18)$$

as we have taken  $\hat{g}_{\alpha\beta}$  to represent the standard Schwarzschild metric, which we recover when  $\psi_1 \rightarrow 0, \gamma_1 \rightarrow 0$ .

The effects of the bumpiness in orbits of test particles will be discussed below, following Vigeland and Hughes [23], as their discussion supersedes the one found in Collins and Hughes [22]. However we will write down the two perturbations used and discuss its effect on periaapse precession and the final superposition of the two used to obtain the pure quadrupole distortion (at least in the weak field). The first perturbations, in Weyl coordinates, are given by

$$\psi_1^{NP} = -\frac{\mu/2}{\sqrt{\rho^2 + (z-b)^2}}, \quad \psi_1^{SP} = -\frac{\mu/2}{\sqrt{\rho^2 + (z+b)^2}}, \quad (4.19)$$

and describe a point with mass  $\mu/2$  near the “north” and “south” pole, respectively. The complete perturbation is given by adding the two and yields (after integration of  $\gamma_1$  chosen to go to zero at large radius) the weak field periapsis precession

$$\Delta\phi^{points} = \Delta\phi_{Schw}(M + \mu) + \Delta\phi_{anom}(\mu) + \Delta\phi_{prol}(\mu, b), \quad (4.20)$$

where

$$\Delta\phi_{Schw}(M + \mu) = \frac{6\pi(M + \mu)}{p} + \frac{3\pi(M^2 + 2M\mu)}{2p^2}(18 + \varepsilon^2), \quad (4.21)$$

$$\Delta\phi_{anom}(\mu) = -\frac{\pi\mu M}{p^2}(1 + 2\varepsilon^2), \quad (4.22)$$

$$\Delta\phi_{prol}(\mu, b) = -\frac{3\pi\mu b^2}{Mp^2}, \quad (4.23)$$

and where  $p$  is the orbit’s semi-latus rectum and  $\varepsilon$  its eccentricity.

The second metric perturbation is a ring of total mass  $\mu$  with radius  $\rho = b$  given by

$$\psi_1^{ring} = -\frac{\mu}{2\pi} \int_0^{2\pi} \frac{d\xi}{[\rho^2 + z^2 + b^2 - 2b\rho \cos \xi]^{1/2}} \quad (4.24)$$

and, again, integration of  $\gamma_1$  leads to the weak field periapsis precession

$$\Delta\phi^{ring} = \Delta\phi_{Schw}(M + \mu) + \Delta\phi_{anom}(\mu) + \Delta\phi_{obl}(\mu, b), \quad (4.25)$$

$$\Delta\phi_{obl}(\mu, b) = \frac{3\pi\mu b^2}{2Mp^2}, \quad (4.26)$$

where  $\Delta\phi_{Schw}(M + \mu)$  and  $\Delta\phi_{anom}(\mu)$  are given by equations (4.21) and (4.22), respectively.

By superposing the two kinds of perturbations a pure quadrupolar deformation was achieved

$$\Delta\phi^{both} = \Delta\phi_{Schw}(M) + \Delta\phi_{quad}(\mu, b), \quad (4.27)$$

where

$$\Delta\phi_{quad}(\mu, b) = \pm \frac{9\pi\mu b^2}{2Mp^2}. \quad (4.28)$$

Collins and Hughes [22] attempt fell short in different ways. Besides only considering the non-rotating case, the perturbations dealt with were non-smooth which made non-equatorial strong-field orbits ill-behaved, as was later realized by Psaltis [23]. In addition, the scheme used allowed only for perturbations at the quadrupole moment.

In two companion papers Vigeland and Hughes [23, 74] carried out a solution of these problems. They continued directly Collins and Hughes approach but used pure multipoles instead of infinitesimal point and ring masses, which solves two of its shortcoming: the ill behaviour of non-equatorial orbits, and the possibility to choose which and how much to deform each multipole. The extension to spinning black holes was implemented by using the Newman-Janis algorithm [140, 141], described in appendix A. They study the effects of the deformation of the multipole on the orbital frequencies of a small orbiting

body, and show how to obtain a bumpy spacetime with a prescribed set of Geroch-Hansen multipole moments from the Weyl multipoles used in the construction of the perturbation functions.

Using the Newman-Janis algorithm (described in appendix A) to generalize bumpy black holes to the rotating case was straightforward and we simply quote the result for the bumpy Kerr metric:

$$\begin{aligned}
ds^2 = & -e^{2\psi_1} \left(1 - \frac{2Mr}{\Sigma}\right) dt^2 + e^{2\psi_1 - \gamma_1} (1 - e^{\gamma_1}) \frac{4a^2 Mr \sin^2 \theta}{\Delta \Sigma} dt dr - e^{2\psi_1 - \gamma_1} \frac{4a Mr \sin^2 \theta}{\Sigma} dt d\phi \\
& + e^{2\gamma_1 - 2\psi_1} \left(1 - \frac{2Mr}{\Sigma}\right)^{-1} \left[1 + e^{-2\gamma_1} (1 - 2e^{\gamma_1}) \frac{a^2 \sin^2 \theta}{\Delta} - e^{4\psi_1 - 4\gamma_1} (1 - e^{\gamma_1}) \frac{4a^4 M^2 r^2 \sin^4 \theta}{\Delta^2 \Sigma^2}\right] dr^2 \\
& - 2(1 - e^{\gamma_1}) a \sin^2 \theta \left[ e^{-2\psi_1} \left(1 - \frac{2Mr}{\Sigma}\right)^{-1} - e^{2\psi_1 - 2\gamma_1} \frac{4a^2 M^2 r^2 \sin^2 \theta}{\Delta \Sigma (\Sigma - 2Mr)} \right] dr d\phi \\
& + e^{2\gamma_1 - 2\psi_1} \Sigma d\theta^2 + \Delta \left[ e^{-2\psi_1} \left(1 - \frac{2Mr}{\Sigma}\right)^{-1} - e^{2\psi_1 - 2\gamma_1} \frac{4a^2 M^2 r^2 \sin^2 \theta}{\Delta \Sigma (\Sigma - 2Mr)} \right] \sin^2 \theta d\phi^2, \tag{4.29}
\end{aligned}$$

where we have the standard Kerr functions  $\Sigma = r^2 + a^2 \cos^2 \theta$  and  $\Delta = r^2 - 2Mr + a^2$ . We can write this metric in the form  $g_{\alpha\beta} = \hat{g}_{\alpha\beta} + b_{\alpha\beta}$ , where  $\hat{g}_{\alpha\beta}$  is the unperturbed Kerr metric and the non-zero components of  $b_{\alpha\beta}$  are given by

$$b_{tt} = -2 \left(1 - \frac{2Mr}{\Sigma}\right) \psi_1, \tag{4.30}$$

$$b_{tr} = -\gamma_1 \frac{2a^2 Mr \sin^2 \theta}{\Delta \Sigma}, \tag{4.31}$$

$$b_{t\phi} = (\gamma_1 - 2\psi_1) \frac{2a Mr \sin^2 \theta}{\Sigma}, \tag{4.32}$$

$$b_{rr} = 2(\gamma_1 - \psi_1) \frac{\Sigma}{\Delta}, \tag{4.33}$$

$$b_{r\phi} = \gamma_1 \left[ \left(1 - \frac{2Mr}{\Sigma}\right)^{-1} - \frac{4a^2 M^2 r^2 \sin^2 \theta}{\Delta \Sigma (\Sigma - 2Mr)} \right] a \sin^2 \theta, \tag{4.34}$$

$$b_{\theta\theta} = 2(\gamma_1 - \psi_1) \Sigma, \tag{4.35}$$

$$b_{\phi\phi} = \left[ (\gamma_1 - \psi_1) \frac{8a^2 M^2 r^2 \sin^2 \theta}{\Delta \Sigma (\Sigma - 2Mr)} - 2\psi_1 \left(1 - \frac{2Mr}{\Sigma}\right)^{-1} \right] \Delta \sin^2 \theta. \tag{4.36}$$

Reduction to the Kerr case is clear when  $\psi_1 \rightarrow 0$ ,  $\gamma_1 \rightarrow 0$ .

Having built the perturbed metric the authors proceed to analyse the shifts in orbital frequencies caused by the mass perturbations and in [74] Vigeland extends the perturbations to the current moments and maps both the mass and current perturbations used to the Geroch-Hansen multipoles.

The calculation of the effect of the deformations on the orbital frequencies was carried out using Hamilton-Jacobi theory. Following Schmidt [33], the orbital frequencies for the unperturbed Kerr metric

$$m\omega^i = \frac{\partial \mathcal{H}^{(aa)}}{\partial J_i} \tag{4.37}$$

where the action variables  $J_i$  are defined by

$$J_r \equiv \frac{1}{2\pi} \oint p_r dr \quad (4.38)$$

$$J_\theta \equiv \frac{1}{2\pi} \oint p_\theta d\theta \quad (4.39)$$

$$J_\phi \equiv \frac{1}{2\pi} \oint p_\phi d\phi \quad (4.40)$$

and  $\mathcal{H}^{(aa)}$  is the formal Hamiltonian reparametrized in terms of the action variables, which for the Kerr case cannot be given explicitly, forcing the calculation of the orbital frequencies to be done with the help of an intermediate matrix and the derivative chain rule. Their closed-form expression was explicitly calculated by Schmidt [33], but these frequencies  $\omega^{r,\theta,\phi}$  are conjugate to the orbit's proper time (they would be measured by an observer riding the orbit). For the frequencies  $\Omega^{r,\theta,\phi}$  measured by a distant observer the conversion is achieved through the formulas

$$\Omega^{r,\theta,\phi} = \frac{\omega^{r,\theta,\phi}}{\Gamma}, \quad \Gamma \equiv \frac{1}{m} \frac{\partial \mathcal{H}^{(aa)}}{\partial J_t} = -\frac{1}{m} \frac{\partial \mathcal{H}^{(aa)}}{\partial E}. \quad (4.41)$$

However for bumpy black hole metrics the equations of motion are not separable which implies that one cannot compute the orbital frequencies by following the procedure used by Schmidt [33]. Instead, the approach taken was to use perturbation theory since the bumpy metric is ‘‘close to’’ to the separable one. Denoting the separable Hamiltonian as  $\hat{\mathcal{H}}$ , we write the full Hamiltonian of the bumpy spacetime as

$$\mathcal{H} = \hat{\mathcal{H}} + \mathcal{H}_1 = \frac{1}{2} g^{\alpha\beta} p_\alpha p_\beta \quad (4.42)$$

where  $\mathcal{H}_1$  represents the perturbation to the separable Hamiltonian and, to first order in  $b_{\alpha\beta}$ , is given by

$$\mathcal{H}_1 = -\frac{1}{2} b_{\mu\nu} p^\mu p^\nu. \quad (4.43)$$

The shifts in the observable frequencies  $\delta\Omega^i$  can be computed through the formula

$$\Omega^i \equiv \hat{\Omega}^i + \delta\Omega^i = \frac{\hat{\omega}^i + \delta\omega^i}{\hat{\Gamma} + \delta\Gamma} \quad (4.44)$$

where it is found that the shifts  $\delta\omega^i$  and  $\delta\Gamma$  can be calculated by averaging  $\mathcal{H}_1$ :

$$m\delta\omega^i = \frac{\partial \langle \mathcal{H}_1 \rangle}{\partial \hat{J}_i}, \quad m\delta\Gamma = \frac{\partial \langle \mathcal{H}_1 \rangle}{\partial \hat{J}_t}, \quad (4.45)$$

again using an intermediate matrix and the chain rule.

As already mentioned, the functions  $\psi_1$  used by Vigeland and Hughes were different than Collins and Hughes' to avoid the ill-behaviour of non-equatorial orbits. Instead they used pure multipoles in the coordinates of the standard form of the Weyl metric. This does not translate into a pure multipolar perturbation of the Geroch-Hansen moments. However for a certain Weyl  $l$  multipole only Geroch-Hansen multipoles of order equal or larger than  $l$  are perturbed. This is calculated explicitly in [74] not just for

the mass perturbations but also for the spin perturbations and the results are condensed in table 4.1. Because the equations for  $\psi_1$  and  $\gamma_1$  (equations (4.9)-(4.11)) are linear in these fields, it is possible to set  $\psi_1$  as a combination of Weyl multipoles that translates into a distortion of the Geroch-Hansen moments for a single order.

			$\delta\mathcal{M}_0$	$\delta\mathcal{M}_1$	$\delta\mathcal{M}_2$	$\delta\mathcal{M}_3$	$\delta\mathcal{M}_4$	$\delta\mathcal{M}_5$
Mass	S	$l = 2$	0	0	$-\frac{1}{2}B_2M^3\sqrt{\frac{5}{\pi}}$	0	$\frac{4}{7}B_2M^5\sqrt{\frac{5}{\pi}}$	0
		$l = 3$	0	0	0	$-\frac{1}{2}B_3M^4\sqrt{\frac{7}{\pi}}$	0	$\frac{2}{3}B_3M^6\sqrt{\frac{7}{\pi}}$
	K	$l = 2$	0	0	$-\frac{1}{2}B_2M^3\sqrt{\frac{5}{\pi}}$	0	–	–
		$l = 3$	0	0	0	$\frac{2}{3}B_3M^6\sqrt{\frac{7}{\pi}}$	0	–
Current	S	$l = 2$	0	0	$i\frac{1}{4}S_2M^3\sqrt{\frac{5}{\pi}}$	0	$-i\frac{1}{28}S_2M^5\sqrt{\frac{5}{\pi}}$	0
		$l = 3$	0	0	0	$i\frac{1}{12}S_3M^4\sqrt{\frac{7}{\pi}}$	0	$-i\frac{1}{36}S_3M^6\sqrt{\frac{7}{\pi}}$
	K	$l = 2$	0	0	$i\frac{1}{4}S_2M^3\sqrt{\frac{5}{\pi}}$	0	–	–
		$l = 3$	0	0	0	$i\frac{1}{12}S_3M^4\sqrt{\frac{7}{\pi}}$	0	–

Table 4.1: Changes to the first few Geroch-Hansen multipole moments of bumpy black holes, for different mass and current perturbations, computed by Vigeland [74]. (S - Schwarzschild, K - Kerr).

We write down the perturbation  $\psi_1$  of order  $l = 2$ , where  $B_2$  is a dimensionless constant that quantifies the magnitude of the perturbation,

$$\psi_1^{l=2}(\rho, z) = B_2M^3 \frac{Y_{20}(\theta_{Weyl})}{(\rho^2 + z^2)^{3/2}} = \frac{B_2M^3}{4} \sqrt{\frac{5}{\pi}} \frac{3 \cos^2 \theta_{Weyl} - 1}{(\rho^2 + z^2)^{3/2}}, \quad (4.46)$$

and where  $\cos \theta_{Weyl} = z/\sqrt{\rho^2 + z^2}$ . Now the procedure is to integrate  $\gamma_1$ , obtain  $b_{\mu\nu}$  and calculate the shifts in orbital frequencies through the derivative of the averaging of  $\mathcal{H}_1 = -\frac{1}{2}b_{\mu\nu}p^\mu p^\nu$ . The results for the three shifts  $\Omega^{r,\theta,\phi}$  are shown in figure 4.1 in function of  $p$ , normalized by  $B_2$  and rescaled by the asymptotic weak-field dependence  $\delta\Omega_{l=2}^x$ , for different values of the eccentricity  $e$  and minimum polar angle reached by the orbit  $\theta_{min}$ . In figure 4.2 the shifts  $\Omega^{r,\theta,\phi}$  are shown for a  $l = 2$  perturbation to the Kerr metric for different values of the spin  $a$ .

### 4.1.2 Quasi-Kerr spacetimes

A different step in the development of the bumpy black hole framework was taken by Glampedakis and Babak [25]. Assuming the spacetime was at most slightly different from Kerr (‘quasi-Kerr’) they quantified this deviation, taking the ‘quasi-Kerr’ spacetime multipolar structure as given by,

$$M_l = M_l^K + \delta M_l, \quad l \geq 2 \quad (4.47)$$

$$S_l = S_l^K + \delta S_l, \quad l \geq 3 \quad (4.48)$$

where the deviations are small.

The approach chosen was to only take in account the quadrupolar deviation and neglect all higher

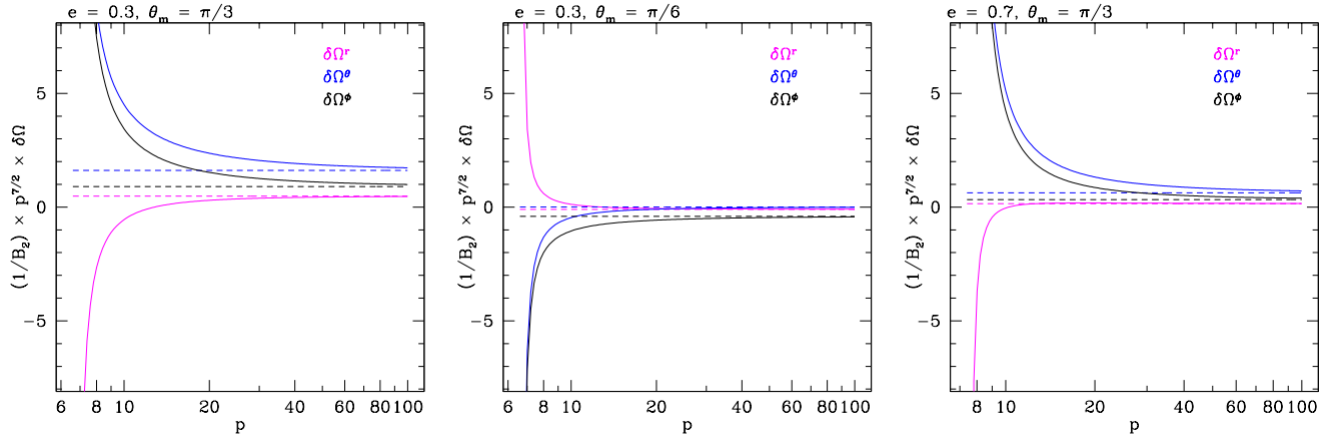


Figure 4.1: Shifts to Schwarzschild black hole orbital frequencies due to an  $l = 2$  bump. The shifts  $\Omega^{r,\theta,\phi}$  are normalized by the bumpiness parameter  $B_2$  and scaled by  $p^{7/2}$ , since in the Newtonian limit  $\Omega^{r,\theta,\phi} \propto p^{7/2}$ . (Figure 1 of [23]).

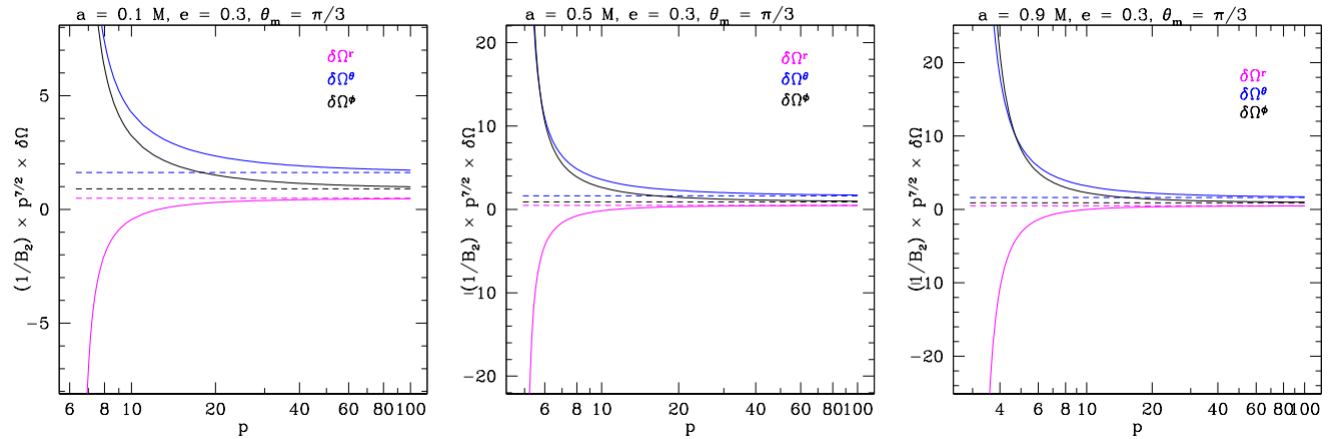


Figure 4.2: Shifts to Kerr black hole orbital frequencies for an  $l = 2$  bump. (Figure 3 of [23]).

order moments. Introducing the dimensionless deviation parameter  $\epsilon$

$$M_2 = M_2^K - \epsilon M^3 \quad (4.49)$$

the quasi-Kerr metric takes the form

$$g_{ab} = g_{ab}^K + \epsilon h_{ab} + O(\delta M_{l \geq 4}, \delta S_{l \geq 3}) \quad (4.50)$$

where  $g_{ab}^K$  is the exact Kerr metric and one is to find the functions  $h_{\alpha\beta}$ .

This was achieved through the Hartle-Thorne (H-T) metric [142] which describes the spacetime of any slowly rotating axisymmetric and stationary body. We will not describe the method explicitly but

will write down the expressions obtained for the contravariant components of the functions  $h_{\alpha\beta}$

$$h^{tt} = (1 - 2M/r)^{-1}[(1 - 3 \cos^2 \theta)\mathcal{F}_1(r)], \quad h^{rr} = (1 - 2M/r)[(1 - 3 \cos^2 \theta)\mathcal{F}_1(r)] \quad (4.51)$$

$$h^{\theta\theta} = -\frac{1}{r^2}[(1 - 3 \cos^2 \theta)\mathcal{F}_2(r)], \quad h^{\phi\phi} = -\frac{1}{r^2 \sin^2 \theta}[(1 - 3 \cos^2 \theta)\mathcal{F}_2(r)] \quad (4.52)$$

$$h^{t\phi} = 0, \quad (4.53)$$

where the functions  $\mathcal{F}_{1,2}(r, \theta)$  are given in appendix A of [25].

As pointed out by Glampedakis and Babak, it is assumed that the spacetime has non-zero higher moments so that terms of order  $O(\epsilon a, \epsilon^2)$  can be neglected. Another point is that the functions  $\mathcal{F}_{1,2}(r, \theta)$  diverge as  $r \rightarrow 2M$  which is a characteristic of the Kerr metric due to the event horizon, but as the quasi-Kerr metric is not associated with a black hole it is unclear what  $r = 2M$  means. However this is not problematic if only orbits sufficiently far from  $2M$  are considered. On the other hand, this metric should be suitable for probing strong-field as it is not an expansion in inverse powers of  $r$ .

Glampedakis and Babak have also studied geodesic motion (mainly on equatorial orbits) and EMRIs gravitational waveforms in the quasi-Kerr spacetime and compared it with the Kerr case. For equatorial orbits the number of cycles  $\mathcal{N}$  required to accumulate  $\pi/2$  in the periastron shift was computed

$$\mathcal{N} = \frac{\pi/2}{|\Delta\phi_K - \Delta\phi_{qK}|}. \quad (4.54)$$

For the pair of orbits with parameters  $(p, e, a) = (10M, 0.5, 0.5M), (15M, 0.5, 0.5M)$ , where  $p$  is the semi-latus rectum and  $e$  the eccentricity, it was found that for a value as low as  $\epsilon = 0.05$  (corresponding to a difference in the quadrupole moment of about 8%) one needs only about  $\sim 100 - 200$  orbits to accumulate a  $\pi/2$  difference in periastron shift. This is shown in figure 4.3.

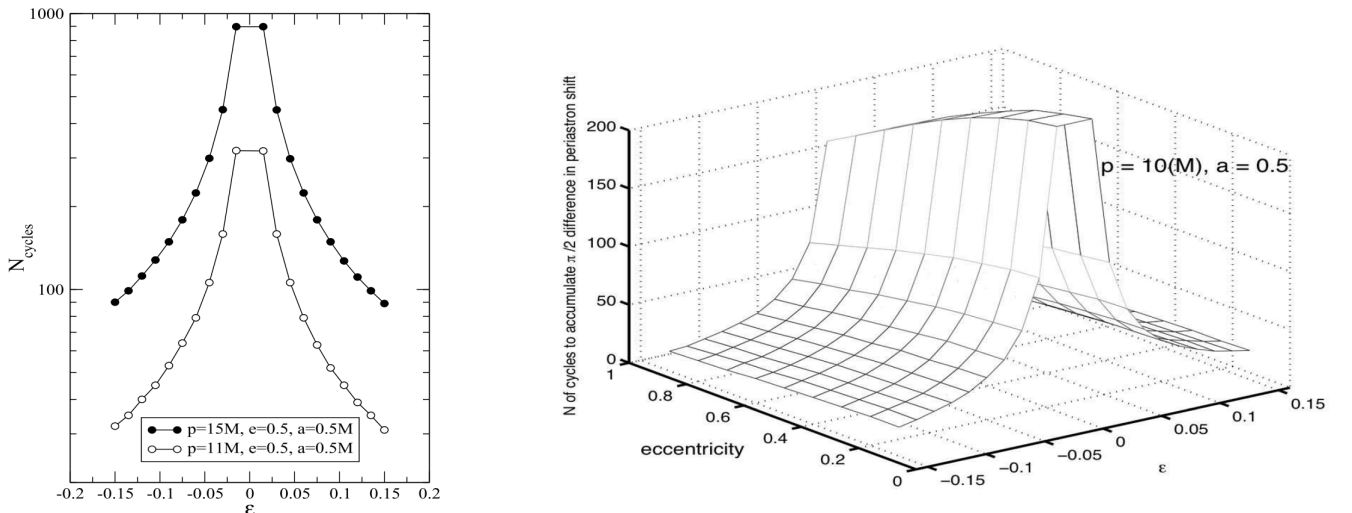


Figure 4.3: Left: Number of cycles  $\mathcal{N}$ , as a function of  $\epsilon$ , required to accumulate  $\pi/2$  difference in periastron shifts, for the two orbits:  $(p, e, a) = (10M, 0.5, 0.5M), (15M, 0.5, 0.5M)$ . Right: Number of cycles  $\mathcal{N}$  required to accumulate  $\pi/2$  difference in periastron shifts as a functions of  $e$  and eccentricity  $e$  for the two fixed parameters  $p = 10M$  and  $a = 0.5M$ . (Figures 1b and 3 of [25]).

The waveform analysis is much harder since, unlike the Kerr case, this quasi-Kerr metric is not of

Petrov type-D which implies that the Teukolsky formalism [143] is not applicable. Instead, Glampedakis and Babak carried out a much simpler and preliminary analysis using approximate waveforms. For the same initial kinematic conditions and the same orbital parameters  $(p, e)$  and spin  $a/M$ , they find that after a time lapse  $\sim T_{RR}$  the accumulated phase-difference between the Kerr and quasi-Kerr waveform is quite significant (see figure 4.4), for  $(p, e, a, \epsilon, \mu/M) = (10M, 0.5, 0.5M, 0.15, \sim 10^{-5})$  which corresponds to a fractional difference of about 40% of the quadrupolar moment ( $T_{RR}$  is defined as the interval of time at which the overlap between Kerr waveforms with and without radiation reaction drops below 95%). Another conclusion drawn is that the phase-difference of the Kerr and quasi-Kerr waveform is more pronounced for smaller  $p$  and smaller  $e$ , which is expected as in this region of the parameter space the body spends more time in the strong-field where the deviation from Kerr is stronger.

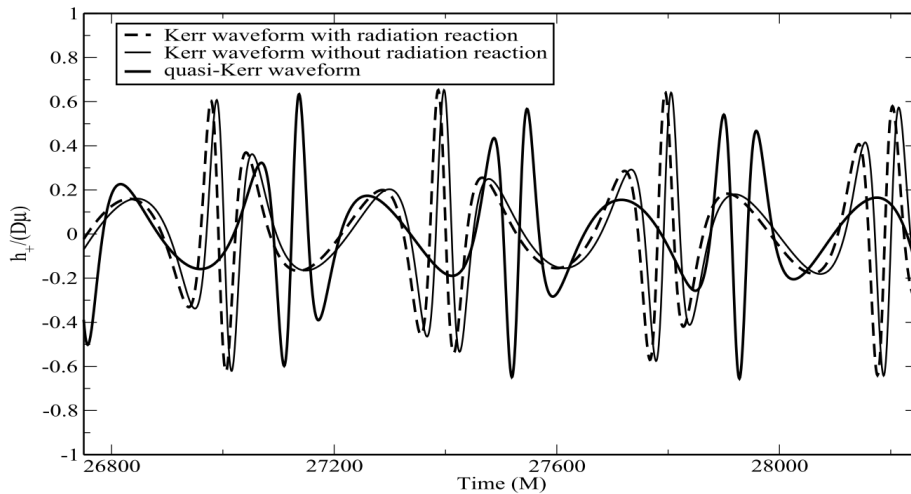


Figure 4.4: Approximate hybrid waveforms of the quasi-Kerr and Kerr metrics (with and without radiation reaction) for the orbit  $p = 10M$ ,  $e = 0.5$ ,  $a = 0.5M$  and for  $\epsilon = 0.15$ , shown at a time window close to the radiation reaction timescale  $T_{RR}$ . (Figure 4 of [25]).

The last section of Glampedakis and Babak’s paper is a prelude to the ‘confusion problem’, which is the possibility of not being able to recognize the difference between a Kerr waveform with a certain set of orbital parameters and quasi-Kerr waveform with a different set of orbital parameters. They give a particular case as an example: for a time interval  $\sim T_{RR}$  there is an overlap of 97.6% between a quasi-Kerr waveform with  $(p, e) = (10M, 0.3)$  and a Kerr waveform with  $(p, e)_K = (9.906M, 0.317)$ , for the particular case of  $\mu/M = 10^{-5}$ ,  $a = 0.3M$  and  $\epsilon = 0.1$ .

### 4.1.3 Bumpy black holes in alternative theories

The bumpy black hole formalism described so far has one key feature that makes it unsuitable for testing alternative theories of gravity: it assumes Einstein’s equations hold, at least to first order. This assumption is imposed as a restraint on the metric perturbations used. Vigeland, Yunes and Stein [24] have suggested a new approach. The idea is to build a scheme that allows for non-GR deviations in a model-independent way while testing the Kerr black hole hypothesis, and they propose two such perturbations: the generalized bumpy Kerr (BK) and the generalized deformed Kerr (DK). In both these schemes the perturbed spacetimes must satisfy the restraint that there exists an approximate

second-order Killing tensor implying the existence of a Carter constant, besides a conserved energy and a conserved angular momentum respectively associated with the stationarity and axisymmetry of the spacetime. The authors note this is not a strictly necessary condition, but that all black hole solutions in alternative theories that are not pathological do possess three constants of the motion [144], such as the slowly rotating solution in dynamical Chern-Simons modified gravity [145] and the spherically symmetric solution found in dynamical quadratic gravity [146, 147].

The generalized bumpy formalism picks up the standard one at the bumpy Kerr metric:

$$g_{\mu\nu} = \bar{g}_{\mu\nu} + \epsilon h_{\mu\nu}^{BK}, \quad (4.55)$$

where  $\bar{g}_{\mu\nu}$  is the background Kerr metric. In the standard bumpy formalism the non-zero components of  $h_{\mu\nu}^{BK}$  are some specific functions of the perturbations  $(\psi_1, \gamma_1, \sigma_1)$  which in turn are functions of  $(r, \theta)$ . The generalization suggested is to take these non-zero components  $(h_{tt}^{BK}, h_{tr}^{BK}, h_{t\phi}^{BK}, h_{rr}^{BK}, h_{r\phi}^{BK}, h_{\theta\theta}^{BK}, h_{\phi\phi}^{BK})$  as arbitrary functions of  $(r, \theta)$ , restricted only by the requirement that there exists an approximate second-order Killing tensor.

This Killing tensor is parametrized as

$$\xi_{\alpha\beta} = \Delta k_{(\alpha} l_{\beta)} + r^2 g_{\alpha\beta} \quad (4.56)$$

where  $g_{\alpha\beta}$  is the full metric so that although the functional form of the Killing tensor is the same,  $k^\alpha$  and  $l^\alpha$  do not necessarily correspond to the Kerr case where, in Boyer-Lindquist coordinates,

$$k^\alpha = \left[ \frac{r^2 + a^2}{\Delta}, 1, 0, \frac{a}{\Delta} \right], \quad l^\alpha = \left[ \frac{r^2 + a^2}{\Delta}, -1, 0, \frac{a}{\Delta} \right]. \quad (4.57)$$

In fact these three quantities are expanded into

$$k^\alpha = \bar{k}^\alpha + \epsilon \delta k^\alpha, \quad (4.58)$$

$$l^\alpha = \bar{l}^\alpha + \epsilon \delta l^\alpha, \quad (4.59)$$

$$\xi_{\alpha\beta} = \bar{\xi}_{\alpha\beta} + \epsilon \delta \xi_{\alpha\beta} \equiv [\delta k_{(\alpha} l_{\beta)} + \delta l_{(\alpha} k_{\beta)} + 2h_{\delta(\alpha} \bar{k}_{\beta)} \bar{l}^{\delta]} + 3r^2 h_{\alpha\beta}^{BK}. \quad (4.60)$$

The Killing tensor equation

$$\nabla_{(\alpha} \xi_{\beta\delta)} = 0 \quad (4.61)$$

becomes then

$$\partial_{(\mu} \delta \xi_{\alpha\beta)} - 2\bar{\Gamma}_{(\mu\alpha}^{\delta} \delta \xi_{\beta)\delta} = 2\delta \Gamma_{(\mu\alpha}^{\delta} \bar{\xi}_{\beta)\delta} \quad (4.62)$$

which consists of 20 partial differential equations, with two additional algebraic equations in the form of

the normalization conditions  $l^\alpha l_\alpha = 0 = k^\alpha k_\alpha$ . This turns out to be solvable and it was found that

$$\begin{aligned}\delta k_{BK}^\alpha &= \left[ \frac{r^2 + a^2}{\Delta} \delta k_{BK}^r + \delta_1, \delta k_{BK}^r, 0, \frac{a}{\Delta} \delta k_{BK}^r + \delta_2 \right] \\ \delta l_{BK}^\alpha &= \left[ \frac{r^2 + a^2}{\Delta} \delta k_{BK}^r + \delta_3, \delta k_{BK}^r + \delta_4, 0, \frac{a}{\Delta} \delta k_{BK}^r + \delta_5 \right]\end{aligned}\quad (4.63)$$

where  $\delta_i$  are arbitrary functions of  $r$ , fully determined by equations involving the metric perturbations and functions of  $r$  and  $\theta$  (which we do not write down).

With these perturbations the approximate constants and first-order equations of the motion can be found, as well as the perturbation of Kepler's law:

$$|\Omega| = |\bar{\Omega}| - \frac{M^{1/2}(r^{1/2}(r - 3M) + 2aM^{1/2})}{r^{5/4}(r^{3/2} + aM^{1/2})} \delta T(r) + \frac{M^{1/2}(r^{1/2}(r - 3M) + 2aM^{1/2})^{1/2}}{r^{5/4}(r^{3/2} + aM^{1/2})} \delta \Phi(r) \quad (4.64)$$

where

$$|\bar{\Omega}| \equiv |\dot{\phi}/\dot{t}| = \frac{M^{1/2}}{r^{3/2} + aM^{1/2}}, \quad (4.65)$$

and where an overhead bar denotes background quantities, such that the full metric  $g_{\mu\nu} = \bar{g}_{\mu\nu} + \epsilon h_{\mu\nu}$  can be decomposed into a background metric and a small perturbation. The perturbations to the potential functions of the geodesic equations are denoted by  $\delta T$  and  $\delta \Phi$  (as described in [24]).

A second similar approach was also put forward: the deformed Kerr (DK) formalism, which perturbs the most general stationary and axisymmetric line element

$$ds^2 = -V(dt - wd\phi)^2 + V^{-1}\rho^2 d\phi^2 + \Omega(d\rho^2 + \Lambda dz^2) \quad (4.66)$$

and proceeds in a similar way to the generalized bumpy Kerr perturbation. The two formalisms differ in some of the perturbed metric components, but the two parametrizations were mapped to each other and to specific black hole solutions in alternative theories of gravity, namely the dynamical Chern-Simons gravity slowly rotating solution [145] and the nonspinning black hole in dynamical quadratic gravity [147]. Gravitational waveforms for these bumpy metrics have been computed by Gair and Yunes [148].

## 4.2 Manko-Novikov spacetimes

Although uniqueness theorems imply that vacuum stationary asymptotically flat generalizations of the Kerr metric within GR will have naked singularities or closed timelike curves, one could still think of using one such metric as a candidate for tests of the Kerr black hole hypothesis. Besides the possibility that the assumptions of the theorems are not in fact realized in nature, one could expect that a generalization sufficiently close to the Kerr case would still contain most of the spacetime properties common to non-Kerr spacetimes.

The Manko-Novikov spacetimes [26] are a family of stationary, asymptotically flat, exact solutions of the Einstein-Maxwell solutions with an infinite number of parameters, generalizing the Kerr-Newman solution. Because astrophysical black holes are thought to be neutral, in this context one usually considers

only the uncharged family. They are characterized by the two parameters  $M$  and  $a$ , and an infinite number of other parameters.

The construction of the solution starts with the Lewis-Papapetrou metric, the most general stationary axisymmetric vacuum case, in prolate spheroidal coordinates:

$$ds^2 = k^2 f^{-1} \left[ e^{2\gamma} (x^2 - y^2) \left( \frac{dx^2}{x^2 - 1} - \frac{dy^2}{y^2 - 1} \right) + (x^2 - 1)(1 - y^2) d\phi^2 \right] - f(dt - \omega d\phi)^2, \quad (4.67)$$

where  $k$  is a real constant and  $f$ ,  $\gamma$  and  $\omega$  are unknown functions of  $(x, y)$ , coordinates that are related to the the cylindrical coordinates  $\rho$  and  $z$  by

$$\rho = k\sqrt{(x^2 - 1)(1 - y^2)}, \quad z = kxy. \quad (4.68)$$

In these coordinates, the Ernst potential is defined by

$$\mathcal{E} = f + i\Omega, \quad (4.69)$$

$$\Omega_x = k^{-1}(x^2 - 1)^{-1} f^2 \omega_y, \quad \Omega_y = k^{-1}(y^2 - 1)^{-1} f^2 \omega_x \quad (4.70)$$

(where the subscripts  $x$  and  $y$  denote partial differentiation) and satisfies the Ernst equation

$$(\mathcal{E} + \mathcal{E}^*)\Delta\mathcal{E} = 2(\nabla\mathcal{E})^2, \quad (4.71)$$

where the operators are given by

$$\Delta = k^{-2}(x^2 - y^2)^{-1} \{ \partial_x [(x^2 - 1)\partial_x] + \partial_y [(1 - y^2)\partial_y] \} \quad (4.72)$$

$$\nabla = k^{-1}(x^2 - y^2)^{-1/2} [x_0(x^2 - 1)^{1/2}\partial_x + y_0(1 - y^2)^{1/2}\partial_y] \quad (4.73)$$

Thus if one has a solution of the Ernst equation by the above equations we can find  $f$  and  $\omega$  (see section 2.2.1), and  $\gamma$  can be found from the two following differential equations:

$$\gamma_x = \frac{1 - y^2}{(x^2 - y^2)(\mathcal{E} + \mathcal{E}^*)^2} [x(x^2 - 1)\mathcal{E}_x\mathcal{E}_x^* - x(1 - y^2)\mathcal{E}_y\mathcal{E}_y^* - y(x^2 - 1)(\mathcal{E}_x\mathcal{E}_y^* + \mathcal{E}_y\mathcal{E}_x^*)] \quad (4.74)$$

$$\gamma_y = \frac{x^2 - 1}{(x^2 - y^2)(\mathcal{E} + \mathcal{E}^*)^2} [y(x^2 - 1)\mathcal{E}_x\mathcal{E}_x^* - y(1 - y^2)\mathcal{E}_y\mathcal{E}_y^* - x(1 - y^2)(\mathcal{E}_x\mathcal{E}_y^* + \mathcal{E}_y\mathcal{E}_x^*)]. \quad (4.75)$$

Gutsunaev and Manko have shown [149] that the Ernst potential of a nonlinear superposition of the Kerr solution with an arbitrary static Weyl solution can be written as follows:

$$\mathcal{E} = e^{2\psi} A_- / A_+ \quad (4.76)$$

$$A_{\mp} \equiv x(1 + ab) + iy(b - a) \mp (1 - ia)(1 - ib) \quad (4.77)$$

where  $\psi$  is any solution of the equation  $\Delta\psi = 0$ , and the functions  $a$  (not to be confused with the usual

Kerr spin parameter) and  $b$  satisfy the first-order differential equations

$$\begin{aligned}
(x-y)a_x &= 2a[(xy-1)\psi_x + (1-y^2)\psi_y], \\
(x-y)a_y &= 2a[-(x^2-1)\psi_x + (xy-1)\psi_y], \\
(x+y)b_x &= -2b[(xy+1)\psi_x + (1-y^2)\psi_y], \\
(x+y)b_y &= -2b[-(x^2-1)\psi_x + (xy+1)\psi_y].
\end{aligned} \tag{4.78}$$

There is an additional sufficient condition that these functions should satisfy so that the solutions are asymptotically flat:

$$\psi = O(1/x), \quad a = -\alpha + O(1/x), \quad b = \alpha + O(1/x) \tag{4.79}$$

when  $x \rightarrow \infty$  and where  $\alpha$  is a constant.

The expressions for the metric functions  $f$ ,  $\gamma$  and  $\omega$  were computed in [150] and are given by

$$f = e^{2\psi} A/B \tag{4.80}$$

$$e^{2\gamma} = e^{2\gamma'} A(x^2-1)^{-1}(1-\alpha^2)^{-2}, \quad \omega = 2ke^{-2\psi} CA^{-1} - 4k\alpha(1-\alpha^2)^{-1} \tag{4.81}$$

$$A \equiv (x^2-1)(1+ab)^2 - (1-y^2)(b-a)^2 \tag{4.82}$$

$$B \equiv [x+1+(x-1)ab]^2 + [(1+y)a+(1-y)b]^2 \tag{4.83}$$

$$C \equiv (x^2-1)(1+ab)[b-a-y(a+b)] + (1-y^2)(b-a)[1+ab+x(1-ab)] \tag{4.84}$$

where  $\gamma'$  is the function  $\gamma$  of the static vacuum solution metric determined by  $\psi' = \frac{1}{2} \ln[(x-1)/(x+1)] + \psi$ . These formulae were used in [150] to construct a superposition of the Kerr metric with the Erez-Rosen solution, a version of which had already been carried out by [151] using the Hoenselaer-Kinnersley-Xanthopoulos (HKX) transformations [152]; however both attempts suffer from two drawbacks: they have a completely singular event horizon and the expression for the metric function  $\gamma$  is extremely cumbersome.

The approach taken by Manko and Novikov was to choose  $\psi$  as a sum of ordinary Weyl multipoles:

$$\psi = \sum_{n=1}^{\infty} \beta_n \psi_n = \sum_{n=1}^{\infty} \beta_n R^{-n-1} P_n(xy/R), \tag{4.85}$$

$$R \equiv (x^2 + y^2 - 1)^{1/2}, \quad \beta_n = \text{const} \tag{4.86}$$

where  $\Delta\psi_n = 0$  is satisfied by each  $\psi_n$ , and  $P_n$  are the Legendre polynomials.

With this choice, the expressions for  $a$  and  $b$  can now be found by integration of equations (4.78) and result in

$$a(x, y) = -\alpha \exp \left( - \sum_{n=1}^{\infty} \sum_{l=0}^n 2\beta_n [(x-y)R^{-l-1}P_l - 1] \right) \quad (4.87)$$

$$b(x, y) = \alpha \exp \left( \sum_{n=1}^{\infty} \sum_{l=0}^n 2\beta_n [(-1)^{n-l+1}(x+y)R^{-l-1}P_l + (-1)^n] \right) \quad (4.88)$$

whereas  $\gamma'$  is given by

$$\begin{aligned} \gamma' = \frac{1}{2} \ln \frac{x^2 - 1}{x^2 - y^2} + \sum_{m,n=1}^{\infty} \frac{\beta_m \beta_n (m+1)(n+1)}{(m+n+2)R^{m+n+2}} (P_{m+1}P_{n+1} - P_m P_n) \\ + \sum_{n=1}^{\infty} \sum_{l=0}^n \beta_n \left( \frac{x-y + (-1)^{n-l}(x+y)}{R^{l+1}} P_l - 1 + (-1)^{n+1} \right). \end{aligned} \quad (4.89)$$

After obtaining all the metric functions of this generalization of the Kerr metric with an infinite number of free parameters  $\beta_n$ , Manko and Novikov calculated [26, 153] its first Geroch-Hansen multipole moments:

$$\begin{aligned} M_0 &= k(1 + \alpha^2)/(1 - \alpha^2), & J_0 &= 0, \\ M_1 &= -k^2\beta_1, & J_1 &= -2\alpha k^2(1 + \alpha^2)/(1 - \alpha^2)^2, \\ M_2 &= -k^3[\beta_2 + 4\alpha^2(1 + \alpha^2)(1 - \alpha^2)^{-3}], & J_2 &= 4\alpha\beta_1 k^3/(1 - \alpha^2), \\ M_3 &= k^4[-\beta_3 + \beta_1(\alpha^4 + 10\alpha^2 + 1)(1 - \alpha^2)^{-2}], & J_3 &= 4\alpha k^4[\beta_2 + 2\alpha^2(1 + \alpha^2)(1 - \alpha^2)^{-3}]/(1 - \alpha^2). \end{aligned} \quad (4.90)$$

Setting  $\beta_1 = 0$  so that the dipole moment is zero, the center of mass is brought to the origin of the coordinate system. It is clear than in order to get a different quadrupole moment than that of Kerr a non-vanishing  $\beta_2$  is needed.

Gair, Li and Mandel [154] have studied in detail the Manko-Novikov spacetime in the case where all the  $\beta_n$  free parameters are equal to zero, except for  $\beta_2$ . This simplifies the formulas above considerably and, writing  $\beta \equiv \beta_2$ , in particular  $\psi$  is given by

$$\psi = \psi_2 = \beta R^{-3} P_2(xy/R). \quad (4.91)$$

Now defining the mass  $M \equiv M_0$ , spin  $a \equiv S_1/M$  and quadrupole deviation  $q \equiv \frac{\Delta M_2}{M^3} \equiv \frac{M_{2,K} - M_2}{M^3}$ , where  $tM_{2,K} = -Ma^2$  is Kerr's quadrupole moment, we can relate these to the three metric parameters  $\alpha$ ,  $k$  and  $\beta$  by

$$\alpha = \frac{-M + \sqrt{M^2 - a^2}}{a}, \quad k = M \frac{1 - \alpha^2}{1 + \alpha^2}, \quad \beta = q \frac{M^3}{k^3} \quad (4.92)$$

From the expressions of the multipole moments (equations (4.90)) we find that the ratio of the deviation to the Kerr quadrupole moment is a decreasing function of  $a$ , which is half the one for  $J_3$ , both of which vanish (independently of the value of  $\beta_2$ ) in the limit of the extremal black hole,  $a \rightarrow M$ :

$$\frac{\Delta M_2}{M_{2,K}} = \beta_2 \frac{(M^2 - a^2)^{3/2}}{Ma^2} = \frac{1}{2} \frac{\Delta J_3}{J_{3,K}} \quad (4.93)$$

Being arbitrarily close to Kerr, one could expect that the Manko-Novikov spacetime still possesses some of its properties. However the no-hair theorem implies that it either lacks an event horizon or else contains closed timelike curves (CTC) exterior to a horizon, and in fact both of these happen. It turns out that the event horizon is singular on the equatorial line and that, not unlike the modified ergosphere, there are regions of closed timelike curves as is shown in figure 4.5, for a positive, a negative and a null value of  $q$ . It can be seen that both the ergosphere and the CTC zone have a multiple lobed structure, and that there are regions of overlap between the two.

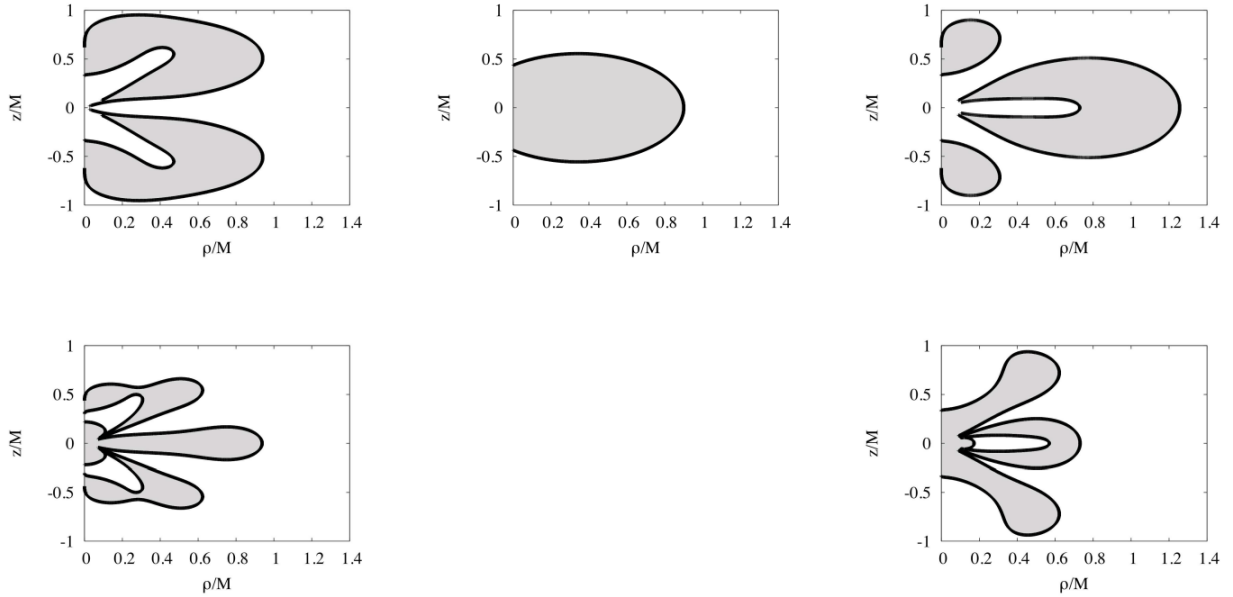


Figure 4.5: Boundaries of the ergoregion and of the region with closed timelike curves for  $a/M = 0.9$ . The upper row shows zeros of  $g_{tt}$  (which defines the boundary of the ergoregion) and the bottom row shows points where  $g_{\phi\phi}$  changes sign (which defines the region where closed timelike curves exist). The left, center and right column correspond to values of  $q = -1, 0, 1$  respectively. Since there is no region of CTCs in the Kerr spacetime the middle bottom panel is empty. (Figure 1 of [154]).

The main results of Gair, Li and Mandel's analysis are: (i) the verification that most of the orbits in the Manko-Novikov spacetime appear to have a fourth integral of the motion and that in general ergodic motion appears only in regions very close to the central body, probably too close for clear observation; (ii) the existence of non-Kerr radial and vertical instabilities of the last stable circular orbit (ISCO); (iii) the calculations of the strong and weak-field precession frequencies of the periaapsis and orbital-plane for nearly circular and nearly equatorial orbits.

As with any stationary axisymmetric spacetime, motion is governed by an effective potential:

$$\frac{1}{2}(\dot{\rho}^2 + \dot{z}^2) + V_{eff}(\rho, z) = 0, \quad (4.94)$$

where the effective potential is determined by the metric functions and given by

$$V_{eff}(\rho, z) = \frac{1}{2}e^{-2\gamma} \left[ f - E^2 + \left( \frac{f}{\rho} (L_z - \omega E) \right)^2 \right]. \quad (4.95)$$

Because  $\frac{1}{2}(\dot{\rho}^2 + \dot{z}^2)$  is always non-negative, orbits are only allowed for regions where  $V_{eff} < 0$ , whose

boundary is the curve  $V_{eff} = 0$ , the so called curve of zero-velocity (CZV) since  $\dot{\rho}$  and  $\dot{z}$  become zero as the orbit approaches it. Figure 4.6 shows these regions for the perturbed and pure Kerr case, and it is found that for  $q < 0$  there are two main disconnected regions where motion is allowed: a small inner region and a much larger outer one. When  $q > 0$ , there is a range of the parameters  $a/M$ ,  $E$  and  $L_z$  for which the inner and outer regions are connected by a neck.

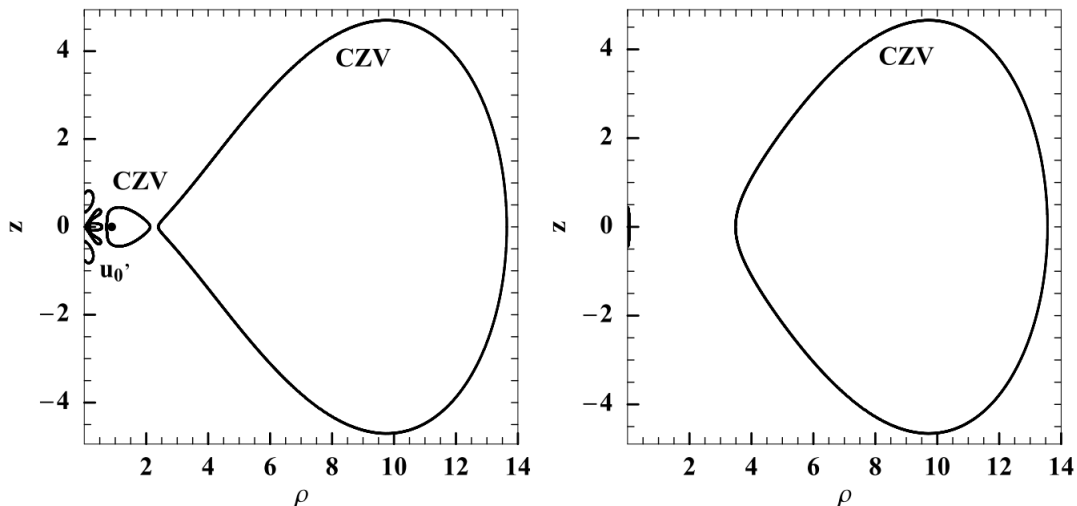


Figure 4.6: Left: The permissible regions (inside the CZVs) of motion on the meridian plane  $(\rho, z)$  for the parameters  $E = 0.95$ ,  $L_z = 3$ ,  $q = 0.95$ ,  $a/M = 0.9$  and  $M = 1$ . Right: The permissible region in the corresponding Kerr case ( $q = 0$  and all other parameters as in the left panel). (Figure 2 of [104]).

Gair, Li and Mandel carry out an analysis of these regions for several values of the parameters, and by plotting Poincaré maps (see figure 4.7) they conclude that all orbits in the outer region appear to be regular, while orbits inside the inner CZV appear to be ergodic. As pointed out by the authors this is only an indication, and in fact a later analysis by Apostolatos, Lukes-Gerakopoulos and Contopoulos [102] revealed the ergodic motion in the outer region as well, as described below.

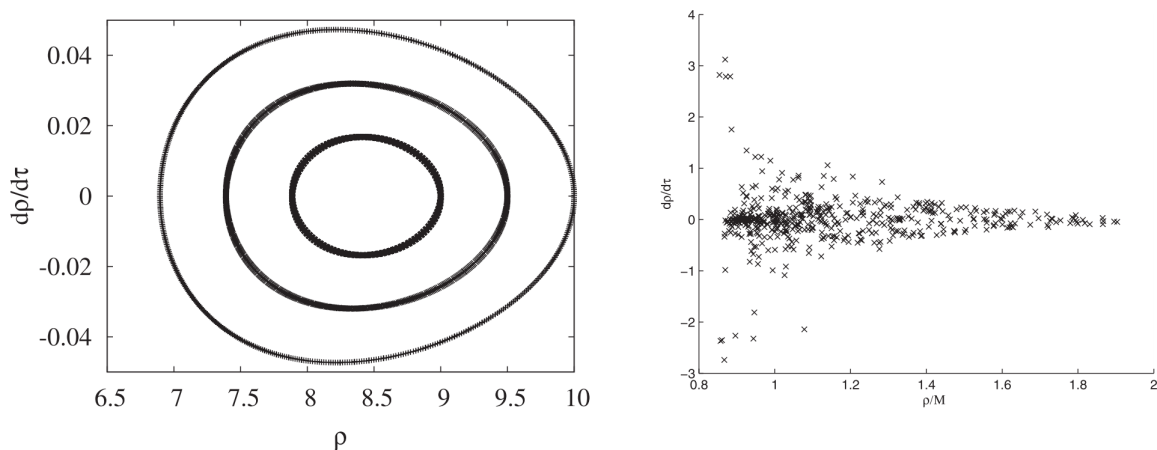


Figure 4.7: Left: Poincaré map showing  $d\rho = d\tau$  vs  $\rho$  for crossings of the  $z = 0$  plane for a sequence of orbits in the outer allowed region of the Kerr spacetime with  $E = 0.95$ ,  $L_z = 3M$ , and  $a/M = 0.9$ . Right: Poincaré map for a geodesic in the inner region. (Figures 5 and 7 of [154]).

An observable feature of the non-Kerrness of the spacetime would be to see an inspiraling orbit make

the transition from regular to ergodic motion, which could be found by frequency component analysis of the  $\rho$  and  $z$  motion. In case of completely regular motion, at some moment the gravitational radiation would cease to be emitted, instead of switching to the chaotic regime. This method was however found to be very unlikely to work due to how close to central body ergodic motion was found to be limited to.

Another observable considered was the orbital frequency of the innermost stable circular orbit (ISCO). It was found that this frequency is significantly dependent on the deviation parameter  $q$ , and that for some values of  $q$  a vertical instability arises, which is not present in the Kerr case. Precession frequencies of the periapsis and orbital-plane for nearly circular and nearly equatorial orbit were calculated and agree in the weak-field with Ryan [69], Collins and Hughes [22] and Glampedakis and Babak [25]. It is argued that this is the first analysis to be valid in the strong-field regime, as it does not rely on perturbation theory or on a weak-field expansion. Its main result is the divergence of one of the precession frequencies which is arrived at from spacetime-independent considerations and should accordingly apply in more general cases than the Manko-Novikov one.

Bambi and Barausse [155, 156] have studied how the structure of thin accretion discs is modified for these spacetimes. Unlike Kerr, there are now regions where equatorial vertical instabilities exist, leading to a different inner edge of the disc, and to the possibility that a thick inner disc forms from trapped particles.

Apostolatos, Lukes-Gerakopoulos and Contopoulos put forward [102–104] a test that could be another ‘smoking gun’ for ergodic motion: the observation of a plateau in the evolution of the ratio of frequencies  $f_\rho/f_z$ , which would be absent in the case of an integrable system like Kerr (see section 3.1).

### 4.3 Johannsen-Psaltis spacetimes

An alternative to the several approaches of the bumpy black hole formalism described above was recently developed by Johannsen and Psaltis [27]. The authors found the need for it because of the pathologies present in the other metric perturbations which they find unsuitable for tests involving observations of the images of inner accretion flows, X-ray observations of relativistically broadened iron lines or of the continuum spectra of accretion disks, for which good behaviour very close to the event horizon is crucial. The approach taken was to perturb the Schwarzschild metric and obtain a rotating metric using the Newman-Janis algorithm. The difference is that they neither impose Einstein’s equations as Glampedakis & Babak [25] and Vigeland & Hughes [23], nor the existence of an approximate Carter constant as Vigeland, Stein & Yunes [24]. Johannsen and Psaltis perturb the Schwarzschild metric

$$ds^2 = -f[1 + h(r)]dt^2 + f^{-1}[1 + h(r)]dr^2 + r^2(d\theta^2 + \sin^2\theta d\phi^2) \quad (4.96)$$

as in [147] (although in this case both component perturbations are the same), where  $f \equiv 1 - 2M/r$  and the perturbation is chosen to be a series of inverse powers of  $r$ :

$$h(r) \equiv \sum_{k=0}^{\infty} \epsilon_k \left(\frac{M}{r}\right)^k \quad (4.97)$$

Then the Newman-Janis procedure is applied (see appendix A) and one arrives at the modified Kerr metric

$$ds^2 = -[1 + h(r, \theta)] \left(1 - \frac{2Mr}{\Sigma}\right) dt^2 - \frac{4aMr \sin^2 \theta}{\Sigma} [1 + h(r, \theta)] dt d\phi + \frac{\Sigma[1 + h(r, \theta)]}{\Delta + a^2 \sin^2 \theta h(r, \theta)} dr^2 + \Sigma d\theta^2 + \left[ r^2 + a^2 + \frac{2a^2 Mr \sin^2 \theta}{\Sigma} + h(r, \theta) \frac{a^2 (\Sigma + 2Mr) \sin^2 \theta}{\Sigma} \right] \sin^2 \theta d\phi^2 \quad (4.98)$$

where

$$h(r, \theta) \equiv \sum_{k=0}^{\infty} \left( \epsilon_{2k} + \epsilon_{2k+1} \frac{Mr}{\Sigma} \right) \left( \frac{M^2}{\Sigma} \right)^k \quad (4.99)$$

and one has the usual Kerr functions

$$\Sigma \equiv r^2 + a^2 \cos^2 \theta, \quad \Delta \equiv r^2 - 2Mr + a^2 \quad (4.100)$$

Constraints on the function  $h(r, \theta)$  were then analysed on the basis that the spacetime is asymptotically flat, that it agrees with the observational weak-field constraints on deviations from the Kerr metric and that the Einstein equivalence principle is valid, but Einstein's equations are not imposed.

Spin	Deviation parameter	Killing horizon topology	ISCO (radial instability)	Vertical instability
$a \leq 0$	$\epsilon_3 < \epsilon_3^{\text{bound}}$	Spherical	Yes	Inside of ISCO
$a \leq 0^a$	$\epsilon_3 \geq \epsilon_3^{\text{bound}}$	Disjoint	Yes	Inside of ISCO
$a > 0$	$\epsilon_3 < \epsilon_3^{\text{bound}}$	Spherical	Yes	Inside of ISCO <sup>b</sup>
$a > 0^a$	$\epsilon_3 \geq \epsilon_3^{\text{bound}}$	Disjoint	No	Yes

Table 4.2: Inner accretion disc edges and Killing horizon topology for the Johannsen-Psaltis spacetime. The value of  $\epsilon_3^{\text{bound}}$  (as a function of  $a$ ) is given by the red curve in the left panel of figure 4.8. (Table I from [157]).

<sup>a</sup>Kerr black hole if  $a = \pm M$  with a spherical Killing horizon and the ISCO located at  $r = M$  and  $r = 9M$ , respectively.

<sup>b</sup>Except for values of the spin and deviation parameter in a narrow region along the boundary  $\epsilon_3^{\text{bound}}$  (see figure 7 of [157]).

Asymptotical flatness requires  $\epsilon_0 = \epsilon_1 = 0$ , and through the parameterized post-Newtonian (PPN) approach we find an observational constraint on  $\epsilon_2$ . In this framework, asymptotic flatness is expressed as

$$ds^2 = -A(r)dt^2 + B(r)dr^2 + r^2 d\Omega \quad (4.101)$$

where

$$A(r) = 1 - \frac{2M}{r} + 2(\beta - \gamma) \frac{M^2}{r^2}, \quad (4.102)$$

$$B(r) = 1 + 2\gamma \frac{M}{r} \quad (4.103)$$

and where the PPN parameters  $\beta$  and  $\gamma$  equal one in general relativity.

The best current constraint on  $\beta$  is from the Lunar Laser Ranging experiment [158]:

$$|\beta - 1| \leq 2.3 \times 10^{-4}, \quad (4.104)$$

which implies

$$|\epsilon_2| \leq 4.6 \times 10^{-4}, \quad (4.105)$$

since it is found that the asymptotic form of this modified Kerr metric identifies

$$\epsilon_2 = 2(\beta - 1), \quad (4.106)$$

$$\gamma = 1. \quad (4.107)$$

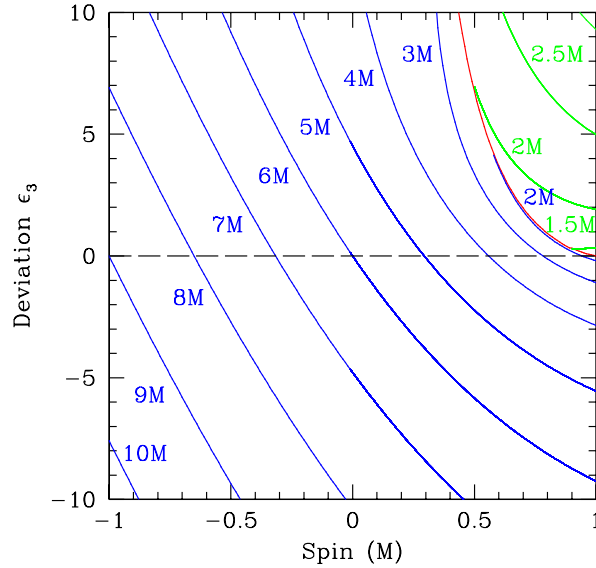


Figure 4.8: ISCO type and location for the Johannsen-Psaltis spacetime. The red curve divides the parameter space in two regions. For the region marked in blue the accretion disc inner edge is radially unstable, and for the region in green it is vertically unstable. (Figure 6 of [157]).

With this constraint, Johannsen and Psaltis chose to set all  $\epsilon_n$  to zero, except for  $\epsilon_3$ , the first unconstrained parameter. The function  $h(r, \theta)$  therefore is now given by

$$h(r, \theta) = \epsilon_3 \frac{M^3 r}{\Sigma^2} \quad (4.108)$$

The properties of the Johannsen-Psaltis metric that have been studied by several authors [27, 157, 159, 160] include the existence of closed event horizons and the structure and dependence of the inner disc edge instabilities. Surprisingly it was found that the parameter space is divided in two disjoint regions: one where the inner disc edge instability is radial *and* there is a closed spherical topology Killing horizon, and a second one where the inner disc edge instability is vertical *and* where the Killing horizon is disjoint.

This is shown in figure 4.8. There is however a third, very thin, region separating the two regions above where the Killing horizon has spherical topology and where the inner edge instability is vertical.

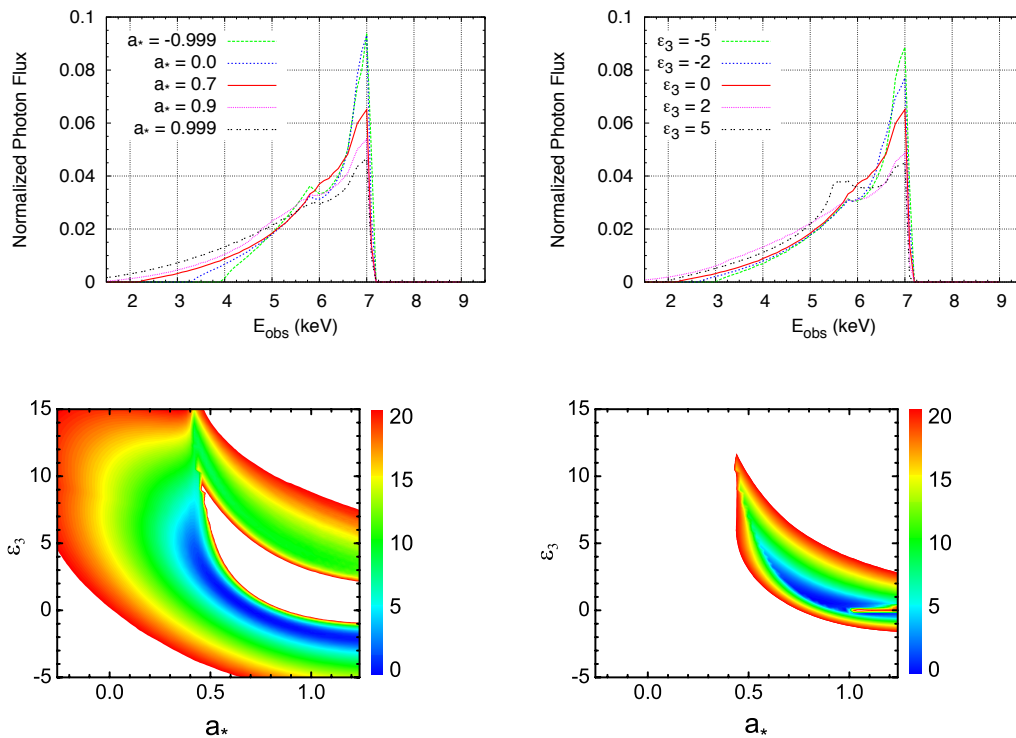


Figure 4.9: Top: Broad K iron line generated around a JP BH as a function of the parameters of the model.

Bottom:  $\chi^2$  from the comparison of the broad K iron line generated around a Kerr BH with spin parameter  $A$  and a JP BH with spin parameter  $a$  and deformation parameter  $\epsilon_3$ . Bottom left:  $a = 0.7$ . Bottom right:  $a = 0.98$ . From [120].

Liu, Chen and Jing [161] investigated the properties of the ergosphere and energy extraction by the Penrose process for this metric, while constraining the extra parameter  $\epsilon_3$  so that the spacetime maintains a closed event horizon. They have found that the ergosphere is sensitive to  $\epsilon$  and becomes wider with its increase, and also that for  $a \leq M$  the maximum efficiency of energy extraction by the Penrose process can be as much as 20.7% larger than for the Kerr black hole. Furthermore, because for the JP metric  $a > M$  is allowed for some range, the maximum efficiency can exceed in 60% the Kerr case. Konoplya and Zhidenko [162] found that scalar, electromagnetic and Dirac fields are stable in the Johannsen-Psaltis spacetime for  $a = 0$ , but the rotating case has not yet been studied due to the non-separability of the equations.

The degeneracy between the spin  $a$  and the parameter  $\epsilon_3$  in the X-ray emission from accretion discs has been investigated in several studies, mostly by Bambi [120, 134, 163, 164]. As shown in figures 4.9 and 4.10 both parameters have a very similar impact on the profiles, since both have a similar impact on the inner edge instability, and a pure Kerr black hole with a certain spin would be hard to distinguish from a Johannsen-Psaltis spacetime with a different value of spin and a non-zero value of  $\epsilon_3$  (see also figures 3.4 and 3.5).

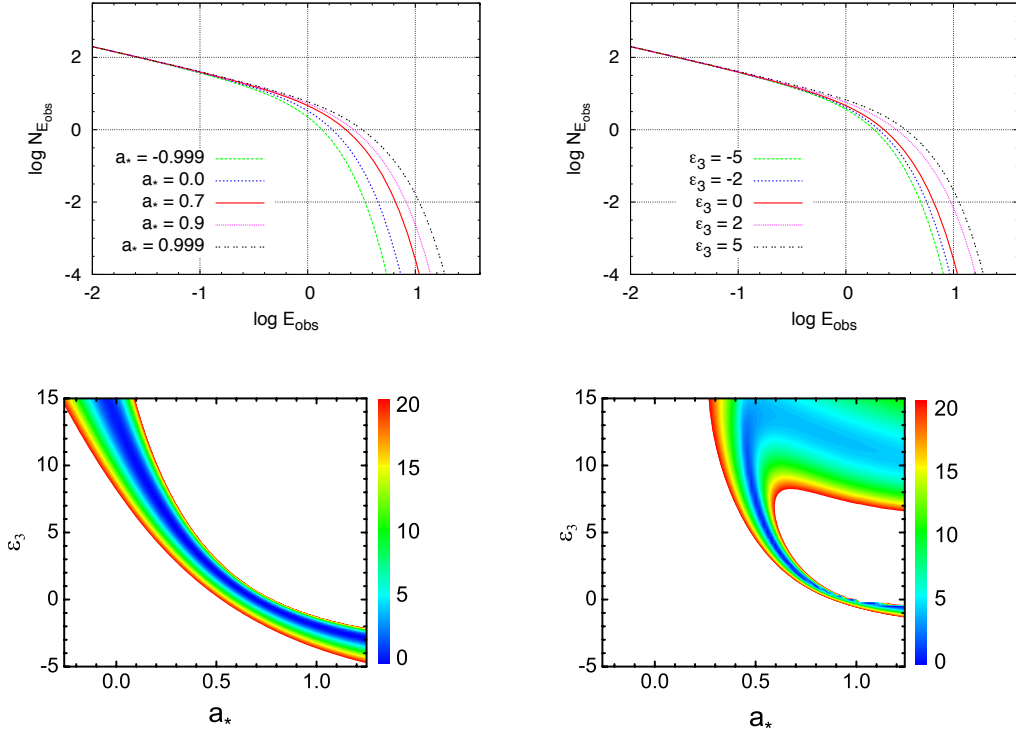


Figure 4.10: Top: Thermal spectrum of a thin disk as a function of the parameters of the model. Bottom:  $\chi^2$  from the comparison of the thermal spectrum of a thin accretion disk around a Kerr BH with spin parameter  $A$  and a JP BH with spin parameter  $a$  and deformation parameter  $\epsilon_3$ . Bottom left:  $a = 0.7$ . Bottom right:  $a = 0.98$ . From [120].

### 4.3.1 Dependence on higher order parameters

In this section, we relax the requirement that all extra parameters in the JP metric except for  $\epsilon_3$  are zero and compute the ISCO location and frequency for different combinations of non-vanishing  $\epsilon_i$ . In particular we show that for any value of the spin the (coordinate-dependent) ISCO can take its Kerr value for a certain combination of at least two non-zero parameters  $\epsilon_i$ , but the same is true of the invariant orbital frequency  $\Omega_\phi$ . This indicates how any experimental approach based on the assumption that  $\epsilon_i = 0$  for  $i \geq 4$  is rendered blind to the possibility that the observed spacetime, for which a certain  $\epsilon_3$  and spin  $a$  would be estimated, is in reality a spacetime with, for example, a much larger value of  $\epsilon_3$  and a non-zero value of  $\epsilon_4$ .

Using the formulas from section 2.2 we calculated the ISCO radius, frequency and energy as a function of  $\epsilon_3$  and  $\epsilon_4$ , shown in the contour plot of figure 4.11, for a spin of value  $a/M = .5$  and  $a/M = .95$ . Similar results were obtained for higher order parameters and different values of the spin. It is clear that a certain value of the ISCO can be obtained for very different values of  $\epsilon_3$ , depending on the value of  $\epsilon_4$ .

This indicates that the estimate of  $\epsilon_3$  of an experimental approach based on the assumption that  $\epsilon_i = 0$  for  $i \geq 4$  is not valid, as the real value of  $\epsilon_3$  could in fact be much larger or even have the opposite sign. This is a fundamental difference from Ryan's approach [69] where the estimate of each of the multipole moments, such as the mass, spin, and quadrupole moment, are independent of the remaining  $\epsilon$  moments.

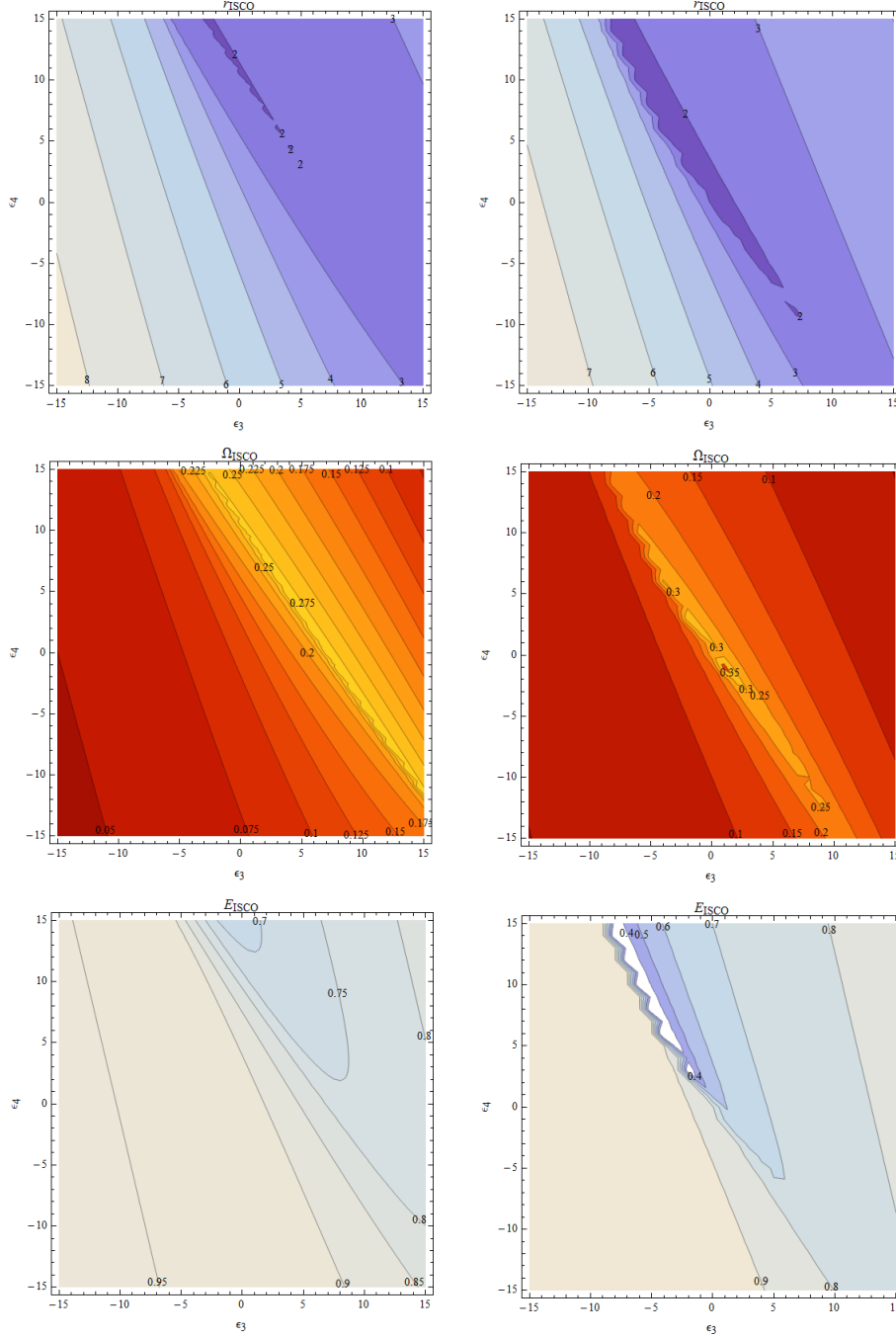


Figure 4.11: ISCO radius, frequency and energy as a function of the parameters  $\epsilon_3$  and  $\epsilon_4$  for a spin value of  $a/M = .5$  (left) and  $a/M = .95$  (right).

By expanding the ISCO radius and frequency as

$$X = X_{\text{Kerr}} + \delta X_3 \cdot \epsilon_3 + \delta X_4 \cdot \epsilon_4 + \delta X_5 \cdot \epsilon_5, \quad (4.109)$$

where  $X$  denotes the quantities  $R_{\text{ISCO}}$  and  $\Omega_{\text{ISCO}}$ , we computed the first-order shifts in the ISCO frequency as a function of  $a/M$ , as shown in the left panel of figure 4.12. The plot shows the hierarchy between different parameters: to higher orders correspond smaller shifts, which is the same result of the

non-linear calculation shown in figure 4.11. Note that this is a nontrivial result because equation (4.97) is a *large distance* expansion which, in principle, is not guaranteed to converge in the strong-field region near the ISCO. Indeed, such hierarchy deteriorates in the near-extremal limit,  $a \rightarrow M$ . As shown in figure 4.12, all linear corrections are roughly equally important in this limit.

### 4.3.2 A generalization of the Johannsen-Psaltis metric

We now study a generalization of this metric, starting from the following seed metric:

$$ds^2 = -f(1+h^t)dt^2 + f^{-1}(1+h^r)dr^2 + r^2(d\theta^2 + \sin^2\theta d\phi^2), \quad (4.110)$$

where  $f \equiv 1 - 2M/r$ , and which differs from the JP metric because we take  $h^t(r) \neq h^r(r)$ , in general. We keep its functional form:

$$h^i \equiv \sum_{k=0}^{\infty} \epsilon_k^i \left(\frac{M}{r}\right)^k, \quad i = t, r. \quad (4.111)$$

Defining the functions

$$K \equiv \sqrt{\frac{1+h^r}{1+h^t}}, \quad H \equiv \sqrt{(1+h^r)(1+h^t)}, \quad (4.112)$$

we carry out a transformation to Eddington-Finkelstein coordinates by the implicit relation

$$du' = dt - f^{-1}Kdr, \quad (4.113)$$

to obtain

$$ds^2 = -f(1+h^t)du'^2 - 2Hdu'dr + r^2(d\theta^2 + \sin^2\theta d\phi^2). \quad (4.114)$$

This and the remaining procedure always reduces to the JP case when  $h^t = h^r$ .

In the same way as JP, we find the contravariant form of the metric and the complex null tetrad:

$$l^\mu = \delta_r^\mu \quad (4.115)$$

$$n^\mu = \frac{1}{H} \left( \delta_u^\mu - \frac{f}{2} \frac{1+h^t}{H} \delta_r^\mu \right) \quad (4.116)$$

$$m^\mu = \frac{1}{\sqrt{2}r} \left( \delta_\theta^\mu + \frac{i}{\sin\theta} \delta_\phi^\mu \right). \quad (4.117)$$

This differs from the JP case only for  $n^\mu$ .

Following the Newman-Janis procedure, we arrive at the rotated metric

$$l^\mu = \delta_r^\mu \quad (4.118)$$

$$n^\mu = \frac{1}{H_{(r,\theta)}} \left( \delta_u^\mu - \frac{f_{(r,\theta)}}{2} \frac{1+h_{(r,\theta)}^t}{H_{(r,\theta)}} \delta_r^\mu \right) \quad (4.119)$$

$$m^\mu = \frac{1}{\sqrt{2}(r+ia\cos\theta)} \left[ ia\sin\theta(\delta_u^\mu - \delta_r^\mu) + \delta_\theta^\mu + \frac{i}{\sin\theta} \delta_\phi^\mu \right], \quad (4.120)$$

where we now have

$$\Sigma \equiv r^2 + a^2 \cos^2 \theta, \quad (4.121)$$

$$f_{(r,\theta)} \equiv \left(1 - \frac{2Mr}{\Sigma}\right), \quad (4.122)$$

$$h_{(r,\theta)}^i \equiv \sum_{k=0}^{\infty} \left( \epsilon_{2k}^i + \epsilon_{2k+1}^i \frac{Mr}{\Sigma} \right) \left( \frac{M^2}{\Sigma} \right)^k, \quad i = t, r, \quad (4.123)$$

$$H_{(r,\theta)} \equiv \sqrt{(1 + h_{(r,\theta)}^r)(1 + h_{(r,\theta)}^t)}. \quad (4.124)$$

Finally this yields a generalized Johannsen-Psaltis (JP2) metric in the covariant form:

$$g_{tt} = -f(1 + h^t), \quad (4.125)$$

$$g_{rr} = \frac{\Sigma(1 + h^r)}{\Delta + a^2 \sin^2 \theta h^r}, \quad (4.126)$$

$$g_{\theta\theta} = \Sigma, \quad (4.127)$$

$$g_{\phi\phi} = \sin^2 \theta [\Sigma + a^2 \sin^2 \theta (2H - f(1 + h^t))], \quad (4.128)$$

$$g_{t\phi} = -a \sin^2 \theta (H - f(1 + h^t)), \quad (4.129)$$

where for ease of notation the dependencies on  $r$  and  $\theta$  have been dropped.

Imposing asymptotic flatness requires  $\epsilon_0^t = \epsilon_1^t = \epsilon_0^r = \epsilon_1^r = 0$ . The PPN bound, which for the JP metric constrained  $\epsilon_2$ , for this generalized metric only constrains  $|\epsilon_2^t| \leq 4.6 \times 10^{-4}$ , while  $\epsilon_2^r$  is unconstrained.

The right panel of figure 4.12 shows the shifts of the ISCO frequency for the JP2 metric in the small parameter limit, obtained using an analogous expansion to (4.109). It reveals that in the slowly rotating limit the  $\epsilon_i^t$  perturbations lead to frequency shifts of higher order than the  $\epsilon_i^r$ , while the reverse is true for the fast spinning case ( $a/M \gtrsim 0.9$ ). This behaviour stems from the fact that the effective potential (see equation (2.12)) does not involve the  $g_{rr}$  component. In the absence of rotation this is the only component involving the  $\epsilon_i^r$  terms, and these scale with the rotation parameter in the  $g_{t\phi}$  and  $g_{\phi\phi}$  components (equations (4.129) and (4.128)). In particular this analysis has shown that the magnitude of the frequency shift related to  $\epsilon_2^r$  is larger than the one from  $\epsilon_3^r$  or  $\epsilon_3^t$  in the fast-spinning case. For the two types of parameters one finds the same hierarchy as in the JP metric: higher order terms are increasingly subdominant.

### 4.3.3 Non-matching to alternative theories

There are at least two analytical solutions of slowly rotating black holes in alternative theories of gravity: one found by Yunes and Pretorius [145] for Dynamical Chern-Simons (CS) Modified Gravity, and another found by Pani, Macedo, Crispino and Cardoso [165] for a class of alternative theories obtained by including all quadratic, algebraic curvature invariants generally coupled to a single scalar field. However we show that the JP metric cannot describe such solutions even when using the more general case derived above with  $h_{(r)}^t \neq h_{(r)}^r$ .

By expanding the JP2 metric in the slow rotation approximation we show that it cannot be mapped

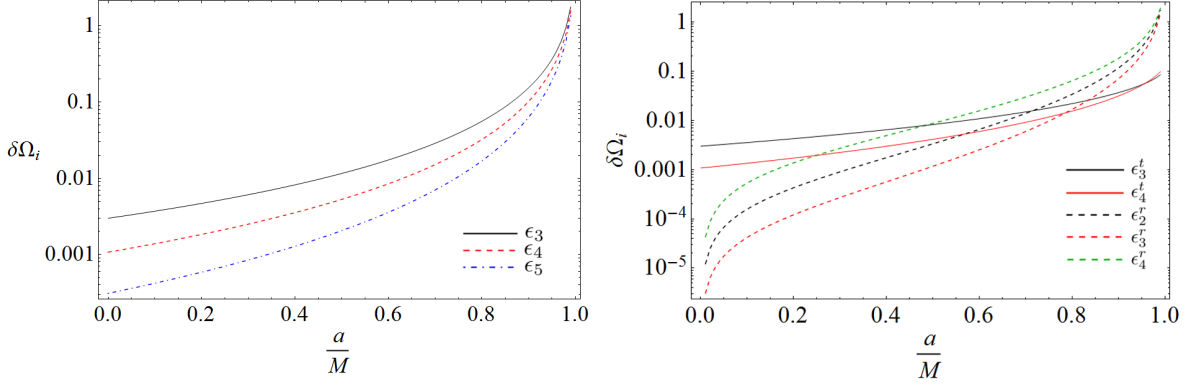


Figure 4.12: Shifts to the ISCO frequencies,  $\delta\Omega_i$ , in the JP (left panel) and JP2 (right panel) metrics, in the small parameter limit, as a function of the spin  $a/M$ .

Left:  $\epsilon_3$  (black),  $\epsilon_4$  (red),  $\epsilon_5$  (blue).

Right:  $\epsilon_2^r$  (dashed green),  $\epsilon_3^r$  (dashed black),  $\epsilon_4^r$  (dashed red),  $\epsilon_3^t$  (black),  $\epsilon_4^t$  (red).

to any of the two known slowly rotating black hole spacetimes in alternative theories, and is unlikely to be matchable to any other future known solution even in the small parameter and small rotation limit. The main reason is because there is not enough freedom over different components: when attempting the match, the terms of different inverse powers of  $r$  of one metric component (e.g.,  $g_{tt}$ ) essentially fix half of the parameters, rendering the matching unfeasible. It is clear that if the JP2 metric cannot be matched the same if true of JP, as the latter is a particular case of the former. One has only two general perturbation functions for three a priori independent metric components.

The  $g_{tt}$  component of the JP2 metric in the small rotation and parameters limits, that is, valid to order  $\mathcal{O}(a^2, \epsilon_i, a\epsilon_i)$ , is given by

$$\begin{aligned}
g_{tt} = & -1 - \epsilon_0^t + \frac{2M}{r} + M \frac{2\epsilon_0^t - \epsilon_1^t}{r} + M^2 \frac{2\epsilon_1^t - \epsilon_2^t}{r^2} - \frac{2a^2 M \cos^2 \theta}{r^3} \\
& + M \frac{(\epsilon_1^t - 2)a^2 \cos^2 \theta + (2\epsilon_2^t - \epsilon_3^t)M^2}{r^3} + M^2 \frac{(\epsilon_2^t - 4\epsilon_1^t)a^2 \cos^2 \theta + (2\epsilon_3^t - \epsilon_4^t)M^2}{r^4} \\
& + M^3 \frac{2(\epsilon_3^t - 2\epsilon_2^t)a^2 \cos^2 \theta + (2\epsilon_4^t - \epsilon_5^t)M^2}{r^5} + M^4 \frac{2(\epsilon_4^t - 3\epsilon_3^t)a^2 \cos^2 \theta + (2\epsilon_5^t - \epsilon_6^t)M^2}{r^6} \\
& + M^5 \frac{3(\epsilon_5^t - 2\epsilon_4^t)a^2 \cos^2 \theta + (2\epsilon_6^t - \epsilon_7^t)M^2}{r^7} + M^6 \frac{(3\epsilon_6^t - 8\epsilon_5^t)a^2 \cos^2 \theta + (2\epsilon_7^t - \epsilon_8^t)M^2}{r^8} + \dots
\end{aligned} \tag{4.130}$$

The  $g_{tt}$  component of the slowly rotating solution for a class of alternative theories obtained by including all quadratic, algebraic curvature invariants generally coupled to a single scalar field [165] is given by:

$$g_{tt} = -1 + \frac{2M}{r} - a^2 \frac{2M \cos^2 \theta}{r^3} - \frac{1}{4} \alpha_3^2 \left( -\frac{49}{40M^3 r} + \frac{1}{3Mr^3} + \frac{26}{3r^4} + \frac{22M}{5r^5} + \frac{32M^2}{5r^6} - \frac{80M^3}{3r^7} \right), \tag{4.131}$$

and is accurate up to order  $\mathcal{O}(a^2, \alpha_i^2, a\alpha_i^2)$ .

Inspection of equation (4.130) makes it clear why matching to the JP2 metric is not possible in general, even for metrics whose terms are just inverse powers of  $r$ . Matching the terms proportional to  $a^2 \cos^2 \theta$  is sufficient to fix almost all parameters. Each  $\epsilon_i^t$  coefficient appears in 4 different terms as a

linear combination with another coefficient (twice with  $\epsilon_{i-1}^t$  and twice with  $\epsilon_{i+1}^t$ ), rendering this into an overconstrained system. Of course, this does not exclude the existence of a coordinate transformation that could allow the matching, but this is unlikely, and one could look at metric invariants, such as curvature scalars at the horizons, to disprove the possibility.

The slowly rotating black hole solution of dynamical Chern-Simons [145] is given by

$$ds^2 = ds_K^2 + \frac{5}{4} \frac{\alpha^2}{\beta\kappa} \frac{a}{r^4} \left( 1 + \frac{12}{7} \frac{M}{r} + \frac{27}{10} \frac{M^2}{r^2} \right) \sin^2 \theta dt d\phi, \quad (4.132)$$

where  $ds_K^2$  is the slowly rotating Kerr metric. Because this reduces to the Schwarzschild solution when  $a = 0$  matching to the JP or JP2 is not possible, since these do not reduce to the Schwarzschild case when  $a = 0$  unless all of the  $\epsilon_i$  parameters are zero.

# Chapter 5

## Conclusions

In this work we reviewed methods and results to test of the Kerr black hole hypothesis, which states that all astrophysical black holes in isolation are described by the Kerr solution and are completely defined by their mass and angular momentum. We presented the essential concepts behind the hypothesis and the related tools from General Relativity: the Kerr solution and the uniqueness theorems, and the properties of general stationary axisymmetric spacetimes, including equatorial circular orbits and relativistic multipole moments.

The current solar system and even binary pulsars tests of gravitational physics do not probe the regimes involving velocities comparable to the speed of light or gravitational potentials of the order of those near the surface of neutron stars or the event horizons of black holes. However with the increasing precision of new electromagnetic and gravitational radiation observatories, the era of experimental tests of the strong-field regime of gravity is around the corner. Although General Relativity has passed every experimental test to date, today there are several alternative theories of gravity which are not excluded by current observations, and that make different strong-field predictions. Unfortunately a general, unbiased framework to test gravity theories and phenomena in this regime is still lacking. Gravitational wave and electromagnetic radiation observations will be the two main avenues for future strong field tests of gravity. The studies reviewed show that extreme mass ratio inspirals and quasinormal ringdown tests have a very good potential to measure the quadrupole moment of black holes, and therefore test the Kerr black hole hypothesis. Electromagnetic observations of accretion discs already probe the strong field regime and today rough estimates of the spin of some black holes are available. The current associated uncertainties will be greatly improved with the precision that new observatories promise, and measurements of higher multipole moments are also expected.

To tackle the problem of measuring deviations from the Kerr metric, different spacetimes have been proposed and studied. These solutions are parametrically deformed from Kerr, that is, they possess additional parameters besides the mass and the spin. These spacetimes can be fitted to observations in order to check whether they agree with the hypothesis that these additional parameters are zero, that is, that astrophysical black holes are described by the Kerr metric of general relativity. The metrics reviewed have different strengths and drawbacks, the most promising proposals so far being the generalized bumpy

and generalized deformed black holes proposed by Vigeland, Yunes and Stein for gravitational wave tests and the Johannsen-Psaltis metric for electromagnetic spectrum tests.

The Johannsen-Psaltis spacetime possesses an infinite number of parameters  $\epsilon_i$ , experimentally unconstrained for  $i \geq 3$ . The existing studies of this metric usually assume only one non-zero additional parameter, namely  $\epsilon_3$ . Here we have relaxed this condition and studied the relative importance of different order parameters. We concluded that there is a hierarchy: higher order terms are subdominant, although in the limit  $a \rightarrow M$  they are roughly equally important. This difference in magnitude however is less than one order of magnitude, and there is a strong degeneracy between parameters of similar order. Therefore if one sets all parameters to zero except, say,  $\epsilon_3$  the experiment is rendered blind to the possibility that the observed spacetime is in reality a spacetime with a much larger value (or even opposite sign) of  $\epsilon_3$  and a non-zero value of  $\epsilon_4$ , for example. This is a fundamental difference from Ryan's approach to probing the spacetime geometry with EMRIs, in which, in a post-Newtonian expansion, higher multipole moments do not affect the measurement of lower multipoles.

We constructed a generalization of the Johannsen-Psaltis metric and studied the importance of the new parameters. To each parameter of the original metric now corresponds two parameters, and the Johannsen-Psaltis metric is recovered in the limit where the two parameters in each pair are equal. We found that the PPN bound does not constrain  $\epsilon_2^r$  unlike in the JP spacetime, where it is set to zero. For this generalized metric we computed the ISCO frequency shifts in the small  $\epsilon_i$  limit, and reached the same conclusion: the parameters are hierarchized by order. However for this metric a different role is played by the different types of parameters. Which one is dominant depends of the value on the rotation parameter. In particular we showed that the magnitude of the frequency shift related to  $\epsilon_2^r$  is larger than the one from  $\epsilon_3^r$  or  $\epsilon_3^t$  in the fast-spinning case. Finally, by using this generalized metric we argued that the Johannsen-Psaltis spacetimes cannot be matched to rotating black holes in alternative theories of gravity, even in the limit of small parameters and slow rotation.

# Appendix A

## The Newman-Janis algorithm

In this appendix we describe, following Drake and Szekeres [141], the Newman-Janis algorithm [140?] as a five steps procedure for obtaining new solutions of the Einstein equation from the known static spherically symmetric ones.

1. Start with a static spherically symmetric seed line element in advanced null coordinates  $u, r, \theta, \phi$

$$ds^2 = e^{2\Phi(r)} du^2 + e^{\Phi(r)+\lambda(r)} dudr - r^2(d\theta^2 + \sin^2 \theta d\phi^2) \quad (\text{A.1})$$

2. Write the metric in terms of a null tetrad

$$g^{\mu\nu} = l^\mu n^\nu + l^\nu n^\mu - m^\mu \bar{m}^\nu - m^\nu \bar{m}^\mu \quad (\text{A.2})$$

using a complex null tetrad

$$Z_a^\mu = (l^\mu, n^\mu, m^\mu, \bar{m}^\mu), \quad a = 1, 2, 3, 4 \quad (\text{A.3})$$

with legs

$$l^\mu = \delta_1^\mu \quad (\text{A.4})$$

$$n^\mu = e^{-\lambda(r)-\Phi(r)} \delta_0^\mu - \frac{1}{2} e^{-2\lambda(r)} \delta_1^\mu \quad (\text{A.5})$$

$$m^\mu = \frac{1}{\sqrt{2}r} \left( \delta_2^\mu + \frac{i}{\sin \theta} \delta_3^\mu \right) \quad (\text{A.6})$$

$$\quad (\text{A.7})$$

that obey the conditions

$$l_\mu l^\mu = m_\mu m^\mu = n_\mu n^\mu = 0, \quad l_\mu n^\mu = -m_\mu \bar{m}^\mu = 1, \quad l_\mu m^\mu = n_\mu \bar{m}^\mu = 0. \quad (\text{A.8})$$

3. Allow the coordinates to take complex values, extending them to a new set of complex coordinates

$\tilde{x}^\rho$ :

$$x^\rho \rightarrow \tilde{x}^\rho = x^\rho + iy(x^\sigma) \quad (\text{A.9})$$

where  $y^\rho(x^\rho)$  are analytic functions of the real coordinates  $x^\rho$ , where the transformation must be such that we recover the old metric when  $\tilde{x}^\rho = \bar{\tilde{x}}^\rho$ .

The tilde transformation is not unique but we will choose the original one by Newman and Janis:

$$\tilde{x}^\rho = x^\rho + ia \cos \theta (\delta_0^\rho - \delta_1^\rho) \quad (\text{A.10})$$

4. Now the metric is obtained by the new tetrad which transform in the usual way

$$\tilde{Z}_a^\mu = Z_a^\nu \frac{\partial \tilde{x}^\mu}{\partial x^\nu} \quad (\text{A.11})$$

so that we have the new legs

$$l^\mu = \delta_1^\mu \quad (\text{A.12})$$

$$n^\mu = e^{-\lambda(r,\theta) - \Phi(r,\theta)} \delta_0^\mu - \frac{1}{2} e^{-2\lambda(r,\theta)} \delta_1^\mu \quad (\text{A.13})$$

$$m^\mu = \frac{1}{\sqrt{2}(r + ia \cos \theta)} \left( ia \sin \theta (\delta_0^\mu - \delta_1^\mu) + \delta_2^\mu + \frac{i}{\sin \theta} \delta_3^\mu \right) \quad (\text{A.14})$$

$$(\text{A.15})$$

and new metric

$$g_{\mu\nu} = \begin{pmatrix} e^{2\Phi(r,\theta)} & e^{\lambda(r,\theta) + \Phi(r,\theta)} & 0 & a \sin^2 \theta e^{\Phi(r,\theta)} (e^{\lambda(r,\theta)} - e^{\Phi(r,\theta)}) \\ \cdot & 0 & 0 & -a e^{\lambda(r,\theta) + \Phi(r,\theta)} \sin^2 \theta \\ \cdot & \cdot & -\Sigma & 0 \\ \cdot & \cdot & \cdot & -\sin^2 \theta (\Sigma + a^2 \sin^2 \theta e^{\Phi(r,\theta)} (2e^{\lambda(r,\theta)} - e^{\Phi(r,\theta)})) \end{pmatrix} \quad (\text{A.16})$$

5. The last step is to write the new metric in Boyer-Lindquist coordinates which is achieved with the transformations

$$u = t + \int g(r) dr, \quad \phi = \psi + \int h(r) dr \quad (\text{A.17})$$

where  $g(r)$  and  $h(r)$  are given by

$$g(r) = -\frac{e^{\lambda(r,\theta)} (\Sigma + a^2 \sin^2 \theta e^{\lambda(r,\theta) + \Phi(r,\theta)})}{e^{\Phi(r,\theta)} (\Sigma + a^2 \sin^2 \theta e^{2\lambda(r,\theta)})} \quad (\text{A.18})$$

$$h(r) = -\frac{a e^{2\lambda(r,\theta)}}{\Sigma + a^2 \sin^2 \theta e^{2\lambda(r,\theta)}} \quad (\text{A.19})$$

We arrive at a final expression for the metric:

$$g_{\mu\nu} = \begin{pmatrix} e^{2\phi(r,\theta)} & 0 & 0 & a \sin^2 \theta e^{\phi(r,\theta)} (e^{\lambda(r,\theta)} - e^{\phi(r,\theta)}) \\ \cdot & -\Sigma / (\Sigma e^{-2\lambda(r,\theta)} + a^2 \sin^2 \theta) & 0 & 0 \\ \cdot & \cdot & -\Sigma & 0 \\ \cdot & \cdot & \cdot & -\sin^2 \theta (\Sigma + a^2 \sin^2 \theta e^{\phi(r,\theta)} (2e^{\lambda(r,\theta)} - e^{\phi(r,\theta)})) \end{pmatrix} \quad (\text{A.20})$$

# Bibliography

- [1] W. Israel, in *Three hundred years of gravitation*, edited by S. W. Hawking and W. Israel.
- [2] R. P. Kerr, *Phys.Rev.Lett.* **11**, 237 (1963).
- [3] W. Israel, *Phys.Rev.* **164**, 1776 (1967).
- [4] D. Robinson, *Phys.Rev.Lett.* **34**, 905 (1975).
- [5] S. Hawking, *Commun.Math.Phys.* **25**, 152 (1972).
- [6] B. Carter, *Phys.Rev.Lett.* **26**, 331 (1971).
- [7] S. Chandrasekhar, in *General Relativity: An Einstein centenary survey*, Vol. 1 (1979) pp. 370–453.
- [8] S. Chandrasekhar, *Shakespeare, Newton, and Beethoven: Or, Patterns of Creativity* (University of Chicago, Center for Policy Study, 1975).
- [9] D. Psaltis, *Living Reviews in Relativity* **11** (2008), arXiv:0806.1531 [astro-ph] .
- [10] N. Yunes and X. Siemens, (2013), arXiv:1304.3473 [gr-qc] .
- [11] S. Schlamminger, K.-Y. Choi, T. Wagner, J. Gundlach, and E. Adelberger, *Phys.Rev.Lett.* **100**, 041101 (2008), arXiv:0712.0607 [gr-qc] .
- [12] C. M. Will, *Theory and experiment in gravitational physics* (Cambridge University Press, 1993).
- [13] C. M. Will, *Living Rev.Rel.* **9**, 3 (2006), arXiv:gr-qc/0510072 [gr-qc] .
- [14] D. Psaltis, *J.Phys.Conf.Ser.* **189**, 012033 (2009), arXiv:0907.2746 [astro-ph.HE] .
- [15] T. Clifton, P. G. Ferreira, A. Padilla, and C. Skordis, *Phys.Rept.* **513**, 1 (2012), arXiv:1106.2476 [astro-ph.CO] .
- [16] J. Abadie *et al.* (LIGO Scientific Collaboration, Virgo Collaboration), *Class.Quant.Grav.* **27**, 173001 (2010), arXiv:1003.2480 [astro-ph.HE] .
- [17] J. E. McClintock, R. Narayan, S. W. Davis, L. Gou, A. Kulkarni, *et al.*, *Class.Quant.Grav.* **28**, 114009 (2011), arXiv:1101.0811 [astro-ph.HE] .
- [18] L. W. Brenneman and C. S. Reynolds, *Astrophys.J.* **652**, 1028 (2006), arXiv:astro-ph/0608502 [astro-ph] .

- [19] J. F. Steiner, R. C. Reis, A. C. Fabian, R. A. Remillard, J. E. McClintock, *et al.*, (2012), arXiv:1209.3269 [astro-ph.HE] .
- [20] R. Wald, *General relativity* (University of Chicago Press, 1984).
- [21] V. Frolov and A. Zelnikov, *Introduction to Black Hole Physics* (Oxford Univ Press, 2011).
- [22] N. A. Collins and S. A. Hughes, Phys.Rev. **D69**, 124022 (2004), arXiv:gr-qc/0402063 [gr-qc] .
- [23] S. J. Vigeland and S. A. Hughes, Phys.Rev. **D81**, 024030 (2010), arXiv:0911.1756 [gr-qc] .
- [24] S. Vigeland, N. Yunes, and L. Stein, Phys.Rev. **D83**, 104027 (2011), arXiv:1102.3706 [gr-qc] .
- [25] K. Glampedakis and S. Babak, Class.Quant.Grav. **23**, 4167 (2006), arXiv:gr-qc/0510057 [gr-qc] .
- [26] V. Manko and I. Novikov, Classical and Quantum Gravity **9**, 2477 (1992).
- [27] T. Johannsen and D. Psaltis, Phys.Rev. **D83**, 124015 (2011), arXiv:1105.3191 [gr-qc] .
- [28] R. Penrose, Riv.Nuovo Cim. **1**, 252 (1969).
- [29] Y. B. Zel'dovich, Pis'ma Zh. Eksp. Teor. Fiz. **14**, 270 (1971) [JETP Lett. **14**, 180 (1971)]; Zh. Eksp. Teor. Fiz **62**, 2076 (1972) [Sov. Phys. JETP **35**, 1085 (1972)] .
- [30] W. H. Press and S. A. Teukolsky, Nature **238**, 211 (1972).
- [31] V. Cardoso, (2013), arXiv:1307.0038 [gr-qc] .
- [32] B. Carter, Phys.Rev. **174**, 1559 (1968).
- [33] W. Schmidt, Class.Quant.Grav. **19**, 2743 (2002), arXiv:gr-qc/0202090 [gr-qc] .
- [34] M. Walker and R. Penrose, Commun.Math.Phys. **18**, 265 (1970).
- [35] R. M. Floyd, *The dynamics of Kerr fields*, Ph.D. thesis, Birkbeck (University of London) (1974).
- [36] L. P. Hughston and P. Sommers, Commun.Math.Phys. **33**, 129 (1973).
- [37] B. Carter, J.Math.Phys. **28**, 1535 (1987).
- [38] C. Collinson, Tensor, NS **28**, 173 (1974).
- [39] P. T. Chrusciel, Contemp.Math. **170**, 23 (1994), arXiv:gr-qc/9402032 [gr-qc] .
- [40] K. S. Thorne, *Black holes and time warps: Einstein's outrageous legacy* (W.W. Norton & Company, 1994).
- [41] P. T. Chrusciel, J. L. Costa, and M. Heusler, Living Reviews in Relativity **15** (2012), 10.12942/lrr-2012-7, arXiv:1205.6112 [gr-qc] .
- [42] H. Elvang and P. Figueras, JHEP **0705**, 050 (2007), arXiv:hep-th/0701035 [hep-th] .
- [43] F. J. Ernst, Phys.Rev. **167**, 1175 (1968).

- [44] W. Israel, Commun.Math.Phys. **8**, 245 (1968).
- [45] P. Mazur, J.Phys. **A15**, 3173 (1982).
- [46] S. Chandrasekhar, Astrophys.J. **74**, 81 (1931).
- [47] J. Oppenheimer and G. Volkoff, Phys.Rev. **55**, 374 (1939).
- [48] R. Penrose, Phys.Rev.Lett. **14**, 57 (1965).
- [49] S. Hawking and R. Penrose, Proc.Roy.Soc.Lond. **A314**, 529 (1970).
- [50] R. Schoen and S.-T. Yau, Commun.Math.Phys. **90**, 575.
- [51] H. Ringström, Living Reviews in Relativity **13** (2010), 10.12942/lrr-2010-2.
- [52] P. S. Joshi, (2011), arXiv:1104.3741 [gr-qc] .
- [53] G. Gibbons, Commun.Math.Phys. **44**, 245 (1975).
- [54] R. Blandford and R. Znajek, Mon.Not.Roy.Astron.Soc. **179**, 433 (1977).
- [55] R. Price, Physical Review D **5**, 2419.
- [56] A. Papapetrou, Annalen der Physik **447**, 309 (1953).
- [57] J. Brink, Phys.Rev. **D78**, 102002 (2008), arXiv:0807.1179 [gr-qc] .
- [58] J. Brink, Phys.Rev. **D81**, 022001 (2010), arXiv:0911.1589 [gr-qc] .
- [59] S. Benenti and M. Francaviglia, Gen.Rel.Grav. **10**, 79 (1979).
- [60] E. G. Kalnins and W. Miller, Jr, SIAM Journal on Mathematical Analysis **12**, 617 (1981).
- [61] M. A. Abramowicz and W. Kluźniak, Astrophysics and Space Science **300**, 127 (2005), arXiv:astro-ph/0411709 [astro-ph] .
- [62] J. M. Bardeen, W. H. Press, and S. A. Teukolsky, Astrophys.J. **178**, 347 (1972).
- [63] F. J. Ernst, Phys.Rev. **168**, 1415 (1968).
- [64] F. J. Ernst, *Solving Einstein's Field Equations (1968-2000)* (2004).
- [65] H. Stephani, D. Kramer, M. MacCallum, C. Hoenselaers, and E. Herlt, Exact Solutions of Einstein's Field Equations, by Hans Stephani, Dietrich Kramer, Malcolm MacCallum, Cornelius Hoenselaers, Eduard Herlt, Cambridge, UK: Cambridge University Press, 2009 **1** (2009).
- [66] G. Fodor, C. Hoenselaers, and Z. Perjés, Journal of Mathematical Physics **30**, 2252 (1989).
- [67] C. Hoenselaers and Z. Perjés, Classical and Quantum Gravity **7**, 1819 (1990).
- [68] T. P. Sotiriou and T. A. Apostolatos, Class.Quant.Grav. **21**, 5727 (2004), arXiv:gr-qc/0407064 [gr-qc] .

- [69] F. Ryan, Phys.Rev. **D52**, 5707 (1995).
- [70] T. P. Sotiriou and T. A. Apostolatos, Phys.Rev. **D71**, 044005 (2005), arXiv:gr-qc/0410102 [gr-qc] .
- [71] R. P. Geroch, J.Math.Phys. **11**, 2580 (1970).
- [72] R. Hansen, J.Math.Phys. **15**, 46 (1974).
- [73] T. Bäckdahl and M. Herberthson, Class.Quant.Grav. **22**, 3585 (2005), arXiv:gr-qc/0506086v2 [gr-qc] .
- [74] S. J. Vigeland, Phys.Rev. **D82**, 104041 (2010), arXiv:1008.1278 [gr-qc] .
- [75] P. Amaro-Seoane, J. Gair, M. Freitag, M. Miller, I. Mandel, C. Cutler, and S. Babak, Class.Quant.Grav. **24**, R113 (2007), arXiv:astro-ph/0703495 [ASTRO-PH] .
- [76] P. Amaro-Seoane, S. Aoudia, S. Babak, P. Binétruy, E. Berti, A. Bohé, C. Caprini, M. Colpi, N. J. Cornish, K. Danzmann, *et al.*, (2012), arXiv:1201.3621 [astro-ph.CO] .
- [77] P. Amaro-Seoane *et al.* (eLISA Collaboration), (2013), arXiv:1305.5720 [astro-ph.CO] .
- [78] J. R. Gair and E. K. Porter, (2012), arXiv:1210.8066 [gr-qc] .
- [79] C. Li and G. Lovelace, Phys.Rev. **D77**, 064022 (2008), arXiv:gr-qc/0702146 [GR-QC] .
- [80] F. D. Ryan, Phys.Rev. **D56**, 1845 (1997).
- [81] L. Barack and C. Cutler, Phys.Rev. **D75**, 042003 (2007), arXiv:gr-qc/0612029 [gr-qc] .
- [82] L. Barack and C. Cutler, Phys.Rev. **D69**, 082005 (2004), arXiv:gr-qc/0310125 [gr-qc] .
- [83] C. L. Rodriguez, I. Mandel, and J. R. Gair, Phys.Rev. **D85**, 062002 (2012), arXiv:1112.1404 [astro-ph.HE] .
- [84] D. Psaltis, D. Perrodin, K. R. Dienes, and I. Mocioiu, Phys.Rev.Lett. **100**, 091101 (2008), arXiv:0710.4564 [astro-ph] .
- [85] E. Barausse and T. P. Sotiriou, Phys.Rev.Lett. **101**, 099001 (2008), arXiv:0803.3433 [gr-qc] .
- [86] P. Pani, V. Cardoso, and L. Gualtieri, Phys.Rev. **D83**, 104048 (2011), arXiv:1104.1183 [gr-qc] .
- [87] C. F. Sopuerta and N. Yunes, Phys.Rev. **D80**, 064006 (2009), arXiv:0904.4501 [gr-qc] .
- [88] P. Canizares, J. R. Gair, and C. F. Sopuerta, Phys.Rev. **D86**, 044010 (2012), arXiv:1205.1253 [gr-qc] .
- [89] P. Canizares, J. Gair, and C. Sopuerta, J.Phys.Conf.Ser. **363**, 012019 (2012), arXiv:1206.0322 [gr-qc] .
- [90] K. Yagi, N. Yunes, and T. Tanaka, Phys.Rev.Lett. **109**, 251105 (2012), arXiv:1208.5102 [gr-qc] .

- [91] C. Everitt, D. DeBra, B. Parkinson, J. Turneare, J. Conklin, *et al.*, Phys.Rev.Lett. **106**, 221101 (2011), arXiv:1105.3456 [gr-qc] .
- [92] I. Ciufolini and E. Pavlis, Nature **431**, 958 (2004).
- [93] N. Yunes and F. Pretorius, Phys.Rev. **D80**, 122003 (2009), arXiv:0909.3328 [gr-qc] .
- [94] P. Jaranowski and A. Królak, Living Reviews in Relativity **15** (2012), 10.12942/lrr-2012-4.
- [95] E. Barausse, L. Rezzolla, D. Petroff, and M. Ansorg, Phys.Rev. **D75**, 064026 (2007), arXiv:gr-qc/0612123 [gr-qc] .
- [96] E. Barausse and L. Rezzolla, Phys.Rev. **D77**, 104027 (2008), arXiv:0711.4558 [gr-qc] .
- [97] N. Yunes, B. Kocsis, A. Loeb, and Z. Haiman, Phys.Rev.Lett. **107**, 171103 (2011), arXiv:1103.4609 [astro-ph] .
- [98] B. Kocsis, N. Yunes, and A. Loeb, Phys.Rev. **D84**, 024032 (2011), arXiv:1104.2322 [astro-ph] .
- [99] M. Kesden, J. Gair, and M. Kamionkowski, Phys.Rev. **D71**, 044015 (2005), arXiv:astro-ph/0411478 [astro-ph] .
- [100] C. F. B. Macedo, P. Pani, V. Cardoso, and L. C. B. Crispino, (2013), arXiv:1302.2646 [gr-qc] .
- [101] P. Pani, E. Berti, V. Cardoso, Y. Chen, and R. Norte, Phys.Rev. **D80**, 124047 (2009), arXiv:0909.0287 [gr-qc] .
- [102] T. A. Apostolatos, G. Lukes-Gerakopoulos, and G. Contopoulos, Phys.Rev.Lett. **103**, 111101 (2009), arXiv:0906.0093 [gr-qc] .
- [103] G. Lukes-Gerakopoulos, T. A. Apostolatos, and G. Contopoulos, Phys.Rev. **D81**, 124005 (2010), arXiv:1003.3120 [gr-qc] .
- [104] G. Contopoulos, G. Lukes-Gerakopoulos, and T. Apostolatos, Int.J.Bifurc.Chaos **21**, 2261 (2011), arXiv:1108.5057 [gr-qc] .
- [105] K. D. Kokkotas and B. G. Schmidt, Living Rev.Rel. **2**, 2 (1999), arXiv:gr-qc/9909058 [gr-qc] .
- [106] E. Berti, V. Cardoso, and A. O. Starinets, Class.Quant.Grav. **26**, 163001 (2009), arXiv:0905.2975 [gr-qc] .
- [107] R. Konoplya and A. Zhidenko, Rev.Mod.Phys. **83**, 793 (2011), arXiv:1102.4014 [gr-qc] .
- [108] O. Dreyer, B. J. Kelly, B. Krishnan, L. S. Finn, D. Garrison, *et al.*, Class.Quant.Grav. **21**, 787 (2004), arXiv:gr-qc/0309007 [gr-qc] .
- [109] E. Berti, V. Cardoso, and C. M. Will, Phys.Rev. **D73**, 064030 (2006), arXiv:gr-qc/0512160v2 [gr-qc] .
- [110] E. Berti and V. Cardoso, Int.J.Mod.Phys. **D15**, 2209 (2006), arXiv:gr-qc/0605101 [gr-qc] .

- [111] E. Berti, J. Cardoso, V. Cardoso, and M. Cavaglia, *Phys.Rev.* **D76**, 104044 (2007), arXiv:0707.1202 [gr-qc] .
- [112] I. Kamaretsos, M. Hannam, S. Husa, and B. Sathyaprakash, *Phys.Rev.* **D85**, 024018 (2012), arXiv:1107.0854 [gr-qc] .
- [113] S. Gossan, J. Veitch, and B. Sathyaprakash, *Phys.Rev.* **D85**, 124056 (2012), arXiv:1111.5819v2 [gr-qc] .
- [114] E. E. Flanagan and S. A. Hughes, *Phys.Rev.* **D57**, 4535 (1998), arXiv:gr-qc/9701039 [gr-qc] .
- [115] J. R. Gair, M. Vallisneri, S. L. Larson, and J. G. Baker, (2012), arXiv:1212.5575 [gr-qc] .
- [116] L.-X. Li, E. R. Zimmerman, R. Narayan, and J. E. McClintock, *Astrophys.J.Suppl.* **157**, 335 (2005), arXiv:astro-ph/0411583 [astro-ph] .
- [117] D. Psaltis and T. Johannsen, *Astrophys.J.* **745**, 1 (2012), arXiv:1011.4078 [astro-ph.HE] .
- [118] C. Bambi, *Astrophys.J.* **761**, 174 (2012), arXiv:1210.5679 [gr-qc] .
- [119] C. W. Misner, K. S. Thorne, and J. A. Wheeler, *Gravitation* (WH Freeman, 1973).
- [120] C. Bambi, *Astron.Rev.* **8**, 4 (2013), arXiv:1301.0361 [gr-qc] .
- [121] A. Fabian, M. Rees, L. Stella, and N. White, *Mon.Not.Roy.Astron.Soc.* **238**, 729 (1989).
- [122] K. Beckwith and C. Done, *Mon.Not.Roy.Astron.Soc.* **352**, 353 (2004), arXiv:astro-ph/0402199 [astro-ph] .
- [123] I. Novikov and K. Thorne, in *Black Holes*, edited by C. D. W. . B. D. Witt (Gordon & Breach, New York, 1973).
- [124] D. N. Page and K. S. Thorne, *Astrophys.J.* **191**, 499 (1974).
- [125] N. Shakura and R. Sunyaev, *Astron.Astrophys.* **24**, 337 (1973).
- [126] C. Bambi, *Mod.Phys.Lett.* **A26**, 2453 (2011), arXiv:1109.4256 [gr-qc] .
- [127] C. M. Will, *Astrophys.J.Lett.* **674**, 25 (2008), arXiv:0711.1677 [astro-ph] .
- [128] D. Merritt, T. Alexander, S. Mikkola, and C. M. Will, *Phys.Rev.* **D81**, 062002 (2010), arXiv:0911.4718 [astro-ph.GA] .
- [129] L. Sadeghian and C. M. Will, *Class.Quant.Grav.* **28**, 225029 (2011), arXiv:1106.5056 [gr-qc] .
- [130] N. Wex and S. Kopeikin, *The Astrophysical Journal* **514**, 388 (1998), arXiv:astro-ph/9811052 [astro-ph] .
- [131] E. Pfahl and A. Loeb, *Astrophys.J.* **615**, 253 (2004), arXiv:astro-ph/0309744 [astro-ph] .
- [132] K. Liu, N. Wex, M. Kramer, J. Cordes, and T. Lazio, *Astrophys.J.* **747**, 1 (2012), arXiv:1112.2151 [astro-ph.HE] .

- [133] T. Johannsen and D. Psaltis, *Astrophys.J.* **726**, 11 (2011), arXiv:1010.1000 [astro-ph.HE] .
- [134] C. Bambi, *JCAP* **1209**, 014 (2012), arXiv:1205.6348 [gr-qc] .
- [135] C. Bambi, *Phys.Rev.* **D83**, 103003 (2011), arXiv:1102.0616 [gr-qc] .
- [136] H. Krawczynski, *Astrophys.J.* **754**, 133 (2012), arXiv:1205.7063 [gr-qc] .
- [137] T. Johannsen and D. Psaltis, *Astrophys.J.* **718**, 446 (2010), arXiv:1005.1931 [astro-ph.HE] .
- [138] C. Bambi, F. Caravelli, and L. Modesto, *Phys.Lett.* **B711**, 10 (2012), arXiv:1110.2768 [gr-qc] .
- [139] C. Liu, S. Chen, and J. Jing, *JHEP* **1208**, 097 (2012), arXiv:1208.1072 [gr-qc] .
- [140] E. T. Newman and A. Janis, *Journal of Mathematical Physics* **6**, 915 (1965).
- [141] S. Drake and P. Szekeres, *Gen.Rel.Grav.* **32**, 445 (2000), arXiv:gr-qc/9807001 [gr-qc] .
- [142] J. Hartle and K. Thorne, *The Astrophysical Journal* **153**, 807 (1968).
- [143] S. Teukolsky, *The Astrophysical Journal* **185**, 635 (1973).
- [144] D. A. Brown, H. Fang, J. R. Gair, C. Li, G. Lovelace, *et al.*, *Phys.Rev.Lett.* **99**, 201102 (2007), arXiv:gr-qc/0612060 [gr-qc] .
- [145] N. Yunes and F. Pretorius, *Phys.Rev.* **D79**, 084043 (2009), arXiv:0902.4669 [gr-qc] .
- [146] S. Mignemi and N. Stewart, *Phys.Rev.* **D47**, 5259 (1993), arXiv:hep-th/9212146 [hep-th] .
- [147] N. Yunes and L. C. Stein, *Phys.Rev.* **D83**, 104002 (2011), arXiv:1101.2921 [gr-qc] .
- [148] J. Gair and N. Yunes, *Phys.Rev.* **D84**, 064016 (2011), arXiv:1106.6313 [gr-qc] .
- [149] T. Gutsunaev and V. Manko, *Gen.Rel.Grav.* **20**, 327 (1988).
- [150] J. Castejon-Amenedo and V. Manko, *Phys.Rev.* **D41**, 2018 (1990).
- [151] H. Quevedo and B. Mashhoon, *Physics Letters A* **148**, 149 (1990).
- [152] C. Hoenselaers, W. Kinnersley, and B. Xanthopoulos, *J.Math.Phys.* **20**, 2530 (1979).
- [153] H. Fang, *Topics in gravitational physics: tidal coupling in gravitational wave searches and Mach's principle*, Ph.D. thesis (2007).
- [154] J. R. Gair, C. Li, and I. Mandel, *Phys.Rev.* **D77**, 024035 (2008), arXiv:0708.0628 [gr-qc] .
- [155] C. Bambi and E. Barausse, *Astrophys.J.* **731**, 121 (2011), arXiv:1012.2007 [gr-qc] .
- [156] C. Bambi and E. Barausse, *Phys.Rev.* **D84**, 084034 (2011), arXiv:1108.4740 [gr-qc] .
- [157] T. Johannsen, (2013), arXiv:1304.8106 [gr-qc] .
- [158] J. G. Williams, S. G. Turyshev, and D. H. Boggs, *Phys.Rev.Lett.* **93**, 261101 (2004), arXiv:gr-qc/0411113 [gr-qc] .

- [159] C. Bambi and L. Modesto, *Phys.Lett.* **B706**, 13 (2011), arXiv:1107.4337 [gr-qc] .
- [160] T. Johannsen and D. Psaltis, (2013), arXiv:1304.7786 [gr-qc] .
- [161] C. Liu, S. Chen, and J. Jing, *Astrophys.J.* **751**, 148 (2012), arXiv:1207.0993 [gr-qc] .
- [162] R. Konoplya and A. Zhidenko, *Phys.Rev.* **D87**, 024044 (2013), arXiv:1210.8430 [gr-qc] .
- [163] T. Johannsen and D. Psaltis, (2012), arXiv:1202.6069 [astro-ph.HE] .
- [164] C. Bambi, *Phys.Rev.* **D87**, 023007 (2013), arXiv:1211.2513 [gr-qc] .
- [165] P. Pani, C. F. Macedo, L. C. Crispino, and V. Cardoso, *Phys.Rev.* **D84**, 087501 (2011), arXiv:1109.3996 [gr-qc] .

